INFORMATION TO USERS

This manuscript has been reproduced from the microfilm master. UMI films the text directly from the original or copy submitted. Thus, some thesis and dissertation copies are in typewriter face, while others may be from any type of computer printer.

The quality of this reproduction is dependent upon the quality of the copy submitted. Broken or indistinct print, colored or poor quality illustrations and photographs, print bleedthrough, substandard margins, and improper alignment can adversely affect reproduction.

In the unlikely event that the author did not send UMI a complete manuscript and there are missing pages, these will be noted. Also, if unauthorized copyright material had to be removed, a note will indicate the deletion.

Oversize materials (e.g., maps, drawings, charts) are reproduced by sectioning the original, beginning at the upper left-hand corner and continuing from left to right in equal sections with small overlaps.

Photographs included in the original manuscript have been reproduced xerographically in this copy. Higher quality 6" x 9" black and white photographic prints are available for any photographs or illustrations appearing in this copy for an additional charge. Contact UMI directly to order.

Bell & Howell Information and Learning
300 North Zeeb Road, Ann Arbor, MI 48106-1346 USA
800-521-0600

Université d'Ottawa · University of Ottawa

Seismic Retrofitting of Concrete Bridge Columns by External Prestressing

by

©Derek Mes

A thesis submitted to the Faculty of Graduate Studies and Research
in partial fulfillment of the requirements for the degree

Masters of Applied Science - Civil Engineering

The Masters of Applied Science - Civil Engineering
is a joint program with Carleton University,
administered by The Ottawa-Carleton Institute for Civil Engineering

University of Ottawa
Ottawa, Ontario, Canada
January 1999

Abstract

Due to recent earthquakes and the ensuing damage, there has been some concern regarding the adequacy of older structures. In particular, there is apprehension as to the adequacy of bridges that were erected prior to the early 1970's. Before this time there was little or no design process which considered seismic behaviour of bridges. Recent codes have been adjusted to compensate for these earlier problems. However, it is not feasible to remove and rebuild all of the previously built bridges. Hence, the only remaining viable approach to improving seismic adequacy of existing bridges is seismic upgrading or retrofitting these structures to improve their strength and/or deformability.

The research program presented in this thesis addresses the problem of reinforced concrete bridge column retrofitting. More specifically, the applicability of a new retrofitting technique, developed at the University of Ottawa for columns of different aspect ratios and reinforcement arrangements, will be verified in terms of concrete confinement and shear resistance. The retrofitting technique consists of wrapping and prestressing high strength steel 7-wire strands around the test columns in order to increase their ductility. The specimen's tested were based on pre-1971 design, and hence had larger transverse reinforcement spacing than the present practice. This results in a lack of concrete confinement which translates into columns with poor shear resistance which tend to have a brittle failure mode. By retrofitting with prestressing strands, placed at closer spacing than the original hoops, the concrete confinement is increased, diagonal tension resistance is improved and a more ductile response is attained.

Experiments from the first phase of this research program, performed by Yalcin (1997), gave very favourable results for a given aspect ratio and reinforcement arrangement. The present experimental research, forming the second phase, examined columns with different aspect ratios and reinforcement arrangements and also gave favourable results.

Acknowledgment

I would especially like to thank Dr. Murat Saatcioglu for his help, support and guidance. I would also like to thank Dr. Cem Yalcin, Dr. Mongi Grira for his assistance in the lab, my fellow graduate students who helped in the lab and my parents for their help and support.

Table of Contents

List of Figures

Notation

A_c	Cross sectional area of core concrete
A_g	Cross sectional area of gross concrete
D	Outside diameter or dimension of column
f'_c	Cylinder compressive strength of concrete specimens
f_{ps}	Stress in prestressing strands
f_{pu}	Tensile capacity of prestressing strands
f_{yh}	Yield strength of transverse reinforcement
F	Applied lateral load
h	Outside diameter or dimension of column
L	Effective cantilever height of column (shear span)
M	Moment
P	Applied axial load
P_o	Axial load capacity of a column
r	Coefficient as defined in Section 4.5.1
s_{ps}	Spacing of prestressing strands
$V_{flexure}$	Flexural capacity of column
V_{shear}	Shear capacity of column
Δ	Lateral tip displacement of column
Δ_y	Lateral tip displacement corresponding to first yield of longitudinal reinforcement
μ	Displacement ductility ratio of column (Δ / Δ_y)
ρ_l	Reinforcement ratio of longitudinal bars
ρ_v	Volumetric transverse reinforcement steel ratio

Chapter 1

Introduction

1.1 General

Due to recent earthquakes and the ensuing damage, there has been some concern regarding the adequacy of older structures. In particular, there is apprehension as to the adequacy of existing lifeline structures, such as bridges that were erected prior to the early 1970's. Before this time there was little or no design process which considered seismic behaviour of bridges. Recent codes have been adjusted to compensate for these earlier problems. However, it is not feasible to remove and rebuild all of the previously built bridges. Hence, the only remaining viable approach to improving seismic adequacy of existing bridges is seismic upgrading or retrofitting these structures to improve their strength and/or deformability. Retrofitting of bridges has been a continuing process in many regions of high seismicity. The focus of bridge retrofitting includes increasing seat widths at the joints, increasing design force levels, providing restrainers between expansion joints, and jacketing columns for improved shear and flexural resistance. The research program presented in this thesis addresses the problem of reinforced concrete column retrofitting. More specifically, the applicability of the new retrofitting technique, developed at the University of Ottawa for columns of different aspect ratios and reinforcement arrangements, will be verified in terms of concrete confinement and shear resistance.

The older bridge piers suffer from insufficient column ductility, which arises from a lack of concrete confinement. One of the objectives of the retrofitting technique used in the current research project is to increase concrete confinement to enhance column ductility. Also, the design shear capacity in pre-1971 codes was not sufficient, and hence shear strength

is another inherent problem in the older bridge columns. In this case, the increase in transverse reinforcement as well as concrete confinement, provided through retrofitting, improve shear capacity and may change the failure mode from a shear dominant brittle failure to a flexural dominant ductile failure, thereby increasing column ductility.

A considerable amount of research has been done recently to examine different retrofitting techniques to resolve the problems in older bridges, such as inadequate shear resistance; inadequate longitudinal bar lap splice lengths within a poorly confined plastic hinging zone; and inadequate flexural strength, ductility and capacity of columns. A literature review of recent experimental research on different retrofitting techniques was conducted. Most of the previous research make direct reference to columns built prior to the early 1970's . Most of the literature review deals with research carried out with direct relation to California and other regions of high seismicity. However, it should be noted that their results are applicable to seismic zones in Canada. A recent survey of bridges built prior to the early 1970's (Yalcin 1997) shows that these Canadian bridges suffer from similar design problems as those inherent in the United States. Although the literature survey includes column retrofitting techniques in general, the emphasis was placed on bridge pier retrofitting. With the high number of bridge piers in need of retrofitting, an effective, quick, easy and economical solution is needed in practice.

1.2 Bridge Pier Retrofitting Literature Review

A brief history of the changes in seismic design philosophy for bridges is presented by Jaradat et al. (1996). After the 1971 San Fernando earthquake and its disastrous effects, major changes were made in the seismic design philosophy. These changes proved to be effective in the subsequent Whittier Narrows (1987), Loma Prieta (1989) and Northridge (1994) earthquakes. However these earthquakes also demonstrated the remaining problems in pre-1971 designs. Before the San Fernando earthquake, bridge columns had very little transverse steel reinforcement, typically, the reinforcement consisted of #3 (9.5 mm dia.) or #4 (12.7 mm dia.) hoops at 305 mm spacing regardless of the column cross-sectional dimensions. Also, these hoops had short overlapping ends within the concrete cover. This

lack of transverse reinforcement made columns susceptible to shear failures, did not allow development of full flexural capacity, and did not restrain longitudinal bars against buckling. The current design code requires about eight times the transverse steel used in pre-1971 designs.

Four tests of typical pre-1971 columns were conducted by Jaradat et al. (1996), and the results were compared with calculated strengths. The authors concluded that plastic hinging regions with poor confinement and lap splices experienced a rapid strength degradation resulting from concrete cracking and splice slippage. However, the columns with continuous longitudinal bars maintained acceptable flexural strength but eventually degraded at large displacement ductilities due to longitudinal bar buckling. The theoretical flexural behaviour closely predicted the experimental results. A shear failure occurred in one of the specimens and the theoretical shear calculation models either gave conservative or slightly under conservative results. The ACI and AASHTO design equations do not take shear strength degradation at increased displacement ductility into consideration.

The problems with bridges and the effects that the recent earthquakes have had on them were examined by Mitchell et al. (1994). The authors examined retrofitting techniques for foundations, concrete columns, concrete cap beams, joints in reinforced concrete bents, span restrainers, bearing improvements, and steel bracing. Notably, for the bridge column retrofitting, the common problems identified for pre-1971 bridge columns are: insufficient lap-splice length; lap-splice in plastic hinging region; insufficient transverse reinforcement resulting in poor concrete confinement and insufficient shear strength to permit development of plastic hinging in column; poor detailing of confinement reinforcement, including large spacing and inadequate end anchorage; and insufficient flexural strength and ductility.

Examining steel jacketing, Mitchell et al. found that the passive confinement increases shear strength, decreases tendency for longitudinal bar buckling and improves column ductility. The authors state that the elliptical steel jackets are more effective than the rectangular steel jackets with external stiffeners. Steel jacketing does not increase the moment capacity of the column, which is desirable, since it does not induce a higher moment demand on the footing. When retrofitting with steel jackets, one must detail the jacket

carefully so as not to trigger other difficulties. The authors also mentioned two active confinement techniques under investigation: prestressed wire-wrapping and pressure-grouted fibre-glass sleeves. In some cases, using reinforced concrete to sleeve the column is also applicable.

Damages incurred by bridges during the 1994 Northridge earthquake are described by Mitchell et al. (1994). The findings were similar to those reported in other literature. Design deficiencies in the pre-1971 bridges include: low design lateral force levels; inadequate reinforcement; lack of longitudinal restraints across expansion joints; and insufficient seat widths at joints and supports. The initial work on bridge retrofitting concentrated on providing adequate restraints at expansion joints. Next, work was done on the columns, jacketing them - mostly with steel jackets. Upon first inspection of 100 retrofitted bridges, it was found that the only apparent damage was limited to some minor spalling of the superstructure at control joint locations. More inspections are currently taking place, looking at the concrete beneath the steel jackets.

The report describes damage and failure of seven different bridges. Notably, the authors discuss shear failures in many of the shorter columns which had lateral confinement of: #4 hoops (12.7 mm diameter) at 305 mm spacing; #5 hoops (16 mm dia.) at 305 mm; #5 spirals with 89 mm pitch; and #5 spirals with 75 mm pitch at top and bottom and 305 mm pitch in the middle, in which case the failure occurred at the change in pitch. "Short column, heavily reinforced to carry vertical or lateral loads, do not perform well if the lateral confinement and shear capacity are not adequate to resist the shears that are developed when plastic hinging forms in the column."

The bridge investigation seems to indicate that, for the most part, the retrofitting techniques used seem to work and damages mostly only occurred to older columns that had not been retrofitted yet.

1.2.1 Experimental Research with Steel Jacketing

The structural problems associated with pre-1971 bridge columns are described by Chai et al. (1991) as being inadequate flexural strength and ductility; inadequate shear

strength; as well as lack of proper joint and footing details. Notably, the authors indicate that the pre-1971 bridge columns do not contain enough transverse reinforcement and that the typical reinforcement consisted of #4 hoops (12.7 mm diameter) placed at 12" (305 mm) spacing, regardless of column dimensions. Also, these hoops were not adequately closed and would unravel and become ineffective once the concrete cover spalled off. For columns with short shear spans, this inadequate transverse reinforcement translated into lower shear capacities than those corresponding to flexural yielding and therefore the failure mode "...involved brittle shear failure with low ductility and poor energy-absorption characteristics.". The solution to these problems involves more closely spaced hoops in the plastic hinge region which improves the confinement of the core concrete, as well as diagonal tension resistance of the column.

The retrofitting technique studied by Chai et al. (1991) involves the confinement of the potential plastic hinge region with a site-welded cylindrical steel sleeve or jacket. The test involved 6 columns of 24" (610 mm) diameter and 12' (3.658 m) height. The testing considered different footings and lap spliced or continuous longitudinal bars. The axial load applied was 1780 kN (17.7% $A_g f'_c$). The lateral load cycling scheme was based on the displacement ductility ratio, μ, which is the ratio of maximum displacement to the displacement needed to cause the first yield of the longitudinal reinforcement. The cycling scheme consisted of three cycles at μ = 1, 1.5, 2, 3, etc. until failure.

The conclusions made by Chai et al. are that pre-1971 circular bridge piers, with lap splices within the plastic hinge region, are likely to fail prematurely due to bond failure, followed by rapid strength degradation. For columns with continuous longitudinal bars, the strength degradation is less rapid, and is caused by lack of concrete confinement. The tests of retrofitted columns showed that high tensile hoop stresses were developed on the compression side, at the top and bottom of the steel jacket. As well, there were high vertical stresses due to local bending, to the point where at large lateral column displacements, the combination of stresses at the bottom of the steel jacket could cause the steel to yield. Analysis also shows that there is relative slip between the jacket and grout infill along the entire length of the jacket. The steel jacket improves the displacement ductility by providing

a good volumetric ratio of confinement steel and increases column stiffness by 10 to 15 %. For the columns with continuous longitudinal bars, the drift level capacity was improved from about 3.5% to above 6%. Tests that are currently in progress, involving oval steel jackets for rectangular columns, are showing similar flexural enhancements.

Further analysis on circular bridge columns retrofitted with steel-jacketing was performed by Chai (1996). The analysis concentrated on how confinement improves the ultimate compressive strain of concrete, and how confinement inhibits the spalling effect. It was found that the compressive strain increased from 4 - 9 times the spalling strain of concrete. There is also a large increase in curvature ductility and tensile strain in the extreme reinforcement. The design for steel jacket thickness, t_j, adopted by Caltrans as given below, was used in the analytical work.

$$t_j = C_j \, {}^{D}/_{200} > 6.4 \text{ mm}$$

where; D = column diameter (in mm)

C_j = 1.0 or 1.2 for continuous or lapped longitudinal bars, respectively

The author also performed computer simulations using COLRET to investigate the effects of jacket thickness on the moment-curvature response of columns. All trials used a 1500 mm diameter column, with $A_s = 2\% A_g$ for longitudinal bars, and #4 (12.7 mm dia.) bars at 305 mm for transverse steel. The study examined the effects of jacket thickness on the curvature ductility factor, f_u / f'_y (ultimate curvature / first-yield curvature), and failure mode. For the unconfined column, f_u / f'_y was 10. For jacket thicknesses of 5, 10 and 15 mm the f_u / f'_y ratio was 31, 51, and 69 respectively. The Caltrans equation, given above, would suggest a jacket thickness of 7.5 mm. For the three thicknesses tried above, the ultimate capacity was governed by the ultimate compressive strain of concrete. When thicker jackets were tried with 20 and 25 mm thickness, and $f_u / f'_y = 79$, the failure was governed by the ultimate tensile strain of the longitudinal steel.

The other contributions of steel jacketing is the increase in lateral stiffness when steel jackets are used along the entire height of the column - which is often done for esthetic

reasons even when not required for performance. Based on current jacket thicknesses used, a 35 - 60% increase in lateral stiffness can be expected for columns with aspect ratios (L/D) of 3 - 9.

An eleven column test regime was conducted by Aboutaha et al. (1996) to examine the use of rectangular steel jackets to improve the behaviour of columns with inadequate lap splices. Different column widths and concrete confinement were used. Retrofitting with and without adhesive anchor bolts, in differing quantities and arrangements, were considered. The loading regime consisted of lateral loads applied with two cycles at every 0.5% drift till failure, without any axial load. The authors concluded that this retrofitting technique could be effective - in some cases maintaining the column's flexural strength when subjected to drift ratios in excess of 4% drift. For larger columns, the adhesive anchor bolts were essential in attaining this performance.

1.2.2 Experimental Research with Reinforced Concrete Jacketing

Four column tests were performed by Rodriguez and Park (1994) to investigate the increase in strength, stiffness and ductility through retrofitting. The tests included damaged and undamaged reinforced concrete columns with a 100 mm thick reinforced concrete jacket. The specimens were based on pre-1970's construction practice with a 350 mm square cross-section and a 3.3 m height, representing column segments between mid-heights of successive stories of a frame. The axial load of 20% $A_g f'_c$ was applied with a lateral loading scheme consisting of 2 cycles at each displacement ductility factor, μ = 1, 2, 3, etc. until failure. According to current codes, these columns were designed with inadequate flexural strength and transverse reinforcement and the two columns tested without retrofitting demonstrated this by showing lack of ductility. These two columns as well as two untested columns were retrofitted and tested. The testing showed a significant increase in strength and stiffness - up to three times that of the original columns. It also showed a large improvement in energy dissipation. Furthermore, the previous damage sustained by columns had no significant effect on the performance of retrofitted columns. The retrofitting technique was successful in improving the strength, stiffness and ductility of columns (from the graphs it appears to have

increased inter-storey drift from about 2% to at most 3%), but as the authors note, the technique is very labor intensive.

1.2.3 Experimental Research with Fibre Wrap

Experiments consisting of five reinforced concrete columns, based on pre-1971 practice, were conducted by Saadatmanesh et al. (1996). The columns had a 305 mm diameter and a height of 1800 mm. Columns with and without lap splices were considered. Both active and passive pressures were applied by means of fiber reinforced plastic (FRP) composite straps, used for retrofitting. The active pressure was achieved using a pressurized grout infill, resulting in a 758 kPa pressure. The applied axial load was 445 kN (17.7% $A_g f'_c$). The lateral loading scheme was based on the displacement ductility factor, μ, and consisted of two cycles at μ = 1, 1.5, 2, 3, 4, etc. until failure. Six layers of FRP straps were wrapped around the plastic region, up to 635 mm above the base. The FRP straps were 0.8 mm thick with a tensile strength of 532 MPa and modulus of elasticity of 18.6 GPa. This retrofitting technique significantly improved the strength and ductility of columns - increasing the displacement ductility level to $\mu = \pm 6$ without any significant strength degradation. For the columns with continuous longitudinal bars the retrofit increased drift capacity from about 3.7% to above 5.5% (estimated). Although the active pressure did have a greater strength enhancing effect than the passive pressure, the resulting improvements may not be significant enough to justify the additional cost.

Tests conducted by Seible et al. (1997) examined the effectiveness of carbon fiber jackets. The emphasis was placed on developing a retrofitting setup which would confine the regions based on necessity. The column height was divided into regions where shear strengthening, flexural hinge confinement, or lap-splice clamping were required. The required wrap thickness was calculated for each section, based on proposed formulae. To validate the proposed retrofitting scheme, 5 columns were tested. The first pair of rectangular columns tested involved shear retrofitting in double bending, with a height of 2.4 m (1.2 m shear span) and a 610 mm by 406 mm cross-section. The axial load was 507 kN (6% $A_g f'_c$) and the lateral loading scheme consisted of 3 cycles at each displacement ductility factor, μ = 1, 2,

3, 4, 6, 8, etc. until failure. The transverse reinforcement consisted of #2 (6.4 mm dia.) bars at 127 mm spacing. The retrofitting layers were: 2.0 mm for 305 mm from top and bottom; 1.0 mm for the next 305 mm; and the middle section had 0.5 mm. The "as built" and retrofitted columns withstood a displacement ductility factor, $\mu = 3$ and 12, respectively.

The second pair were rectangular cantilever columns for testing flexural retrofitting. The columns had a height of 3.658 m and a cross-section of 730 mm by 489 mm. The axial load was 1780 kN ($14.5\%A_g f'_c$) and the lateral loading scheme consisted of 3 cycles at each displacement ductility factor, μ = 1, 2, 3, 4, 6, 7, 8, or until failure. The transverse reinforcement consisted of #2 (6.4 mm dia.) bars at 127 mm spacing. The retrofitting layers were: 10.2 mm for 914 mm from the bottom, then 5.1 mm for the next 457 mm, and the rest, all the way to the top, had 0.5 mm. The "as built" and retrofitted columns withstood a displacement ductility factor, $\mu = 3$ and 7, respectively.

The last column was tested to investigate lap-splice clamping in circular flexure dominant columns. The specimen height was 3.658 m with an outside diameter of 610 mm. The axial load was 1780 kN ($17.5\%\ A_g f'_c$) and the lateral loading scheme consisted of 3 cycles at each displacement ductility factor, μ = 1, 2, 3, 4, 6, 8, etc. until failure. The transverse reinforcement consisted of #2 bars at 127 mm spacing. The retrofitting layers were: 5.1 mm for 457 mm from the bottom, then 2.5 mm for the next 457 mm, and then tapering off over the next 152 mm (the rest of the column not being wrapped). The column was first tested with the retrofitting described above, and demonstrated debonding of the lap splice at a displacement ductility factor, $\mu = 5$. It was then determined that the retrofitting used was 20% less than the calculated amount required. The carbon wrap thickness was increased and the column was tested again. This time a displacement ductility factor, $\mu = 10$, was achieved. The results from the tests lend confidence to the formulae and method for determining carbon fiber wrap thickness requirements.

Five rectangular bridge columns, retrofitted with fiber reinforced plastic (FRP) composite straps, were tested by Saadatmanesh et al. (1997). The retrofitting consisted of FRP straps wrapped around the potential plastic hinging region of columns, estimated as twice the effective depth of column cross-section (635 mm above the footing). The column

dimensions were 240 x 368 mm with a height of 1800 mm. The lateral reinforcement consisted of 9 gauge steel wire (3.8 mm dia.) at 89 mm spacing along the entire height. The tests examined columns with and without lap splices; rectangular and oval retrofitting configurations using fast curing cement; and active and passive pressures for retrofitting. For the active pressure a pressurized epoxy infill was used, resulting in a 550 kPa pressure. The applied axial load was 445 kN (15% $A_g f'_c$) and the lateral load was based on the displacement ductility factor, μ, with two cycles at μ = 1, 1.5, 2, 3, 4, etc. until failure.

This retrofitting technique significantly improved the strength and ductility of columns. For the column retrofitted with active pressure and a rectangular configuration, the test examined specimens with lap splices within the plastic hinging region. The control specimen exhibited a significant reduction in lateral load carrying capacity when pushed beyond μ = 3; whereas the retrofitted specimen showed little strength degradation even up to μ = 6. For the other three columns, which had continuous longitudinal bars, the control specimen failed in shear during the first push to μ = 3. The two retrofitted columns, one with a rectangular and the other with an oval configuration (both with passive pressure), sustained μ = 6 (limit of hydraulic actuator's stroke) with no strength degradation. The difference in oval and rectangular configuration could not be determined in this limited test program.

Xiao and Ma's (1997) conducted experimental research, consisting of three columns with a diameter of 610 mm and a height of 2440 mm. The column reinforcement consisted of #2 hoops (6.4 mm dia.) at 127 mm spacing and 20 #6 (19.1 mm dia.) longitudinal bars which were lap spliced for a length of 381 mm at the bottom. The columns were subjected to a constant axial load of 712 kN (about 5% of capacity) and a lateral load based on the displacement ductility factor, μ, with two cycles at μ = 1, 1.5, 2, 3, 4, 6, 8, etc. until failure. The retrofitting technique utilized prefabricated glass fiber composite jackets, 3.2 mm in thickness, with an ultimate tensile strength of 552 MPa. Different layering schemes were used: 3 layers for 1220 mm above base with a 4th layer in the bottom 610 mm; 3 layers for 2211 mm with 4th and 5th layer in the bottom 1220 mm; and for the repaired column, 4 layers for 1220 mm. The control column could withstand a displacement ductility factor, μ, of 1, whereas the 4-layer and 5-layer retrofitted columns could withstand μ = 6 (about 4% drift)

before experiencing some strength degradation. The ductility of the repaired control column was improved to $\mu = 4$. An analytical model was proposed to predict the behaviour of lap spliced columns with or without jacketing, which compared favorably with the experimental results.

1.2.4 Experimental Research with Prestressed Hoops

Observations made by Coffman et al. (1993) also indicate behavioural deficiencies for seismic resistance in long circular concrete bridge columns built between 1950 and the mid 1970's. The authors conclude that the minimal amount of hoops provided had questionable effectiveness. In particular, the poorly confined (or questionably confined) lap-splice regions within potential plastic hinges were investigated. The retrofitting technique tested consisted of #3 (9.5 mm diameter) and #4 (12.7 mm diameter) grade 60 bars (grade 400 MPa) formed into a semicircular shape, connected by swaged couplers, which were tightened to give the hoops a prestress level of approximately 350 MPa. The tests consisted of four 456 mm diameter, 10' (3.048 m) high columns. One column was tested as a control specimen and the other three had different configurations of #3 and #4 bars at 3" (76.2 mm) to 4" (101.6 mm) spacing. The retrofitting was limited to the bottom quarter of the column, which corresponded to 1.8 h, where h represents the outside column diameter. The columns were subjected to a constant axial load of 20% $A_g f'_c$ and lateral deformation cycles based on displacement ductility ratio, μ. The cycling was as follows: one cycle at 0.75μ, two cycles at 1μ and 2μ, and then cycling at 4μ till failure. The data indicate that a displacement level of 4μ corresponds to about 3.5% lateral drift. Failure was defined as 20% reduction in horizontal load-carrying capacity (as cited by Park in the New Zealand structural design code). It was concluded that this retrofitting technique did not change the column stiffness or increase its strength. It did, however, slightly increase the energy dissipation in a given cycle and significantly increased the number of cycles that could be sustained before failure. The conclusions made by Coffman et al. were that this technique of retrofitting would be good "...for columns of this era where shear is not a significant failure feature, and where shaking is of medium intensity and long duration.".

1.2.5 Experimental Research with Prestressing Strands

A retrofitting technique was developed in 1997 for circular and square columns at the University of Ottawa, as part of the first Phase of the current research program (Yalcin 1997; Saatcioglu, M. and Yalcin, C., 1998). The new retrofitting technique involves external prestressing of concrete columns using prestressing strands, or high-strength steel straps. The experimental part of the research program included 7 column tests. The columns were 1485 mm in height, of which five had a circular cross-section (610 mm diameter), and two had a square cross-section (550 by 550 mm). The columns had typical reinforcement for pre-1971 bridge columns, i.e., they consisted of twelve # 25 (25 mm dia.) longitudinal bars uniformly spaced, and #10 (10 mm dia.) hoops at 300 mm spacing, with the first one placed at 75 mm from the base. The loading regime for all columns consisted of an axial load of 15% P_o, and a cyclic lateral loading pattern of 3 cycles at 0.5%, 1%, 2%, 3%, etc. drift, or until failure. P_o is defined as the concentric capacity of the column and drift is defined as the lateral displacement at the tip of the column over the total column height.

For the circular columns, one was tested as a control column without any retrofitting, another one was retrofitted using steel strapping, and three others were retrofitted by external prestressing, using 7-wire strands. The high strength steel straps had a yield strength of 910 MPa at 0.52% strain and an ultimate strength of 1010 MPa at 9% strain, with strain hardening beginning at 2.1%. The straps were spaced at 150 mm. The prestressing strands used were size 9, grade 1860 MPa, 7-wire strands. They were placed around the column in individual hoops with the ends joined with a Dywidag twisted ring anchor. Different spacing and initial prestress levels were used as test parameters.

The non-retrofitted circular column failed in shear when subjected to 2% drift. The column retrofitted with the high strength steel straps withstood the 2% drift cycles, but at the beginning of the 3% cycles some of the straps ruptured and column failure followed shortly after - this retrofitting technique was not considered to be very effective. For the columns retrofitted with prestressing wires, three different configurations were used: wires at 300 mm with 25% f_{pu} (tensile capacity); wires at 150 mm with 25% f_{pu}; and wires at 150 mm with 5% f_{pu} (passive pressure). In general, external prestressing improved both strength and

deformability of columns. The failure mode changed from a brittle shear dominant response to a ductile flexure dominant response. The 300 mm spacing was not as effective as 150 mm, and one of the wires in the column with 300 mm spacing started to fail during the 3% drift cycle, and significant strength degradation soon followed. However, the 150 mm spacing with 25% f_{pu} was very effective, with no strands showing signs of failure and no strength degradation until 5% lateral drift. With the 150 mm spacing and 5% f_{pu}, behaviour was also good, but the strength degradation occurred suddenly when the 5% drift level was reached. It was concluded that using prestress wires as a method of retrofitting was effective, with the best results achieved using a wire spacing of 150 mm and an initial prestress level of 25% f_{pu}. This method of retrofitting is easy to install and would be a very economical retrofitting solution.

The non-retrofitted square column also failed in shear when subjected to 2% drift, in much the same manner as the companion circular column. The retrofitting technique for square columns with prestressing strands is the same as for the circular columns except that spacers are placed on the column faces to raise the prestress wire at three locations on every face, so as to achieve confining force at these three locations on each face - as well as on the corners. The strands were placed at 150 mm spacing with an initial prestress of 25% f_{pu}. The retrofitted column demonstrated good behaviour, reaching 5% drift before any significant strength degradation occurred. At 5% drift, the strength degradation was slow, and column failure occurred at 6% drift.

1.3 Discussion and conclusions from literature review

Researchers have concluded that bridge columns built based on the pre-1971 code have inadequate seismic resistance for zones of high seismicity. For reinforced concrete bridge columns, the problems are due in part to insufficient transverse reinforcement. This lack of sufficient transverse reinforcement results in inadequate shear resistance and inadequate flexural ductility. To overcome these inadequacies, research has been performed on columns designed prior to 1971, in order to develop retrofitting techniques which would properly improve strength and ductility of these columns. All the techniques researched have

successfully improved the behaviour of these columns; however, some were more successful and proved to be applicable in more circumstances. The most frequently used technique in practice is the steel jacketing. However, this technique is expensive and labour and material intensive. Other techniques such as carbon fibre wrap and prestressing strands are viable alternatives which have been proven effective in the laboratory, but have not been used extensively or at all in practice.

1.4 Objectives and scope

The objective of this research project is to investigate the effectiveness of external prestressing as a viable retrofitting methodology for concrete columns with different aspect ratios and different reinforcement arrangements. Both square and circular columns, with spiral and tied reinforcement, are included.

The scope includes the following steps:

- Literature review of previous experimental research on seismic column retrofitting.
- Design, preparation and instrumentation of 6 large scale reinforced concrete columns for testing.
- Retrofitting columns through external prestressing.
- Preparation of test set-up for simulated seismic loading.
- Testing 6 concrete columns under combined constant axial compression and incrementally increasing lateral deformation reversals.
- Evaluation of test data.
- Analysis of columns and drawing practical conclusions for retrofitting seismically inadequate concrete bridge columns.
- Preparation of a thesis and presentation of results.

Chapter 2

Test Specimens and Apparatus

2.1 General

Tests of reinforced concrete columns were conducted using a retrofitting technique consisting of prestressing strands wrapped around the outside of the test specimens. The tests were conducted to examine the deficiencies of pre-1971 columns and to establish the improvements resulting from this retrofitting technique. The experimental research included columns with different aspect ratios and reinforcement configurations. The columns were built in pairs and tested, one as a control column the other as a retrofitted column - in all, three pairs were tested. The specimen details, material properties, instrumentation and test setup are presented in the following sections.

2.2 Test Specimen Details

2.2.1 Circular Columns with Tied Reinforcement (BR-C6 & BR-C7)

The first pair of columns were circular with a diameter of 508 mm and a height of 1725 mm, and were labeled BR-C6 and BR-C7, following the labeling scheme used in the earlier phase of the same investigation. The total effective height of the column (shear span) was 2.0 m, taken to the point of application of the horizontal actuator (see Fig. 2.12c). The reinforcing steel was of grade 400 MPa, and consisted of twelve #20 longitudinal bars and #10 hoops with overlapping ends. The hoop spacing was 300 mm, starting at 125 mm from the column base. The outside dimension of the hoops was 410 mm, leaving a clear cover of 50 mm. The hoop spacing reflects the common design practice used prior to 1971. The longitudinal reinforcement and column aspect ratio were chosen to give the column a flexure

dominant failure mode. The column dimensions and reinforcement details are illustrated in Figure 2.1.

The retrofitting consisted of prestressing strands placed at 150 mm spacing, with the first wire placed at 125 mm from the column base. Each wire was stressed using a Dywidag twisted ring anchor. The prestressing strands and prestress level are described in Section 2.3.3. The retrofitting details are illustrated in Figure 2.2.

2.2.2 Square Columns (BR-S3 & BR-S4)

The second pair of columns had a 500 mm square cross-section with an effective height (shear span) of 2.0 m. These columns were labeled BR-S3 and BR-S4. The reinforcement consisted of twelve #20 longitudinal bars and #10 hoops with 135° bends at the ends. The spacing of hoops was 300 mm, starting at 150 mm above the column base. The outside dimension of the hoops was 410 mm leaving a clear cover of 45 mm. As for the previously described circular columns, the longitudinal reinforcement and column aspect ratio were chosen to give the column a flexure dominant failure mode. The column dimensions and reinforcement details are illustrated in Figure 2.3.

The prestressing strands for the retrofitted column were placed at 150 mm spacing, with the first wire at 125 mm from the footing. On each column face, the prestressing strands were raised at three points, using raiser discs attached to an HSS section, in order to distribute the prestress load over four faces of the column. The spacing of the last two wires was increased to 250 mm as this was well beyond the plastic hinging zone and the retrofitting no longer needed to be as stringent. The retrofitting details are illustrated in Figure 2.4.

2.2.3 Circular Columns with Spiral Reinforcement (BR-SP1 & BR-SP2)

The third pair of columns were circular with a diameter of 610 mm and an effective height of 1.55 m. These columns were labeled BR-SP1 and BR-SP2. The reinforcement consisted of twelve #20 longitudinal bars and a #10 spiral with a 75 mm pitch. The spiral's outside dimension was 500 mm, leaving a clear cover of 55 mm. The column dimensions and reinforcement details are illustrated in Figure 2.5.

The prestressing strands for retrofitting were placed at 150 mm spacing along the entire height of the column. The column dimensions and reinforcement details are illustrated in Figure 2.6. A fiber-reinforced concrete shell was placed on the retrofitted column, to investigate the behaviour of a concrete jacket that may be required for protection against corrosion, as well as improved aesthetics. Before the concrete shell was placed, the concrete on the outside of the column was roughened using a small compressed air chisel. Concrete nails were also hammered in at a spacing of roughly 150 mm in both directions, protruding 20 mm from the surface. The concrete was soaked and surface dried, and a bonding agent, SikaTop Armetec 110, was applied to the surface on one side. The other side of the surface, perpendicular to the direction of loading, was not treated with the bonding agent to assess the effectiveness of and the need for a bonding agent. Concrete with 10 mm maximum aggregate size and 25 mm plastic fibers was poured and vibrated into a form. This produced a 25 mm concrete shell with a test day strength of 37 MPa.

2.3 Material Properties

2.3.1 Concrete

The column bases were poured in pairs and the concrete had 28 day strengths of 46 MPa for the footings of the circular columns with tied reinforcement, 34 MPa for the footings of the square columns and 39 MPa for the footings of the circular columns with spiral reinforcement. These different strengths were not intentional but resulted from the use of different batches of concrete. However, although the strength of footing concrete was not expected to influence the behaviour of columns, the same batch of concrete was used for each pair to eliminate any doubt on potential effect of footing concrete on column behaviour. It should be noted that the footings were very well reinforced, making them very rigid to provide full fixity.

The columns were all poured simultaneously from the same batch of concrete, with a 28 day strength of 34 Mpa. The concrete strength during the column test period was 35 MPa. Standard cylinder tests were conducted in accordance with the relevant CSA Standard. The results for column concrete are shown in Fig. 2.7 and Fig. 2.8.

2.3.2 Reinforcing Steel

Tension coupon tests were conducted on #10 and #20 reinforcing steel used in preparing column cages. For the #10 rebars, the three coupons tested had a yield strength of 440 MPa at a strain level of 0.2%, and an ultimate strength of 690 MPa at a strain level greater than 12% strain. For the #20 rebars, the three coupons tested had a yield strength of 440 MPa at a strain level of 0.2%, and an ultimate strength of 600 MPa at a strain level greater than 10%. Test data is plotted in Figure 2.9 and Figure 2.10 for # 10 and # 20 bars, respectively.

2.3.3 Pre-stressing Strands

The seven-wire strands used for retrofitting were of size 9 and grade 1860 MPa. The nominal strand diameter was 9.53 mm, while the nominal area was 51.6 mm^2. The prestressing strand was not tested in the lab. The stress-strain curve was obtained from the supplier, and is shown in Fig. 2.11. The ultimate tensile capacity, f_{pu}, was about 2180 MPa. Yielding began at 1720 MPa with a strain level of about 0.75%. The 0.2% offset curve intersects at 2035 MPa with a strain level of 1.1%. When retrofitting the columns, the prestressing strands were stressed to approximately 25% f_{pu}. This was established in the earlier phase of the research by Yalcin (1997), to be a suitable stress level for shear dominant short-span columns.

2.4 Test Setup

Three servo-computer controlled MTS hydraulic actuators were used to apply the required load and/or deformation. The actuators had a capacity of 1000 kN, both in tension and compression. Two actuator were placed vertically, one on either side of the column, to apply the vertical load. The third actuator was placed horizontally and was attached to the tip of column to apply lateral deformation reversals. The test setup is illustrated in Fig. 2.12.

The column footing was secured to the laboratory strong floor with four bolts. The two vertical actuators were attached to the column footing at one end, and to the steel loading beam at the other end, to compress the column, simulating vertical gravity loading.

Each end of the actuators was attached using 4 high-strength bolts.

For the two shorter columns, BR-SP1 and BR-SP2, the horizontal actuator was lowered by 460 mm and a second 460 mm concrete spacer was added to the top loading beam to allow for the length of the vertical actuators. These details are shown in Fig. 2.12.

2.5 Instrumentation

Electric resistance strain gauges were used to measure steel strains in column reinforcement, as well as prestressing strands. Strain gauges were placed on longitudinal and transverse reinforcement as illustrated in Figs. 2.13, 2.14 and 2.15. As well, each prestressing strand had a strain gauge, though the bottom five strands had two gauges each.

LVDTs (Linear Voltage Displacement Transducer) were used to measure the flexural rotation of the columns. The LVDTs were connected to threaded rods which were cast in column concrete on each side, at h and h/2 (where h is the cross-sectional dimension of column) distances from the base. LVDT locations are illustrated in Fig. 2.16.

Temposonic LVDTs (Linear Variable Differential Transformer) were used to measure column tip deflection and longitudinal reinforcement extension at the column-footing interface. An LVDT was placed on each side of the column for this purpose, as close to the column-footing interface as possible, attached to threaded rods cast in column concrete. A third LVDT was attached to the center point of the horizontal actuator - at the effective height of the column. The Temposonic LVDTs are shown along with the other LVDTs in Fig. 2.16.

2.6 Loading

A constant vertical load was applied to the columns, during testing, representing the effects of gravity loading. The level of axial compression was approximately 15% P_o, where P_o is defined as the concentric capacity of the column. This level of load is a good representation of actual bridge loads applied in practice. The vertical load was kept at the same level for the entire duration of the test. Specifically, the loads applied to the circular columns with tied reinforcement, the square columns and the circular columns with spiral

reinforcement were: 1260 kN (15% P_o, 17.7% $A_g f'_c$); 1510 kN (15% P_o, 17.3% $A_g f'_c$); and 1750 kN (15% P_o, 17.7% $A_g f'_c$), respectively.

The horizontal loading was applied in deformation controlled mode at incrementally increasing displacement reversals. Column drift level was used as the basis for lateral displacements, where drift was defines as the column tip deflection / column height. The columns were subjected to three full cycles at each drift level of 0.5%, 1.0%, 2.0%, 3.0%, etc. until failure. A sketch of the horizontal loading program is illustrated in Fig. 2.17.

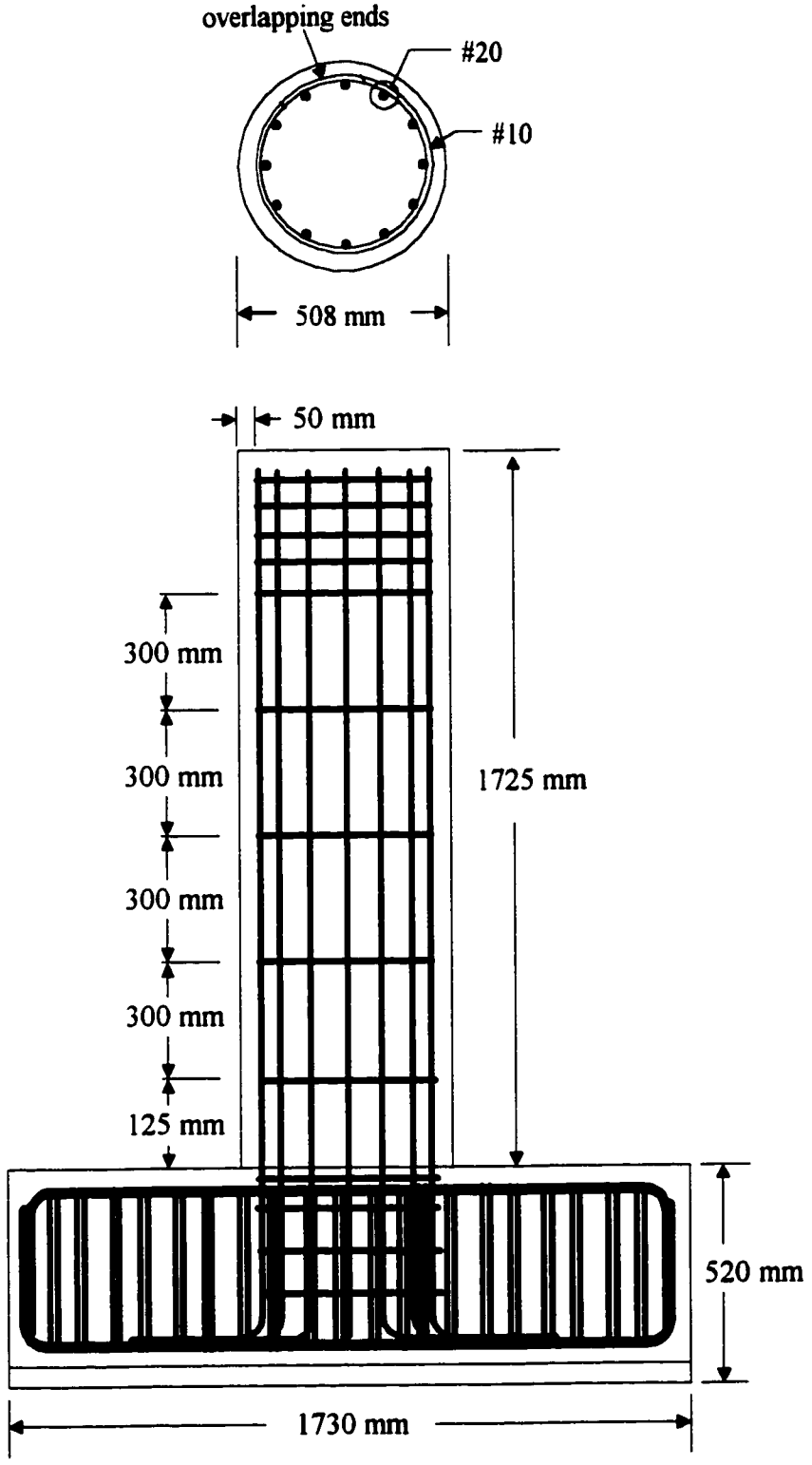

Fig. 2.1 Dimensions and reinforcement details for columns BR-C6 and BR-C7

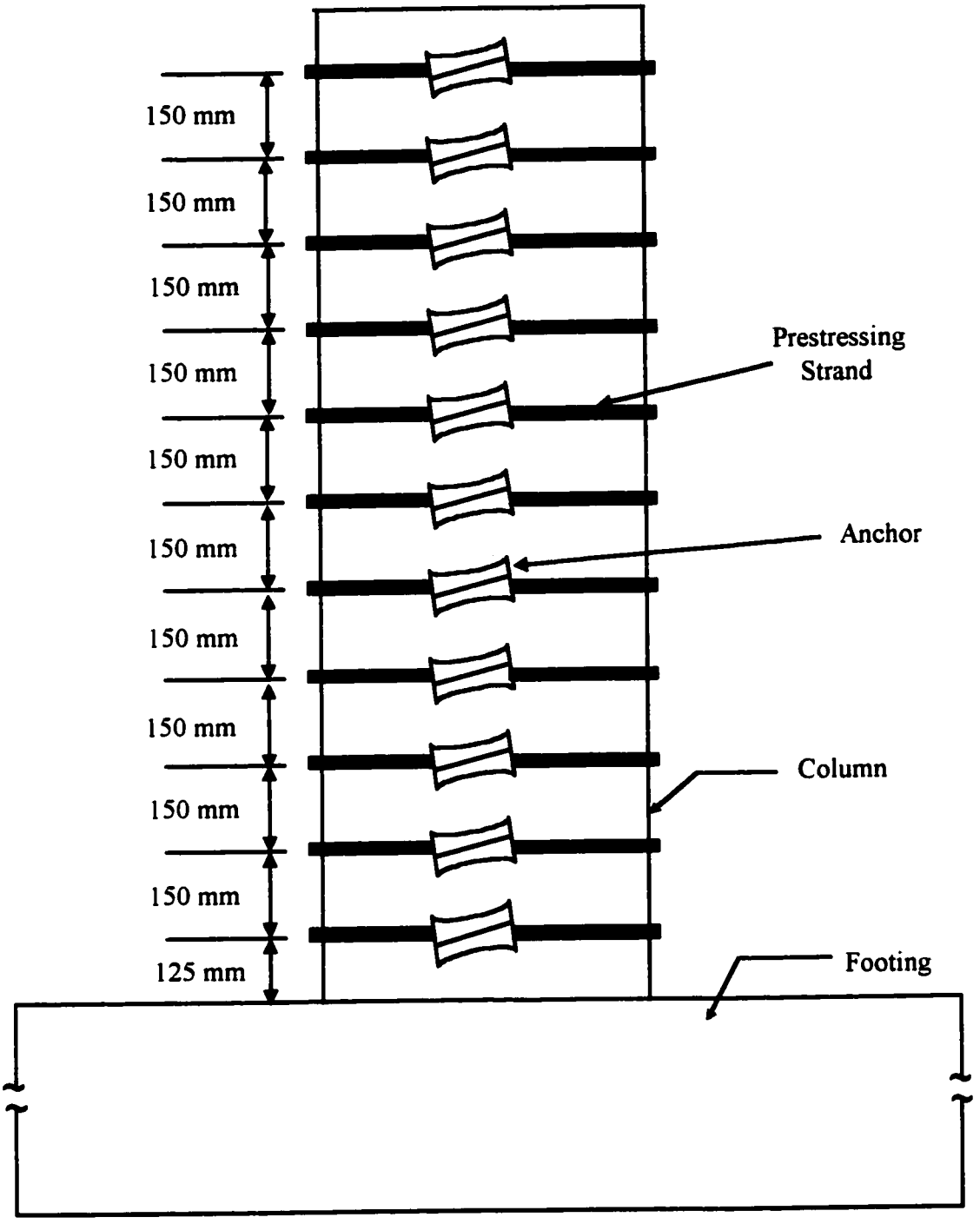

Fig. 2.2 Retrofitting details for columns BR-C7

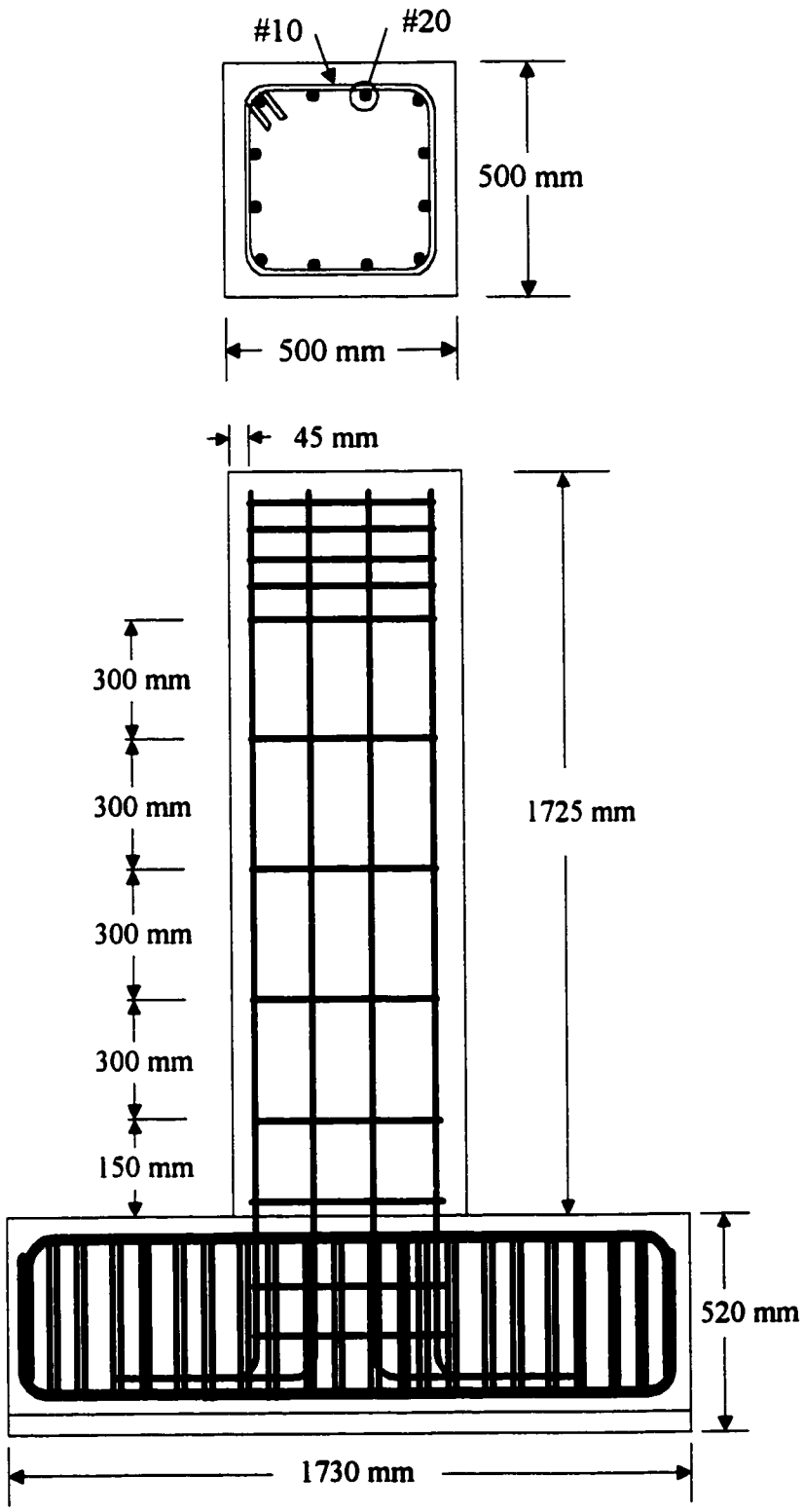

Fig. 2.3 Dimensions and reinforcement details for columns BR-S3 and BR-S4

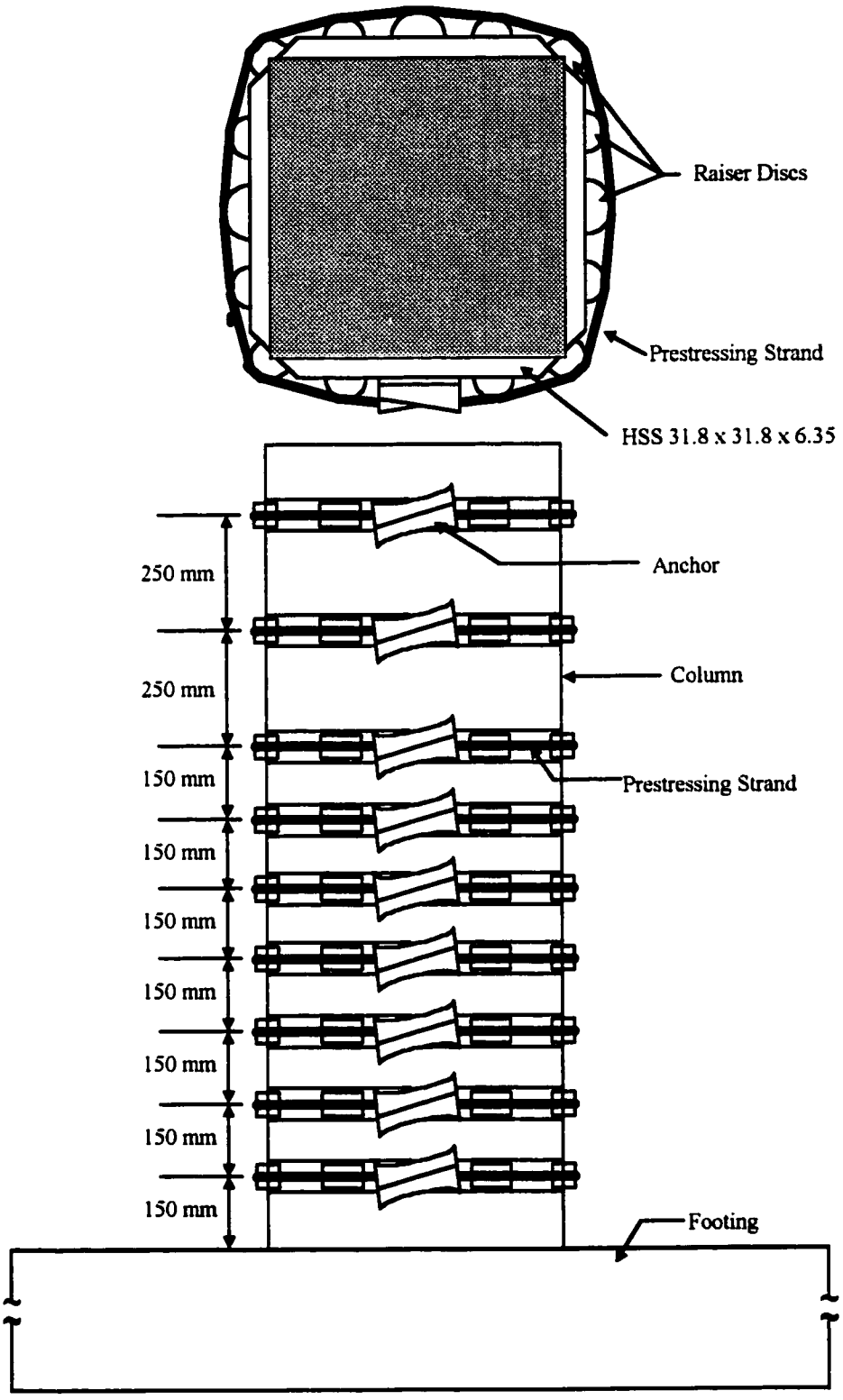

Fig. 2.4 Retrofitting details for columns BR-S4

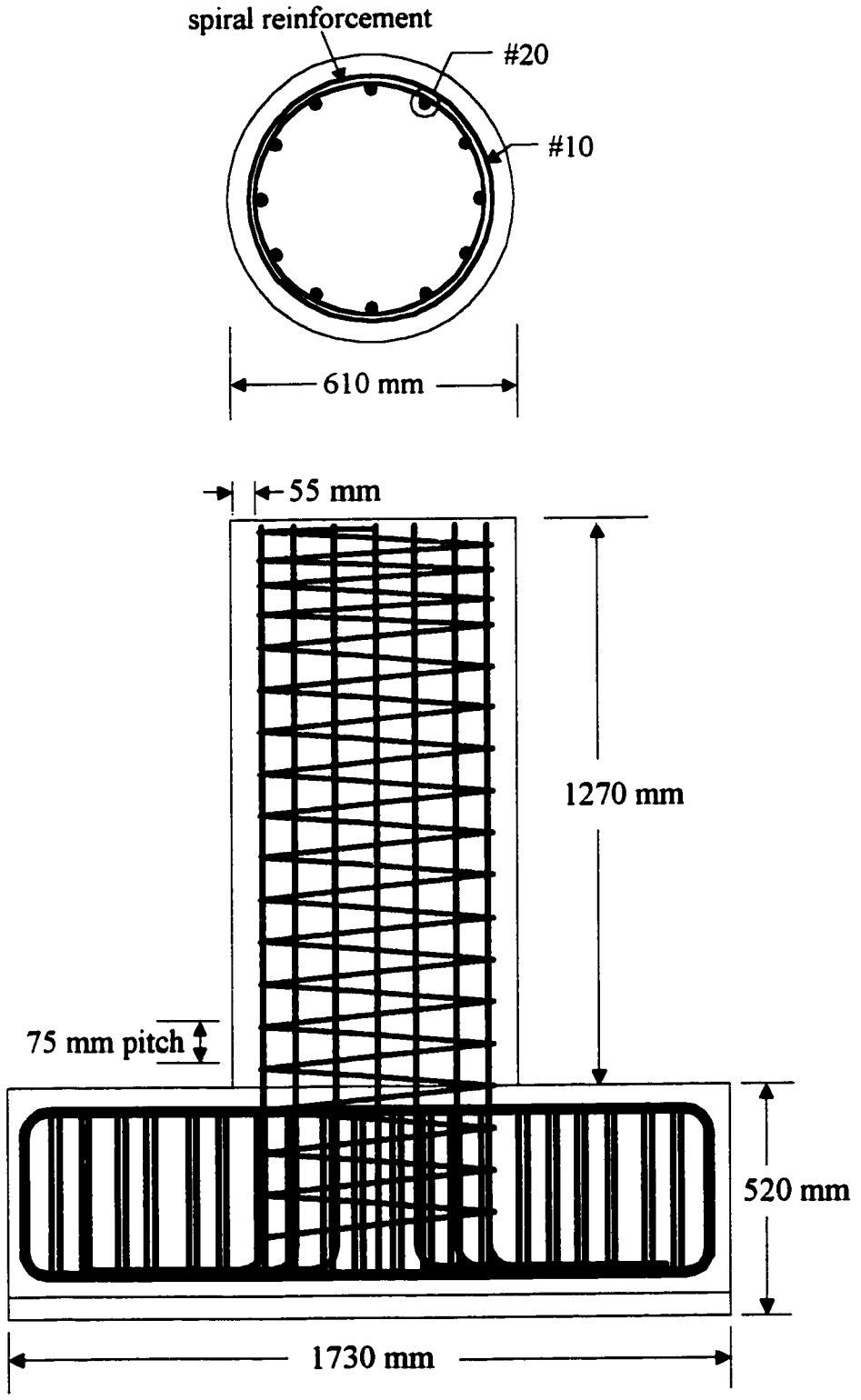

Fig. 2.5 Dimensions and reinforcement details for columns BR-SP1 and BR-SP2

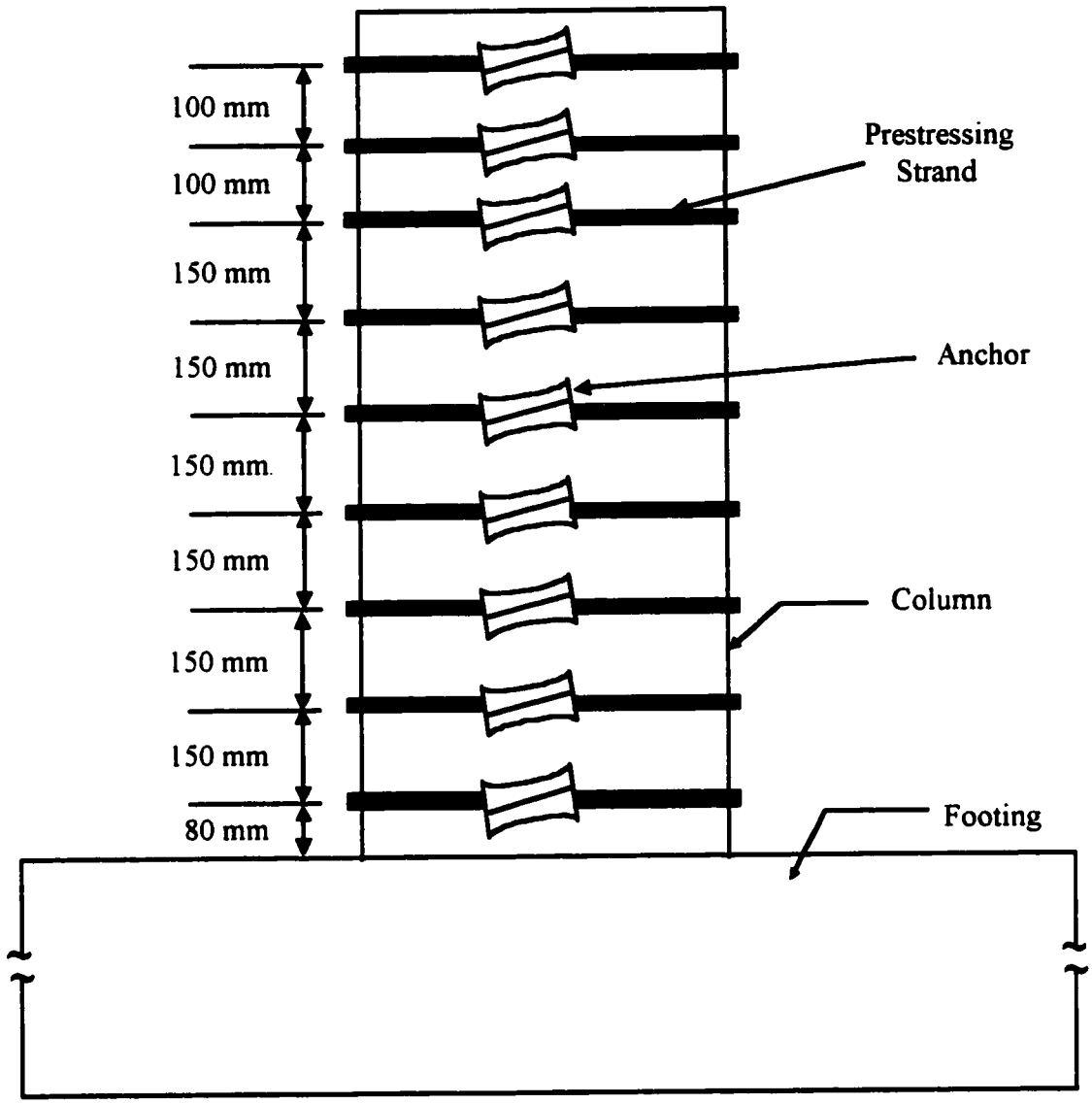

Fig. 2.6 Retrofitting details for columns BR-SP2

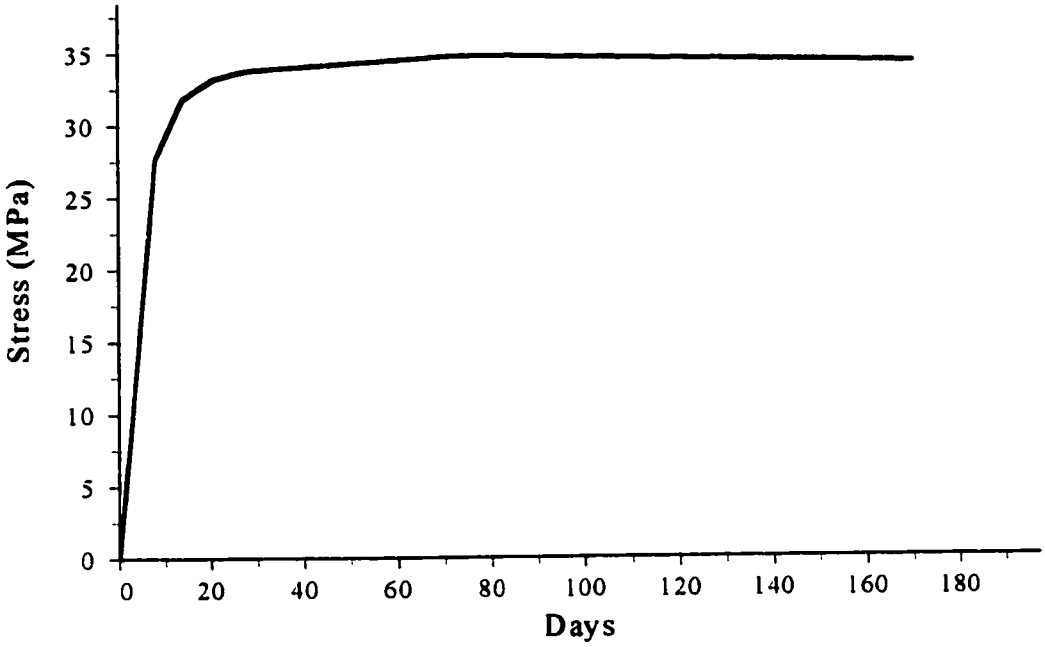

Fig. 2.7 Stress development over time of concrete test cylinders

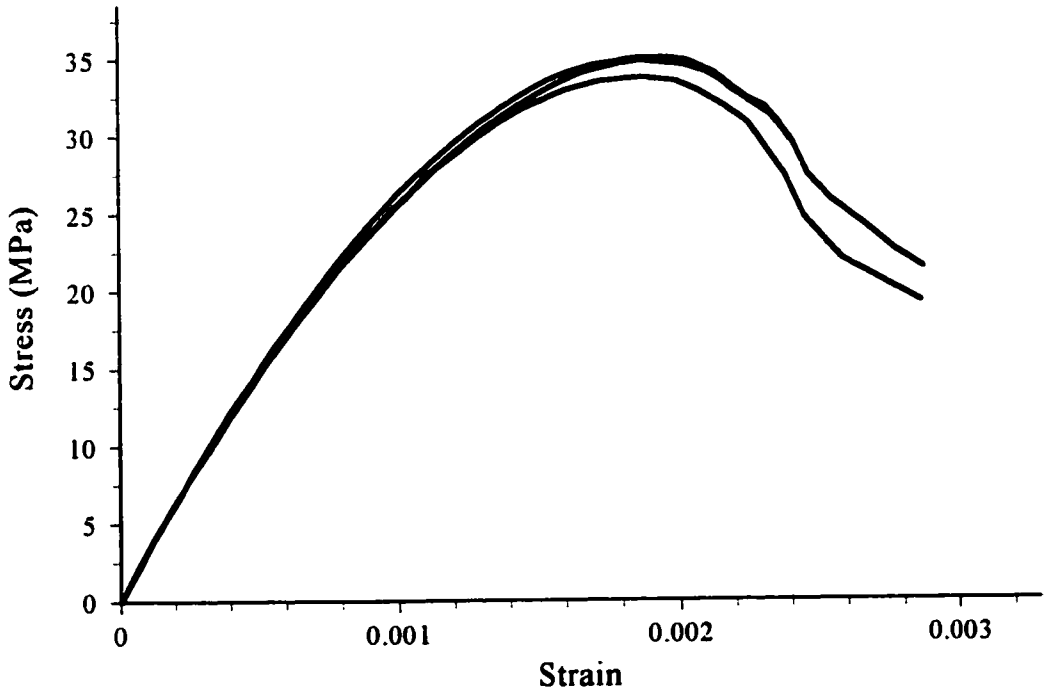

Fig. 2.8 Stress-strain relationship of concrete test cylinders

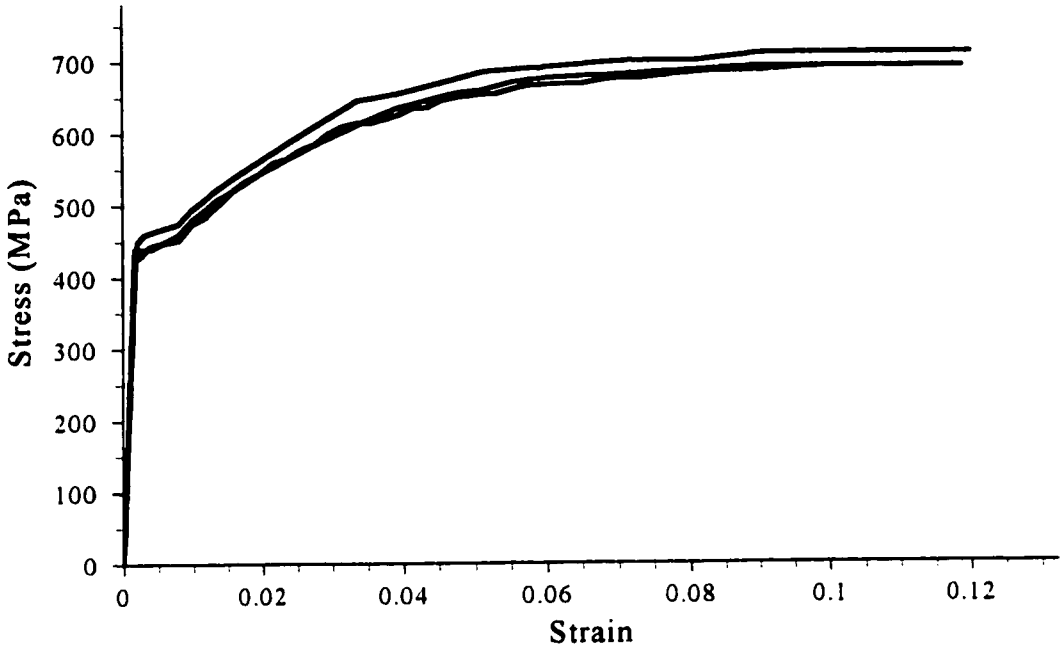

Fig. 2.9 Stress-strain relationship of grade 400, #10 reinforcing steel bar

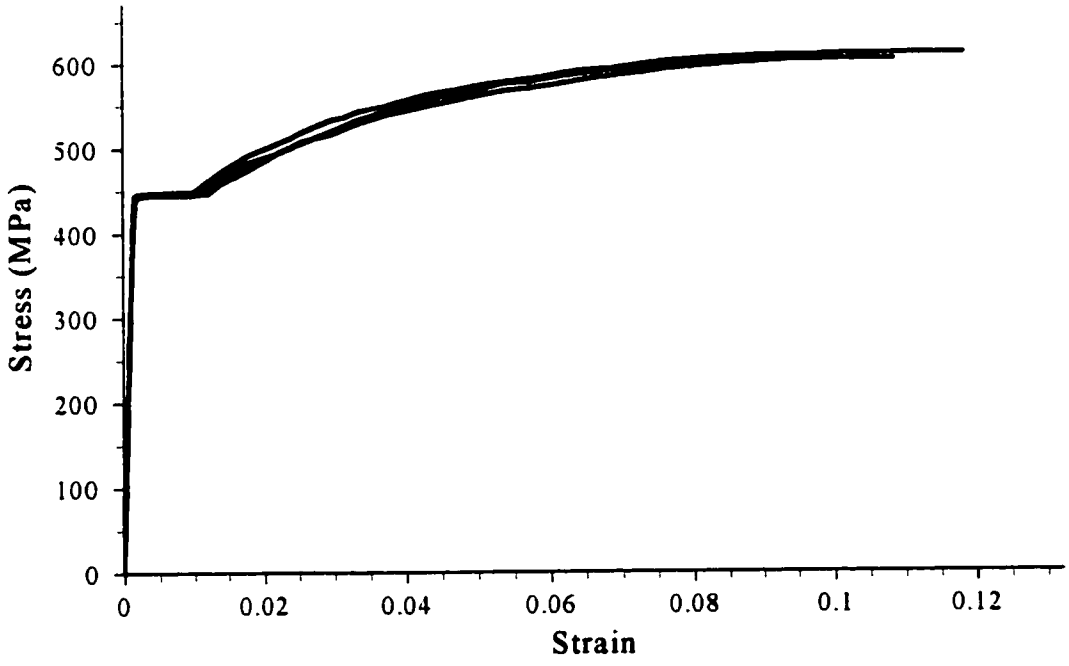

Fig. 2.10 Stress-strain relationship of grade 400, #20 reinforcing steel bar

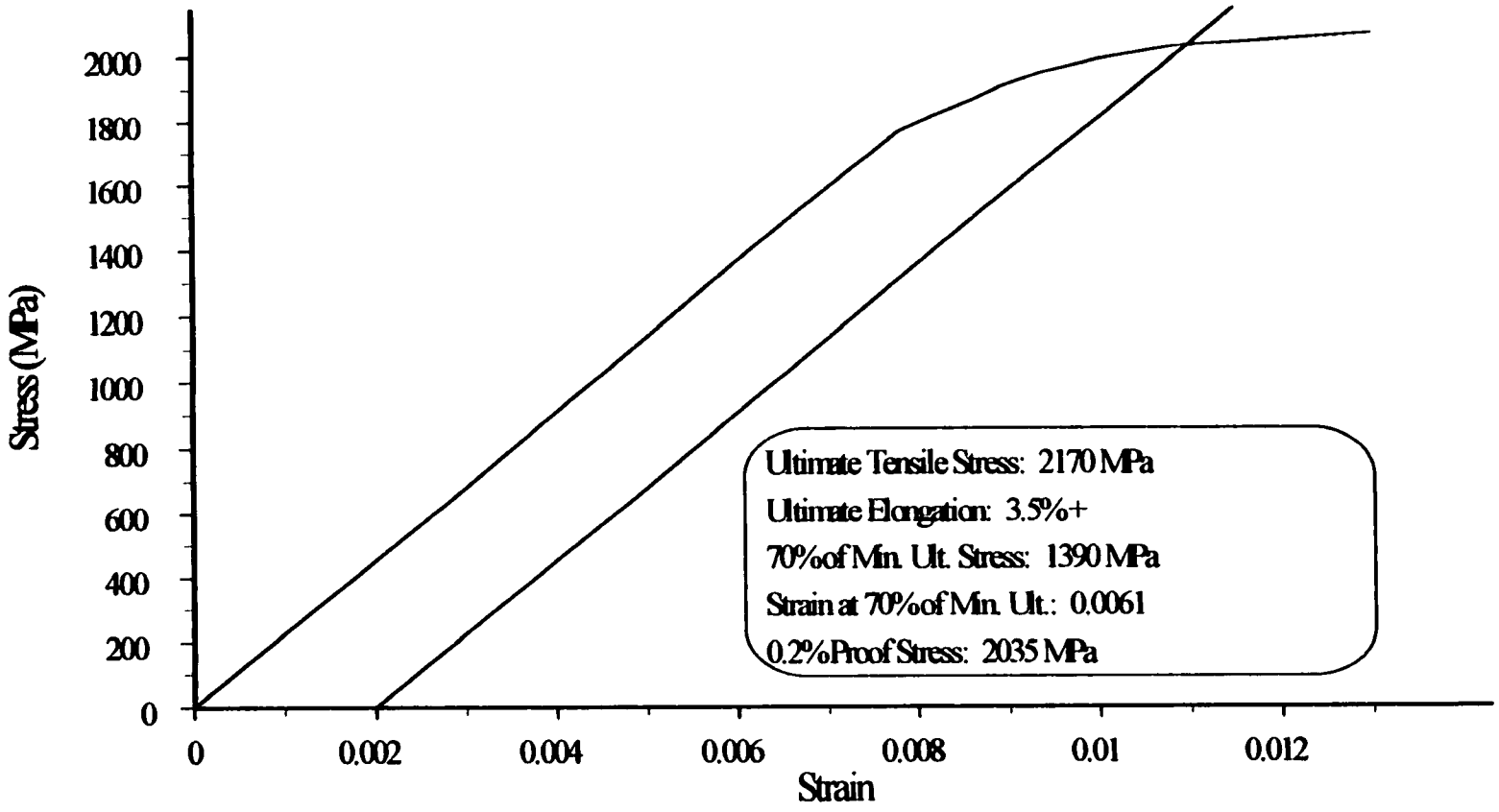

Fig. 2.11 Stress-strain relationship of size 9, grade 1860, seven-wire prestressing strands

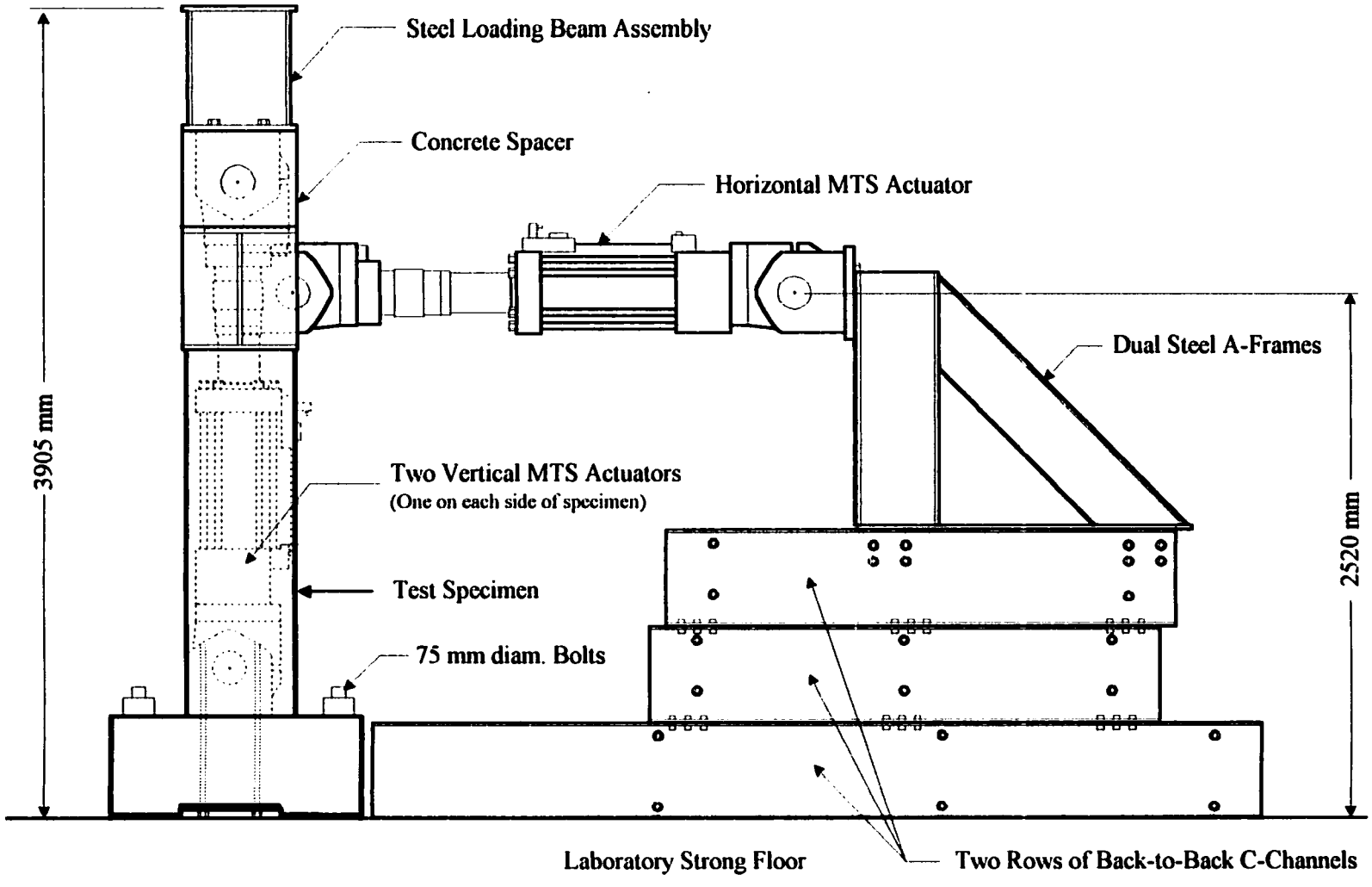

Fig. 2.12a Schematic drawing of test setup: Side view

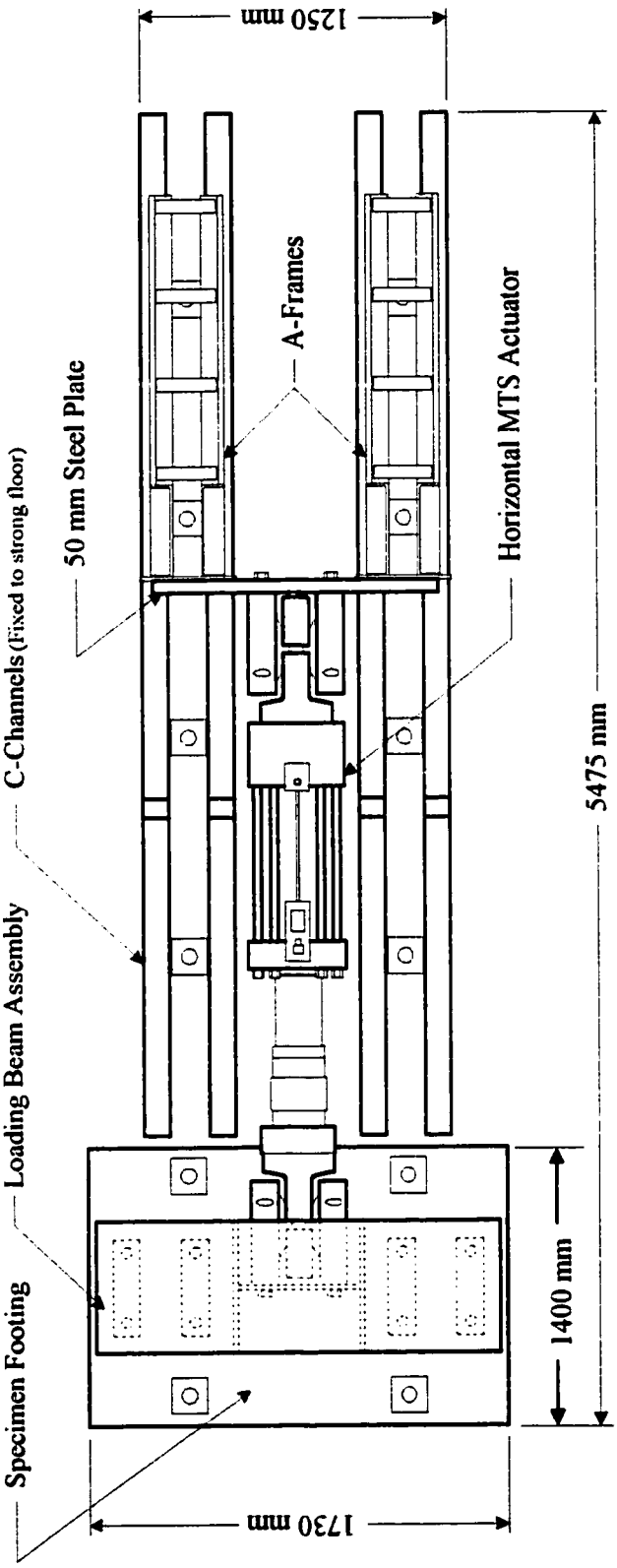

Fig. 2.12b Schematic drawing of the test setup: Plan view

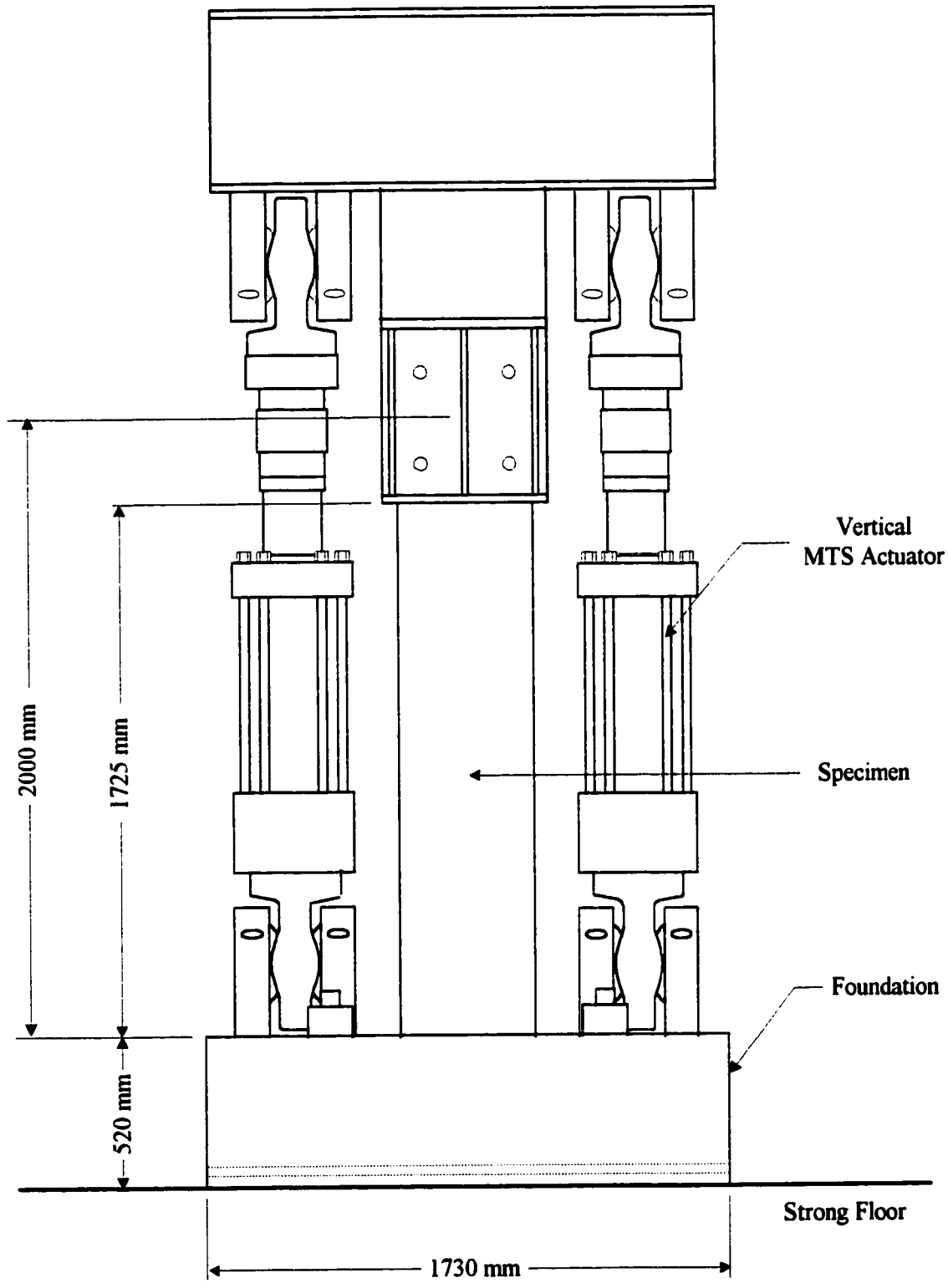

Fig. 2.12c Schematic drawings of the test setup: Front view

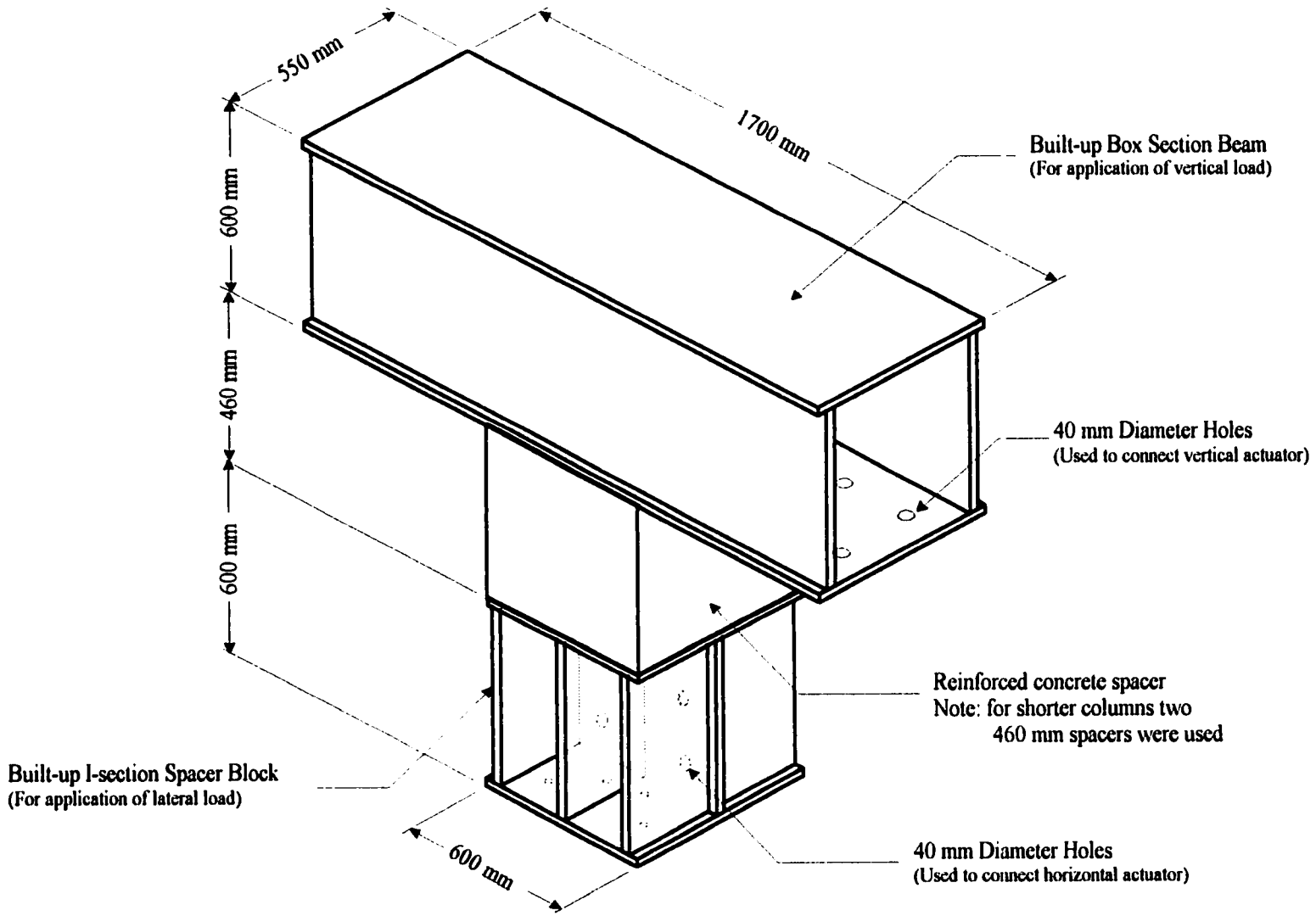

Fig. 2.12d Schematic drawing of the test setup: Details of loading beam assembly

Gauges	Location
1,2	third stirrup layer, 725 mm above footing
3,4	second stirrup layer, 425 mm above footing
5,6	first stirrup layer, 125 mm above footing
7,8	longitudinal bar, 125 mm above footing
9,10	longitudinal bar, at column/footing interface
11,12	longitudinal bar, 125 mm into footing

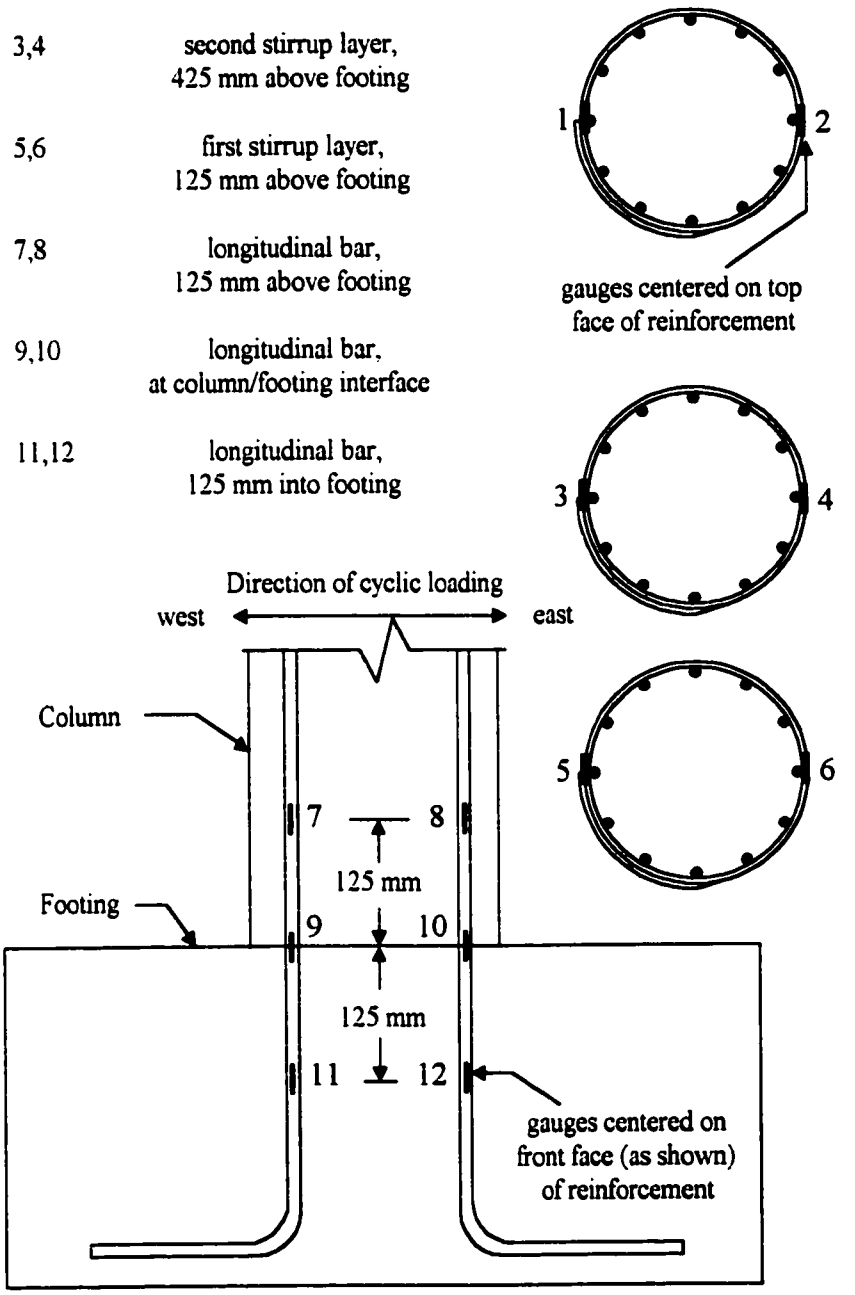

Fig. 2.13 Strain gauge location on reinforcing steel for columns BR-C6 and BR-C7

Gauges	Location
1,2	third stirrup layer, 750 mm above footing
3,4,5,6	second stirrup layer, 450 mm above footing
7,8	first stirrup layer, 150 mm above footing
9,10	longitudinal bar, 125 mm above footing
11,12	longitudinal bar, at column/footing interface
13,14	longitudinal bar, 125 mm into footing

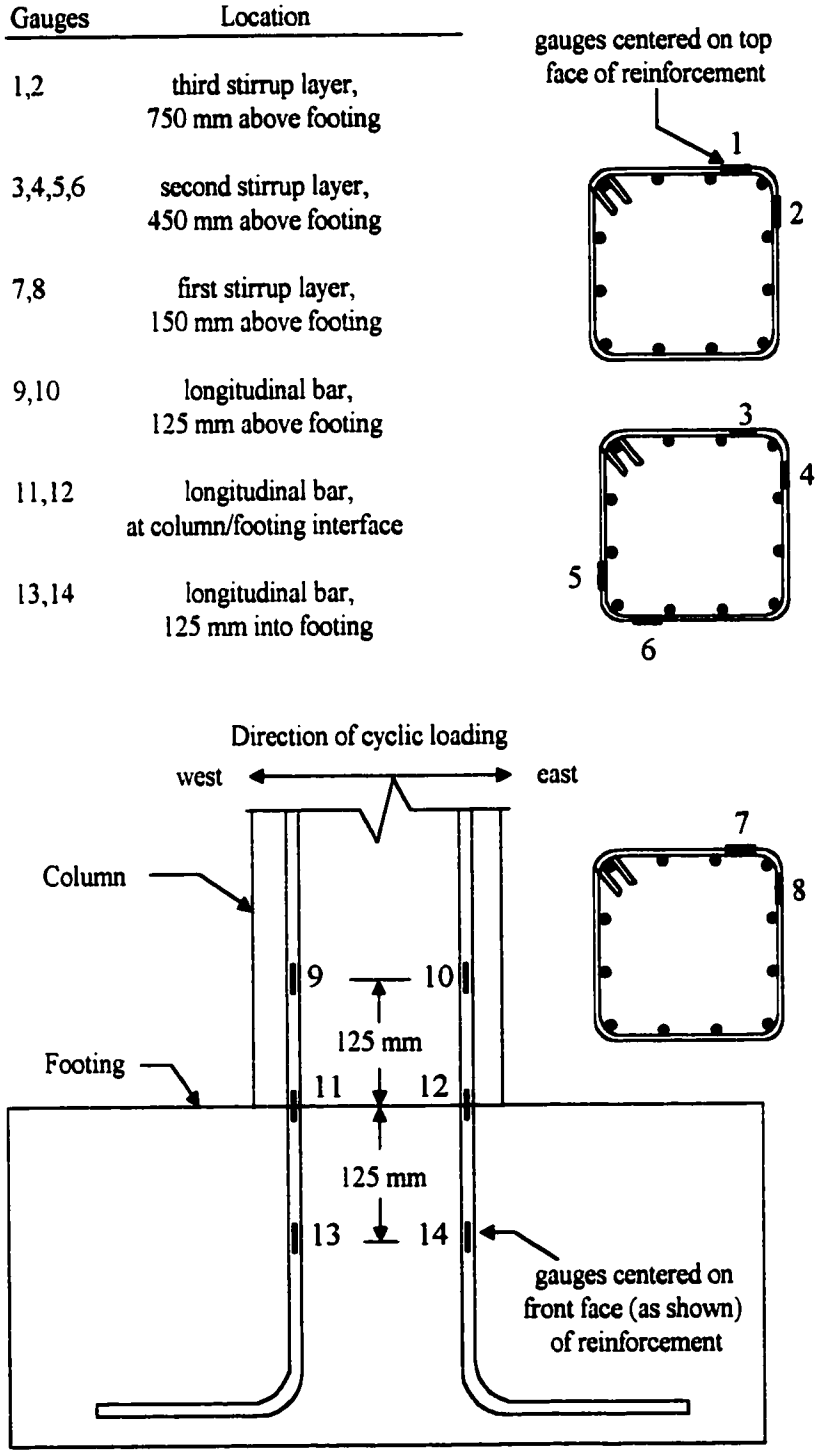

Fig. 2.14 Strain gauge location on reinforcing steel for columns BR-S3 and BR-S4

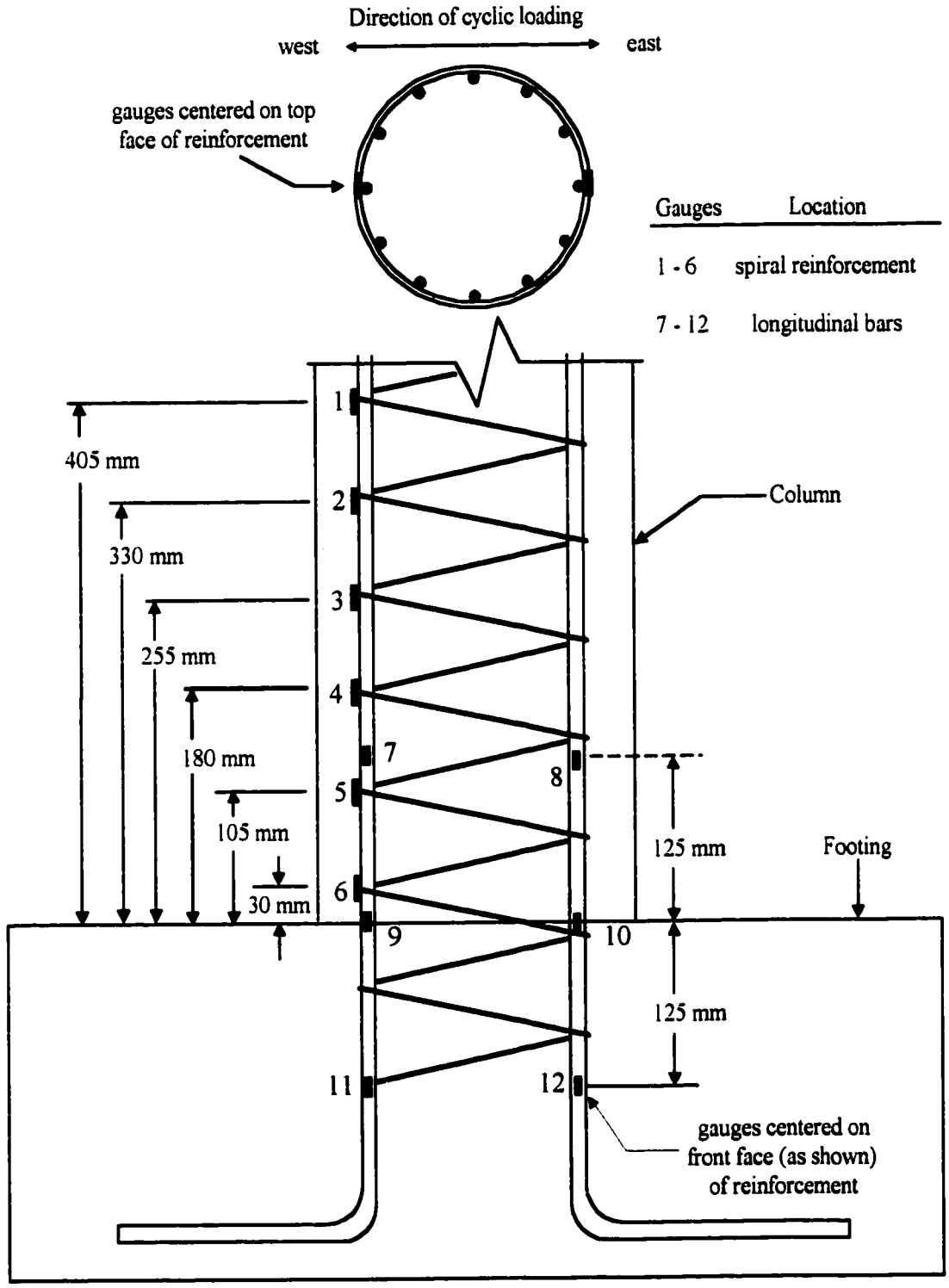

Fig. 2.15 Strain gauge location on reinforcing steel for columns BR-SP1 and BR-SP2

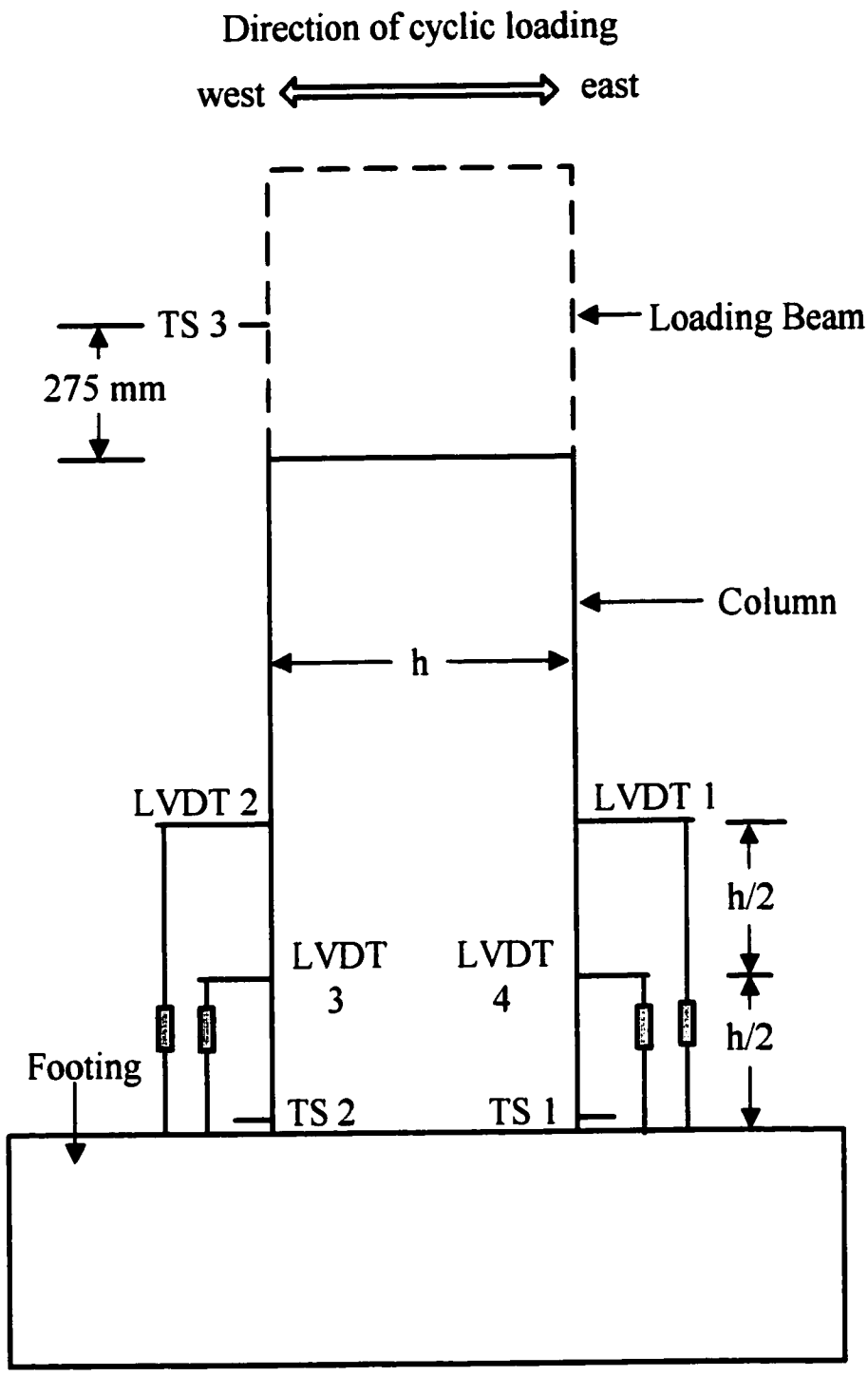

Note: TS = Temposonic LVDT

Fig. 2.16 Column instrumentation

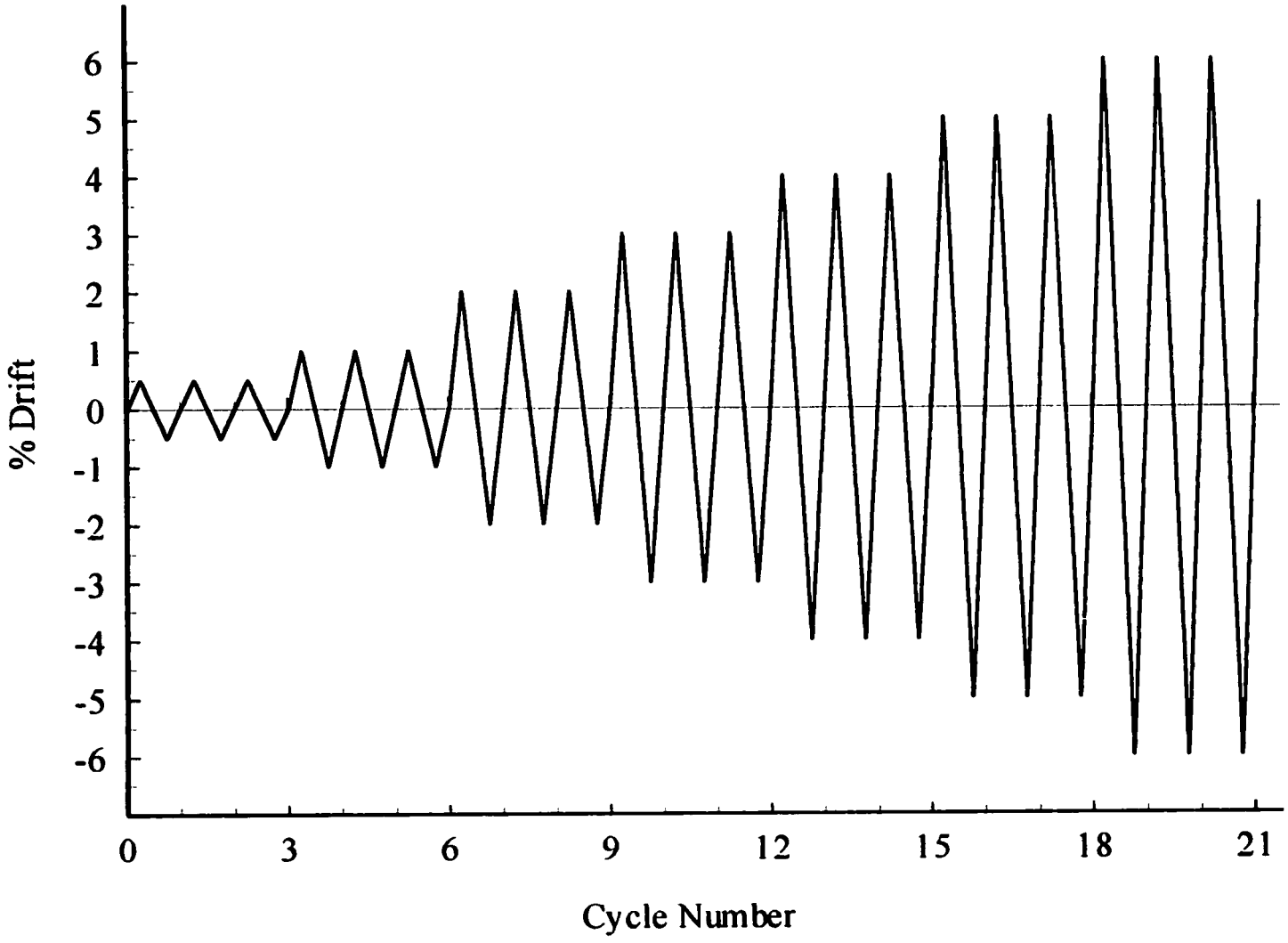

Fig. 2.17 Loading Program

Chapter 3

Test Results

3.1 General

This chapter presents the results of the six column tests conducted as part of the experimental phase of this research program. First, the data recorded for each column is presented individually with observations made during testing. Then, companion columns are compared to examine the effectiveness of retrofitting for columns with different transverse reinforcement and aspect ratios.

The data collected from the strain gauges do not always continue till the end of the test due to the rupture of the wires or damage of strain gauges. The data is presented until the gauges ceased to record data. Similarly, for some of the other data collected using LVDTs, it is indicated in data analysis the test stage beyond which the data was discontinued.

Note that circular columns with tied reinforcement (hoops) are referred to as "tied circular columns" and the circular columns with spiral reinforcement are referred to as "spiral circular columns".

3.2 Tied Circular Columns - Test Results and Analysis

3.2.1 Non-Retrofitted Column (BR-C6) - Test Observations

The progression of damage observed during testing is illustrated in Fig. 3.1, at different stages of loading. Initial flexural cracks formed in the bottom half of the column during the cycles at 0.5% drift. No other signs of deterioration were noted at this load level. The lateral load resistance during the first cycle at 0.5% drift reached 172 kN. The load resistance increased to 228 kN during the initial cycle at 1% drift. The cycles at 1% drift

caused yielding of longitudinal bars and lengthening of the flexural cracks.

By the end of the cycles at 2% drift, there were signs of shear cracking on side faces, as well as crushing and spalling of concrete under flexural compression at the base of the column. The flexural cracks started to widen and the strain gauges recorded values reaching up to half the yield strength in hoops. The lateral load resistance reached its peak value of 246 kN during the initial cycle at 2% drift, and did not drop below 95% of this value during the subsequent cycles at 2% drift. The lateral load resistance dropped to 206 kN (85% of peak lateral load) during the initial cycle at 3% drift. It continued to drop to 176 kN and below 100 kN in the second and third cycles, respectively. A lateral load resistance of less than 80% of the peak capacity is considered by many researchers to represent column failure. Therefore, this column would be considered failed after having completed the first cycle at 3% drift. At the start of the cycles at 3% drift, the lowest level hoop yielded and the concrete cover started to spall more severely. By the second cycle, the concrete cover in the lower portion of the column was completely spalled off and buckling of the longitudinal bars was evident. The second hoop from the bottom of the column (425 mm above the footing) opened during the third cycle. This caused all the longitudinal bars to buckle out, and the column to collapse. The failure was quite sudden and explosive once the hoop opened up, which was a good indication that hoops with overlapping ends were unreliable once the concrete cover spalled off.

3.2.2 Non-Retrofitted Column (BR-C6) - Data Analysis

The test observations mentioned in the previous section were substantiated by the test data collected and plotted. Figure 3.2 depicts Force-Displacement and Moment-Displacement hysteretic relationships recorded for Column BR-C6, clearly showing the degradation of load resistance under cyclic loading. The column behaved quite well until the first cycle at 3% drift, after which, it deteriorated quite rapidly.

The rotation of the hinging region, as well as the rotation due to anchorage slip are shown in Fig. 3.3. Anchorage slip consists of reinforcement slip and extension, however in the column tests performed the anchorage slip is due to reinforcement extension, as the

longitudinal reinforcement is continuous and well anchored in both the column and footing. Rotation measurements were taken at 508 mm and 254 mm (h and h/2 respectively) above the column base. The term h is defined as the cross-sectional dimension of the column - in this case the sectional diameter. These two graphs illustrate that much of the rotation occurred within the first 254 mm as the two graphs are quite similar in magnitude. The third graph, anchorage slip rotation, shows how much of the total rotation illustrated in the two previous graphs can be attributed to anchorage slip and not to flexure. The difference between total rotations measured and the rotation due to anchorage slip indicates column rotation caused by flexure.

The strains recorded in reinforcement are illustrated in Figs. 3.4 and 3.5. The positive strain indicates tension, with the yield point of the steel being about 0.2% strain or 2000 microstrain (strain x 10^{-6}). Many of the hoops exceeded the yield point. Yielding in longitudinal bars was generally reached during the cycles at 1% drift, with the yield plateau being developed under increasing lateral drift. The yield plateau is well illustrated by Gauges no. 11 and no. 12 in Fig. 3.5. The compression plateau occurred well before 0.2% strain, which was a good indication that the longitudinal bars were buckling.

3.2.3 Retrofitted Column (BR-C7) - Test Observations

The photographs taken during the test, illustrating various stages of column damage, are shown in Fig. 3.6. The retrofitted column behaved in much the same way as the non-retrofitted column during the 0.5%, 1% and 2% drift cycles. During the cycles at 0.5% drift, the lateral load resistance was 174 kN, and some flexural cracks formed. The lateral load resistance was increased to 230 kN and the flexural cracks lengthened at 1% drift. The peak load resistance was attained during the first cycle at 2% drift, at a magnitude of 256 kN. It did not drop below 95% of peak during the remainder of the cycles at 2% drift. There were signs of crushing at the base of the column with a little bit of spalling. A crack was noticeable at column footing interface, signifying anchorage slip.

The column showed stable behaviour during the cycles at 3% drift. The lateral load resistance barely dropped, reaching a level of 250 kN during the first cycle. The load

resistance was maintained at 237 kN (92% of peak) on the third cycle. The flexural cracks widened and there was more crushing and spalling of concrete cover at the base of the column, but was confined to the first 100 mm from the footing. The strength was maintained during the cycles at 4% drift. The initial lateral load resistance was 245 kN (96% of peak) and did not drop more than 5%, indicating a substantial increase in column ductility. The crushing of concrete cover continued to rise up the column, reaching the second prestressing hoop (275 mm above the footing). At this stage the hoop started to dig into the column concrete. A close up picture of this is shown in Fig. 3.6b.

Increased strength decay was observed during the cycles at 5% drift. The initial lateral load resistance of 210 kN (82% of peak) reduced to 170 kN (20% drop) by the third cycle. The column can be considered to have failed after the first cycle at 5% drift, which is a substantial improvement over the non-retrofitted column, which failed after the first cycle at 3% drift. The test was continued for a full cycle at 6% drift, during which a lateral load resistance of 135 kN (52% of peak) was developed. The load resistance dropped during the second cycle to 97 kN (38% of peak), at which point the test was stopped.

3.2.4 Retrofitted Column (BR-C7) - Data Analysis

The data for column BR-C7 is illustrated in the same manner as column BR-C6. The data is plotted using the same scale for both columns to facilitate a direct comparison of corresponding graphs. Figure 3.7 illustrates Force-Displacement and Moment-Displacement hysteretic relationships for column BR-C7. The column behaviour was much improved compared to its companion column, as it maintained its moment capacity until after the first cycle at 5% drift, after which point it began to deteriorate below 80% of peak capacity.

Column rotation and slip rotation measurements are plotted in Fig. 3.8. The total rotation within the hinging region were measured at 508 mm and 254 mm (h and h/2 respectively) above the column base. These two graphs illustrate that much of the rotation occurred within the first 254 mm, as the two graphs are quite similar in magnitude. The third graph, illustrating anchorage slip rotation, excludes any rotation due to flexure. The difference in values between the total rotation and anchorage slip rotation give the rotation

caused by flexure. It should be reported that the slip rotation data for this column appears to be questionable, as it shows asymmetric behaviour. This may be attributed to instrumentation problems that may have arose at later stages of loading when the concrete cover was significantly damaged.

The strains in column reinforcement are shown in Figs. 3.9 and 3.10. Many gauges were damaged during testing. Hence, limited results are available for this column. The strains in the prestressing strands were also measured and the results are shown for each individual strand in Fig. 3.11. These graphs show that the strands near the base of the column were the ones being strained the most - up to 3000 microstrain above the initial prestress strain of 2000 microstrain. This total of 5000 microstrain is below 50% of the initial yield point for the strands. It should also be noted that for the two lower level strands, the strain dropped below the initial 2000 microstrain, which demonstrates the importance of applying the initial prestress. If it was not applied, there could be a problem with strands slipping down the column. Although in this case, the release in stress was perhaps due to the strands digging into the column concrete, as illustrated in Fig. 3.6b. This figure displays the strand located 275 mm above the base. Figure 3.12 shows the maximum strain profiles of strands at selected drift levels.

3.2.5 Tied Circular Columns - Comparison

The improvements achieved due to retrofitting can clearly be seen when comparing the Moment-Displacement hysteretic relationships of the two columns (Fig. 3.2 and Fig. 3.7). The retrofitted column withstood 5% drift before exhibiting significant strength degradation, whereas its companion column lost its strength very quickly after the first cycle of 3% drift, collapsing during the third cycle at 3% drift. The retrofitted column had gradual failure. It lost its lateral capacity slowly, when being cycled at 5% and 6% drift. The comparison of strength degradation is displayed in Fig. 3.13, which shows the Moment-Drift envelope for both columns.

The moment capacity is not significantly altered by retrofitting. The longitudinal reinforcement strains indicate little or no difference between the two columns. The transverse

steel does however show some differences, as seen by strain gauges no.3 and no.4 (Fig. 3.4 and Fig. 3.9). These gauges were connected to the hoop located 425 mm above the footing. In column BR-C6 the hoop strain increased beyond 2000 microstrain (steel yield point), whereas in column BR-C7 the strain in the hoop was limited to 1000 microstrain (50% of yield). This can be attributed to the fact that there was also a prestressed strand at this location (425 mm above the footing) which helped resist diagonal tension and lateral expansion of concrete.

3.3 Square Columns - Test Results and Analysis

3.3.1 Non-Retrofitted Column (BR-S3) - Test Observations

The observed behaviour of Column BR-S3 is illustrated in Fig. 3.14. The figure contains photographs taken during the test, showing the degree of damage at various stages of loading. During the cycles at 0.5% drift, flexural cracks formed in the bottom half of the column. No other signs of deterioration were noted at this stage of loading. The lateral load resistance reached 234 kN during the first cycle at 0.5% drift. The load resistance increased to 295 kN during the initial cycle at 1% drift. It was observed that the longitudinal bars started to yield at this load stage, while the flexural cracks became longer and wider. Formation of shear cracks was also observed during the cycles at 1% drift.

The flexural cracks started to widen during the cycles at 2% drift. The concrete also started to crush near the base. There were visible signs of anchorage slip, as indicated by widening of the crack at the column-footing interface. The lateral load resistance reached its peak of 308 kN during the initial cycle at 2% drift. It subsequently dropped by approximately 5% during the remaining two cycles. The load resistance decreased to 290 kN (94% of peak) during the first cycle at 3% drift. It further dropped to 246 kN (80% of peak) by the end of the third cycle. The column continued to deteriorate during the cycles at 3% drift. The cracks widened and the concrete started to spall off, exposing the longitudinal bars. One of the corner longitudinal bars showed signs of buckling. The column was considered to have failed after the last cycle at 3% drift. The column was pushed to 4% drift with a lateral load resistance of only 130 kN (42% of peak) as all the bars on the compression side buckled

between the first and second stirrups. Upon reversing the load, the core concrete crushed, causing the column to collapse.

3.3.2 Non-Retrofitted Column (BR-S3) - Data Analysis

Experimentally recorded Force-Displacement and Moment-Displacement hysteretic relationships are shown in Fig. 3.15 for Column BR-S3. The column faired well until the last cycle at 3% drift, after which it deteriorated suddenly when an attempt was made to push the column to 4% drift. This is clearly shown in both graphs, as a sudden drop in lateral force or moment resistance, when the column was pushed just beyond the 3% drift mark.

The recorded column rotations within the assumed hinging region are illustrated in Fig. 3.16. The figure also includes anchorage slip rotations. Column rotations were measured within the bottom 500 mm and 250 mm (h and h/2 respectively) segments above the base. These rotations included those caused by anchorage slip. The data indicate that much of the rotation was caused by flexure within the first 250 mm segment. The anchorage slip rotation values appear to be questionable, as they show asymmetry. This may be attributed to potential problems with instrumentation at later stages of loading, when the concrete at the base of the column was significantly damaged.

The strains in reinforcement are shown in Figs. 3.17 and 3.18. The strains in lateral reinforcement do not exceed the yield point, except at the very end of the test - during column failure. The large strain readings recorded by gauge no. 5 (Fig. 3.17) may be attributed to a failure in the gauge. However, those recorded by gauges no.7 and 8, which were located on the hoop 150 mm above the footing, appear to have reached the yield point right before collapse. Yielding of longitudinal reinforcement was generally reached during the cycles at 1% drift. The yield plateau in both tension and compression is well illustrated in the case of strain gauge no. 13 (Fig. 3.18). The compression plateau occurred well before 0.2% strain was developed, which was a good indication that the longitudinal bars suffered buckling.

3.3.3 Retrofitted Column (BR-S4) - Test Observations

Figure 3.19 depicts the observed damage in Column BR-S4 at various stages of

loading. Initially, only one or two small flexural cracks appeared on either side of the column during the cycles at 0.5% drift. No other damage was observed at this load stage. The magnitudes of lateral load in opposite directions showed variations. In the west direction, the load was only about 80% of that in the east direction. The lateral loads referred to in this section are the average of the two. The lateral load resistance in the first cycle at 0.5% drift was 225 kN. It increased to 290 kN during the initial cycle at 1% drift. Cycles at 1% drift caused yielding of longitudinal reinforcement and increased flexural cracking.

During the cycles at 2% drift, the flexural cracks started to widen; shear cracks started to appear on the side faces of column; and the concrete started to crush near the base. There was also a visible crack at column-footing interface, as depicted in Fig. 3.19b, which was a good indication that there was some anchorage slip between the column reinforcement and footing. The lateral load resistance reached 318 kN at this stage. However, unlike the non-retrofitted column (BR-S3), this was not the peak. The peak resistance of 321 kN was reached during the first cycle at 3% drift. The resistance did not drop any more than 5% during the subsequent cycles at 3% drift. A few more flexural cracks appeared, the shear cracks lengthened and there was some concrete spalling in the lower 150 mm of the column.

The load resistance dropped to 318 kN during the first cycle at 4% drift. By the third cycle, the resistance was maintained at 306 kN (95% of peak). The damage observed did not change during the current load cycles, with the exception of widening of cracks and additional spalling of concrete near the base. The load resistance remained at 306 kN during the initial cycle at 5% drift. It dropped to 275 kN (85% of peak) by the third cycle. The column continued to deteriorate during these cycles. The crack widths increased and the concrete continued to spall off in the lower 150 mm segment of column.

The lateral load resistance dropped to 236 kN (73% of peak) during the first cycle at 6% drift, as one of the longitudinal bars ruptured. Therefore, this column failed during the first cycle of this deformation level. The strength degradation was observed to be rapid after this point. The load resistance dropped to about 50% of the peak by the third cycle at 6% drift, as other longitudinal bars also ruptured (see Fig. 3.19d). At this stage, the column resistance was terminated by longitudinal bar rupturing, beyond which the retrofitting

technique employed could not provide any further improvements in ductility. The column was then pushed to 7% drift for one cycle, with a limited lateral load resistance of 136 kN (42% of peak).

3.3.4 Retrofitted Column (BR-S4) - Data Analysis

The data for column BR-S4 is illustrated in the same manner as column BR-S3. The data is plotted using the same scale for both columns to facilitate a direct comparison. For BR-S4, the hysteretic behaviour is illustrated in Fig. 3.20 in terms of Force-Displacement and Moment-Displacement relationships. The column behaviour is much improved, compared to the companion column, as it maintained its moment capacity until the first cycle at 6% drift, at which point it deteriorated below 80% of peak capacity.

Column rotations recorded during the test are shown in Fig. 3.21. The rotation measurements were taken at 500 mm and 250 mm (h and h/2 respectively) above the column base, relative to the column footing. Rotations caused by anchorage slip were also measured as close to the base as possible. The graphs shown in Fig. 3.21 illustrate that much of the rotation occurred due to flexure within the first 250 mm segment from the base. The third graph, given in Fig. 3.21, shows anchorage slip rotations. These rotations are significantly lower than those caused by flexure.

Steel strain readings, recorded on column reinforcement, are shown in Figs. 3.22 and 3.23. The strains in lateral reinforcement (Fig. 3.22) never exceed the yield point. They were lower than those recorded in column BR-S3. Yielding of longitudinal reinforcement was recorded during the cycles at 1% drift. The yield plateau can be seen clearly in the strains recorded by gauge no. 13 (Fig. 3.23). The compression plateau occurred well before 0.2% strain, which was an indication of buckling of longitudinal bars.

Strains were also measured in the prestressing strands used for retrofitting. The variation of strains throughout the test is shown for each strand in Fig. 3.24. From this data it can be concluded that the prestressing strands used for retrofitting developed highest strains near the base. At this location the increase in strain due to the lateral expansion of concrete was approximately equal to 3000 microstrain above the initial prestress strain of 2000

microstrain. This total of 5000 microstrain remained below 50% of the initial yield. It should be noted that the strand strains dropped only slightly below the initial 2000 microstrain. This can be compared to column BR-C7, where a possible cause of this drop below 2000 microstrain was attributed to the strands digging into the concrete. In the case of BR-S4, the strands were not in contact with concrete. Instead, hoop tension was distributed over the area of the hollow steel sections, which formed part of the retrofitting scheme. The strands did however drop a little bit below 2000 microstrain, indicating that the initial prestress remains to be an important requirement for retrofitting. Figure 3.25 also shows the variation of strains in prestressing strands, but this time displaying maximum strain profiles over the height for selected drift levels.

3.3.5 Square Columns - Comparison

The comparisons of Moment-Displacement hysteretic relationships for columns with and without retrofitting, shown in Figs. 3.15 and Fig. 3.20, clearly demonstrate the improvements attained in column deformability. The retrofitted column withstood three cycles at 5% drift before exhibiting significant strength degradation when pushed to 6% drift. The companion column withstood the cycles at 3% drift, but lost its strength rapidly beyond this level of deformation and collapsed during the first attempt towards 4% drift. The retrofitted column showed gradual failure as it slowly lost its lateral load resistance while being cycled at 6% drift. The column maintained some capacity even after the rupturing of some of the longitudinal bars at 7% drift. The rate of strength decay can be seen in Fig. 3.26, which shows Moment-Drift envelopes for both columns.

The retrofitted column reacted to initial loading in much the same manner as the control column prior to the strength decay. The moment capacity was not significantly altered by retrofitting. Strain gauge no. 13 placed on one of the longitudinal bars showed similar readings in both columns, providing further evidence that the moment resistance remained essentially unchanged due to retrofitting. These bars both reached the steel yield point during the cycles at 1% drift and showed a yield plateau when pushed to 2% drift. As observed in the tied circular columns, the strain in transverse steel reduced in the retrofitted

column, since the retrofitting helped to counter the lateral expansion of concrete.

3.4 Spiral Circular Columns - Test Results and Analysis

3.4.1 Non-Retrofitted Column (BR-SP1) - Test Observations

The observed damage in column BR-SP1 is illustrated in Fig. 3.27. The figure includes photographs taken at selected stages of loading. During the initial cycle at 0.5% drift, a few small flexural cracks appeared and widened as the column was cycled more. There was also a crack visible at column-footing interface. Some narrow shear cracks were noticed near the top of the column. The strain level in the longitudinal bars indicated that the steel had approximately reached 50% of yield strength. The magnitude of lateral load in each direction showed some differences. When the column was pushed in the west direction the lateral loads were only about 77% of the load required to pull the specimen towards the east. This difference in lateral load diminished as the test progressed. The lateral loads reported in this section are the average of the two force values recorded. The lateral load resistance reached 354 kN during the first cycle at 0.5% drift. It increased to 435 kN during the initial cycle at 1% drift. The cycles at 1% drift caused yielding of longitudinal bars and increased flexural and shear cracking.

The flexural and shear cracks continued to widen and the concrete cover started to break up and crush near the base, when the column was deformed to 2% lateral drift. The lateral load resistance reached its peak value of 462 kN during this stage of loading. The lateral load started at 453 kN during the initial load cycle at 3% drift, and dropped to 423 kN (92% of peak lateral load) during the subsequent cycles at 3% drift. There was a bit of spalling in the lower portion of the column. The load resistance was 441 kN (95% of peak) during the first cycle at 4% drift. The column maintained a lateral load resistance of 420 kN (91% of peak) during the third cycle. There was no further damage, other than a continuation of the widening of cracks and additional spalling of concrete in the bottom 350 mm segment.

Cycles at 5% drift started with a lateral load resistance of 429 kN, which subsequently dropped to 412 (89% of peak) by the third cycle. The column continued to deteriorate during the cycles at this deformation level, exhibiting widened cracks and increased spalling of cover

concrete in the lower portion of column. The load resistance was maintained at 412 kN during the first cycle at 6% drift, but dropped to 362 kN during the third cycle, which is below 80 % of peak lateral load resistance. Hence, the column was considered to have failed at 6% drift.

When the column was pushed to its first cycle at 7% drift, a longitudinal bar ruptured before the column had even reached the 6% drift mark. The lateral load resistance dropped quickly during this first cycle to 290 kN (60% of peak) when the column reached 7% drift. The column was also pulled back to 7% drift in the opposite direction, and longitudinal bars ruptured on the other side of the column (see Fig. 3.27c). At this point the test was stopped. The column showed ductile behaviour, with the capacity dictated by longitudinal bar fracture. Retrofitting this column would have introduced very little or no improvement.

3.4.2 Non-Retrofitted Column (BR-SP1) - Data Analysis

The hysteretic behaviour of Column BR-SP1 is illustrated in Fig. 3.28 in terms of Force-Displacement and Moment-Displacement relationships. The column behaved very well until the end of the cycles at 6% drift, beyond which the longitudinal bars started to rupture.

Column rotations, including those due to anchorage slip, are shown in Fig. 3.29. The rotation measurements were taken at 610 mm and 305 mm (h and h/2 respectively) above the column base, relative to column footing. The graphs in Fig. 3.29 illustrate that much of the rotation was caused by flexure within the first 305 mm segment. It should be noted that the data plotted for the first two graphs in Fig. 3.29 include points recorded up to the first push at 6% drift and midway through 6% drift cycling, respectively. The data after these points was affected by the limits of instruments or a disruption in the instrumentation setup. The third graph, showing anchorage slip, indicates how much of the total rotation measured and plotted in the two previous graphs is attributed to anchorage slip. The difference between total rotations recorded and those caused by anchorage slip gives rotations caused by flexure.

The strain gauge data recorded on column reinforcement are plotted in Figs. 3.30 and 3.31. The positive strain indicates tension, with a yield point of about 2000 microstrain (strain x 10^{-6}). The longitudinal bars generally reached their yield point during the first cycle

at 1% drift. Yield plateau was developed under increasing drift level, as can be seen in the graph for gauge no. 11 (Fig. 3.31). As the drift level was increased, some yielding in the spiral reinforcement was observed. This is illustrated in the graph for gauge no.3 (Fig. 3.30), which was located 255 mm above the footing.

3.4.3 Retrofitted Column (BR-SP2) - Test Observations

Although retrofitting was not required due to the superior performance exhibited by companion column (BR-SP1), the second circular column with spiral reinforcement was retrofitted and tested. This was done because the second column had already been prepared, since the excellent behaviour shown by the companion column had not been anticipated, although somewhat improved behaviour was expected. To take advantage of this column specimen, it was retrofitted and tested to check the adequacy of a potential concrete jacket that may be needed for corrosion protection and aesthetics. Consequently, a 25 mm concrete cover was added on top of the retrofitting strands, - which in practice could be used to enhance the appearance and to cover and protect the steel from corrosion. A 25 mm cover was used due to the space limitations in the test setup. This thickness is conservative in terms of behaviour, as thicker concrete shells would be more stable under cyclic loading.

The photographs taken during the test are shown in Fig. 3.32. A few hair-line flexural cracks appeared during cycles at 0.5% drift, only on the west side of the column. The magnitudes of lateral loads in two opposite directions showed some variation during the cycles at 0.5% and 1% drift. When pushing the specimen in the west direction the lateral loads were only about 83% of those required to pull the specimen to the east. This difference disappeared once the cycles at 2% drift were imposed. The average of lateral loads resisted in two directions was 363 kN at 0.5% drift, and 455 kN at 1% drift. Yielding of longitudinal reinforcement was recorded at 1% drift. Flexural cracks appeared on both sides, and existing cracks widened. The flexural cracks continued to widen during cycles at 2% drift, with vertical cracks propagating from them. Cracks were noticeable on both sides at the base of the column. The lateral load reached 492 kN at 2% drift, which was the peak lateral resistance of column.

The lateral load resistance was maintained at 490 kN during the first cycle at 3% drift. It dropped to 468 kN (95% of peak lateral load) during subsequent cycles at 3% drift. There was widening of the flexural cracks and additional propagation into vertical cracks, resulting in different sized pieces of rectangles in the concrete shell. The first cycle at 4% drift showed a lateral load resistance of 477 kN (97% of peak). This resistance showed a slight drop during the subsequent two cycles, reducing to 455 kN (92% of peak). There was no additional damage observed in column shell, other than widening of the cracks, accompanied by the initiation of some spalling of concrete shell at the bottom. Cycles at 5% drift resulted in continued but slow degradation of strength. The column developed a lateral load resistance of 475 kN during the first cycle at 5% drift, followed by a drop to 450 kN (91% of peak) at the end of three cycles at 5% drift.

The column was subjected to the first cycle at 6% drift with 462 kN (94% of peak) load resistance. By the third cycle, although the load capacity had only dropped to 362 kN (85% of peak) one of the longitudinal bars ruptured, marking the flexural capacity of the column. Further loading reduced the lateral load resistance. The load dropped to 410 kN (83% of peak) when the column was pushed to 7% drift. Other longitudinal bars ruptured on either side of the column, as illustrated in Fig. 3.32b. After the first cycle at 7% drift the test was stopped. Although retrofitting was not needed in this column, it did improve the column performance by maintaining its lateral load resistance at high drift levels. But this slight benefit would hardly warrant retrofitting the column. This test did however show the successful use and applicability of a concrete shell over retrofitting strands, which may be required in practice.

3.4.4 Retrofitted Column (BR-SP2) - Data Analysis

The hysteretic behaviour of Column BR-SP2 is illustrated in Fig. 3.33 in terms of Force-Displacement and Moment-Displacement relationships. The column behaved very well until the end of 6% drift, beyond which the longitudinal bars started to rupture.

The rotation data are plotted in Fig. 3.34. Column rotation measurements were taken at 610 mm and 305 mm (h and h/2 respectively) above the column base. The anchorage slip

rotation was measured as close to the base of the column as possible, essentially measuring the crack width at column-footing interface, resulting from the extension of main column reinforcement in the footing. The graphs illustrate that much of the rotation was caused due to flexure within the first 305 mm segment near the base. It should be noted that the graph for "h" location only shows data up to 4% drift. The data after this points was affected by the limits of the instruments. The third graph, depicting slip rotation, shows data up to the end of 3% drift, as the data after this point was affected by the instrumentation setup, as the cord connected to the Temposonic LVDT was coming in contact with the lower corner of the shell.

The strains in reinforcement are plotted in Figs. 3.35 and 3.36. Many of the gauges were damaged in this column, limiting the available data. Strains were also measured in prestressing strands used for retrofitting. The strains throughout the test were recorded and are shown for each individual strand in Fig. 3.37. The data indicates that the strands near the base of the column strained the most, developing up to 1500 microstrain above and below the initial prestress strain of 2000 microstrain. Note that the strain in the three lower prestressing hoops dropped below the initial 2000 microstrain, which demonstrates the importance of applying this initial stress to the strands. The release in pressure may be caused by sinking of strands into the concrete, as in column BR-C7. Figure 3.38 shows maximum strain profiles for strands over the height of the column, for given drift levels.

3.4.5 Circular Columns with Spiral Reinforcement - Comparison

Although retrofitting was not needed for this column, it did improve column deformability. The comparison of the Moment-Displacement relationships for these two columns (Fig. 3.28 and Fig. 3.33) shows the slight improvement observed in column ductility. The strength degradation is also displayed in Fig. 3.39, which shows the Moment-Drift envelope for both columns. The other notable improvement, resulting from retrofitting, is the reduction in the strain in steel spiral (Fig. 3.30 and Fig. 3.35).

Fig. 3.1a Column BR-C6 at 1% drift (upper left), 2% drift (upper right) and 1st and 2nd cycles of 3% drift (lower left and right respectively)

Fig. 3.1b Column BR-C6 at the end of the third cycle at 3% drift (left) and at the end of test (right)

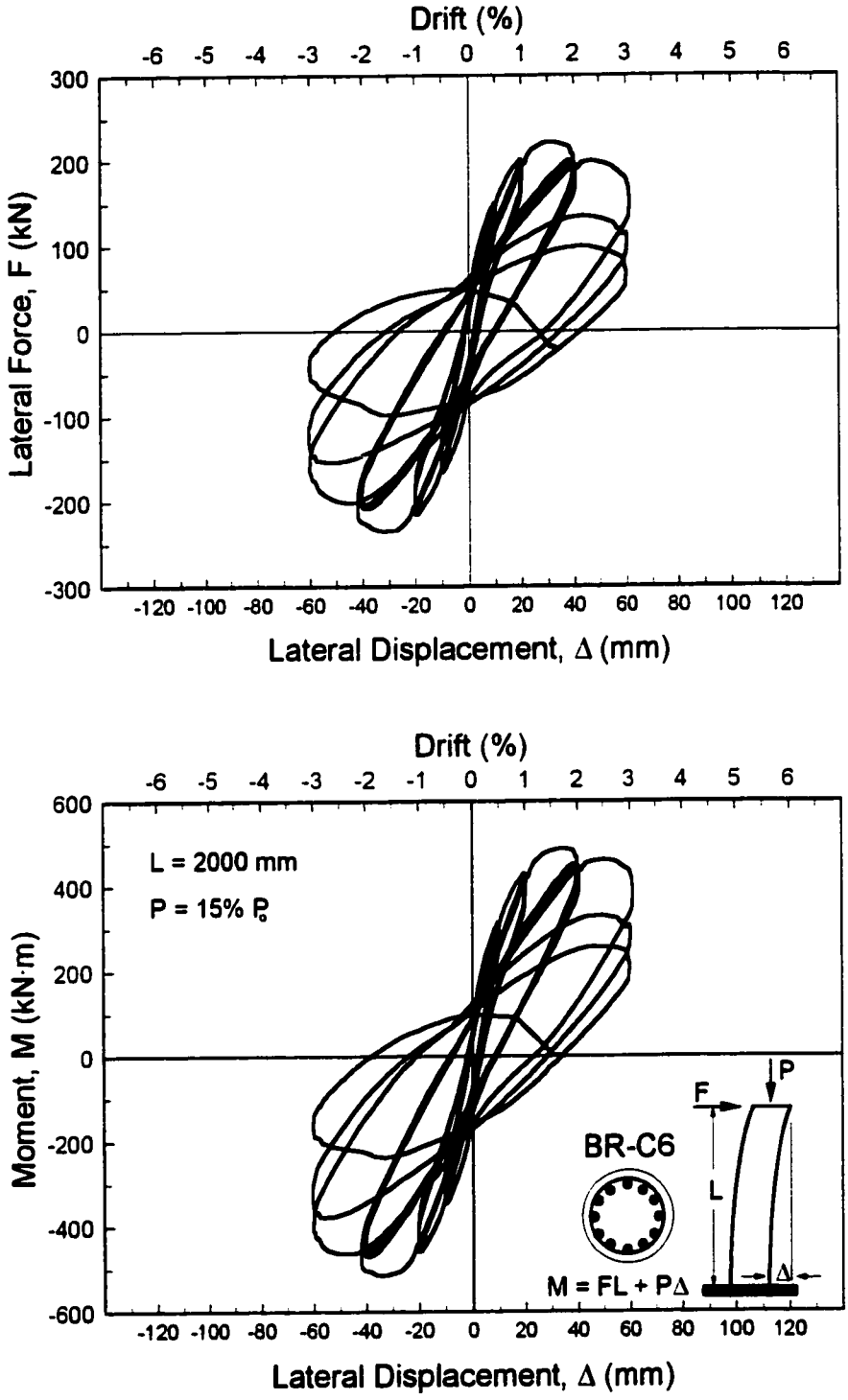

Fig. 3.2 Force and Moment-Displacement relationships for column BR-C6

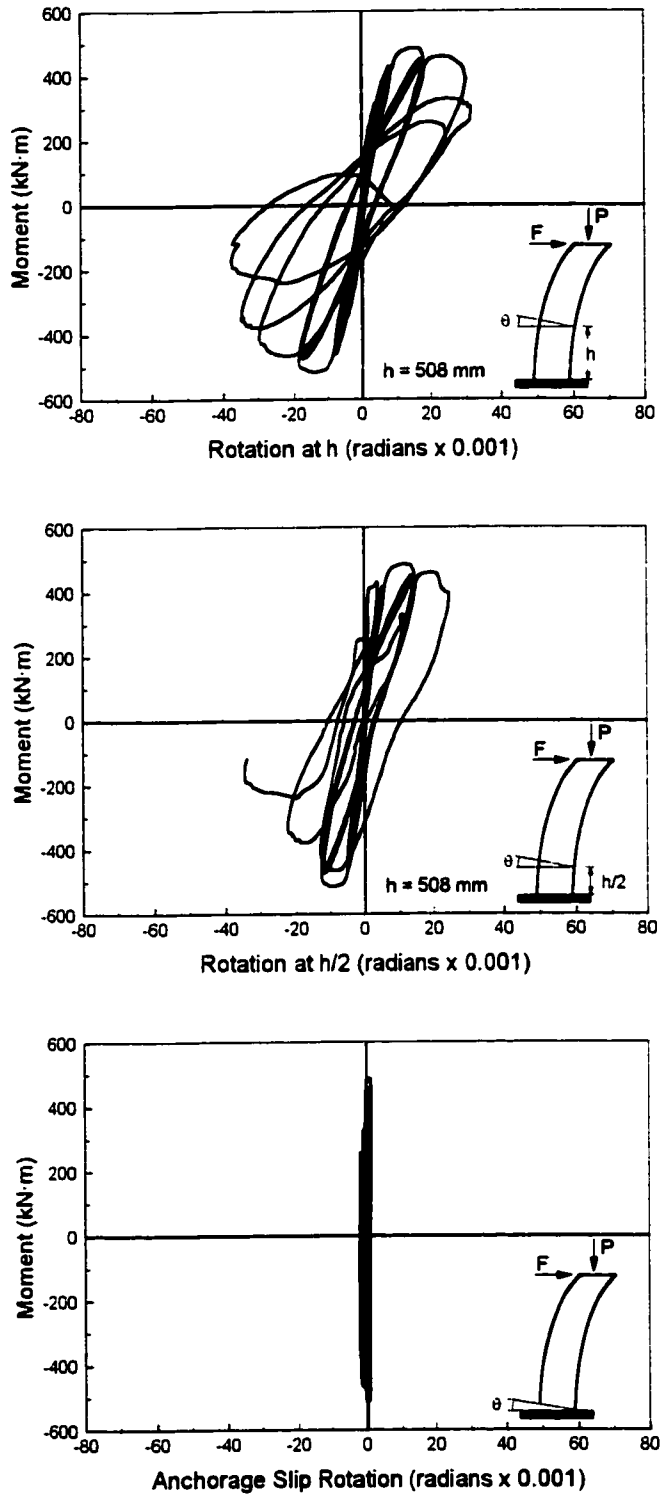

Fig. 3.3 Moment-Rotation relationships for column BR-C6

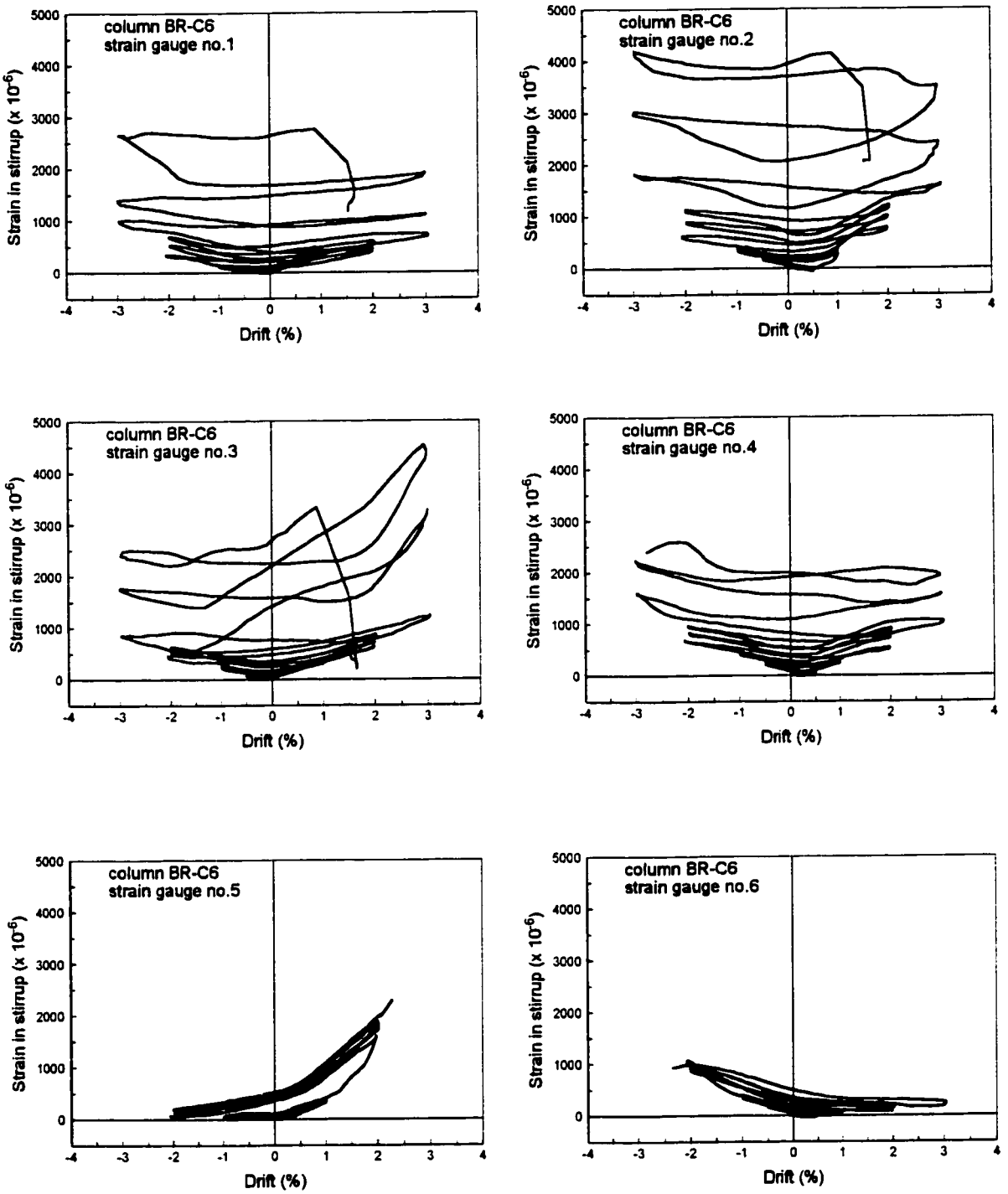

Fig. 3.4 Transverse reinforcement steel strains for column BR-C6
(for strain gauge locations refer to Fig. 2.13)

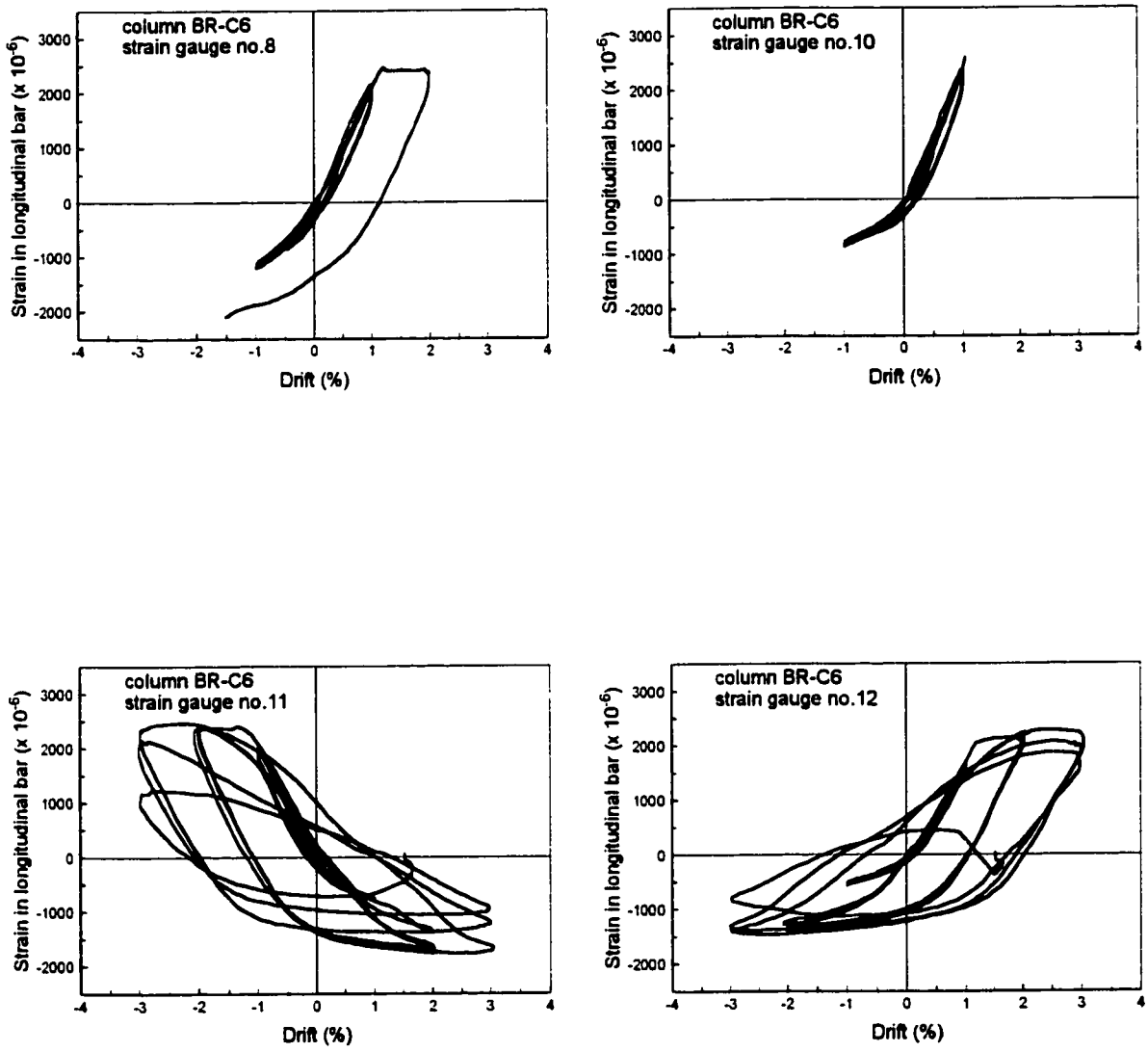

Fig. 3.5 Longitudinal reinforcement steel strains for column BR-C6 (for strain gauge locations refer to Fig. 2.13)

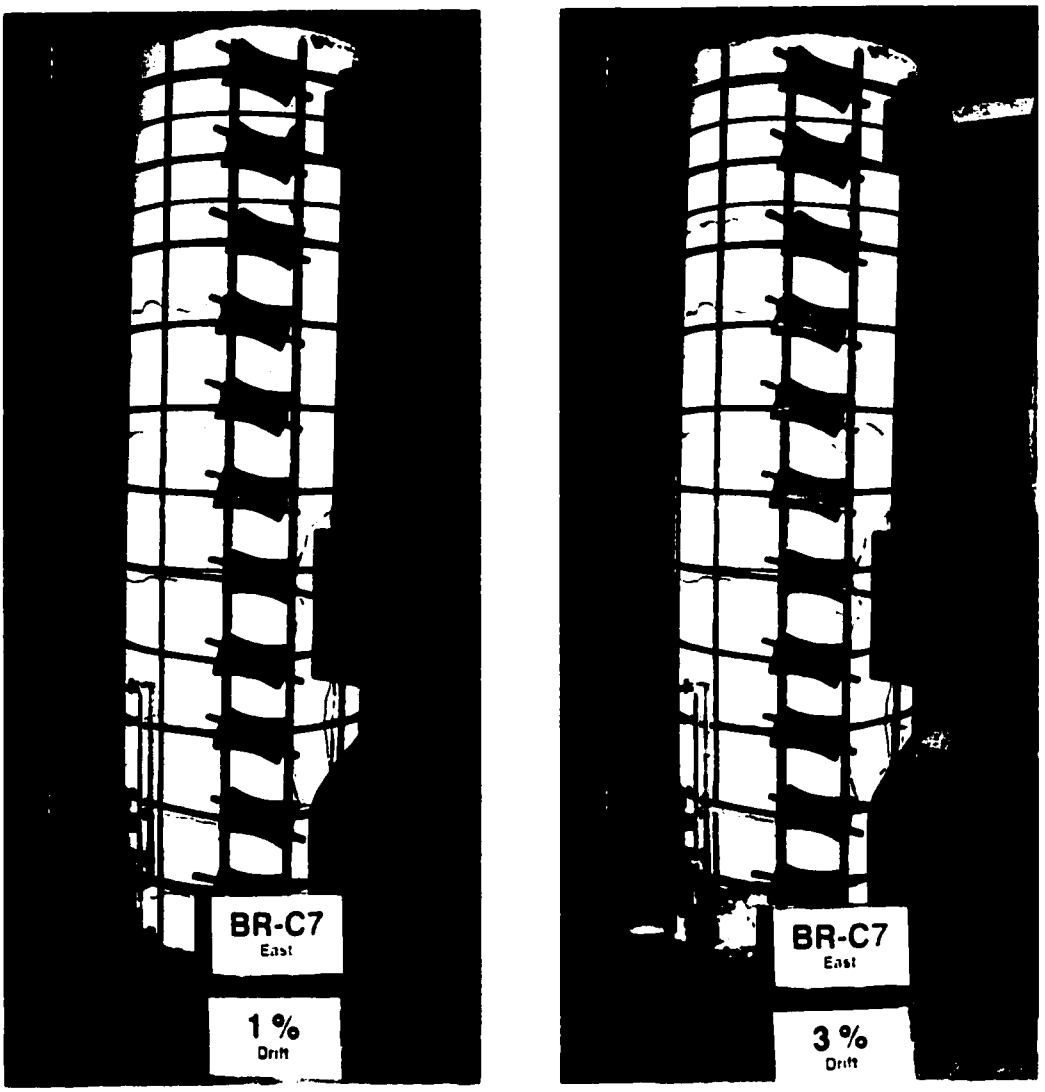

Fig. 3.6a Column BR-C7 at 1% drift (left) and 3% drift (right)

Fig. 3.6b Column BR-C7 at 4% drift: Prestressing strand digging into concrete cover

Fig. 3.6c Column BR-C7 at 5% drift (left) and 6% drift (upper right) and at the end of test (lower right)

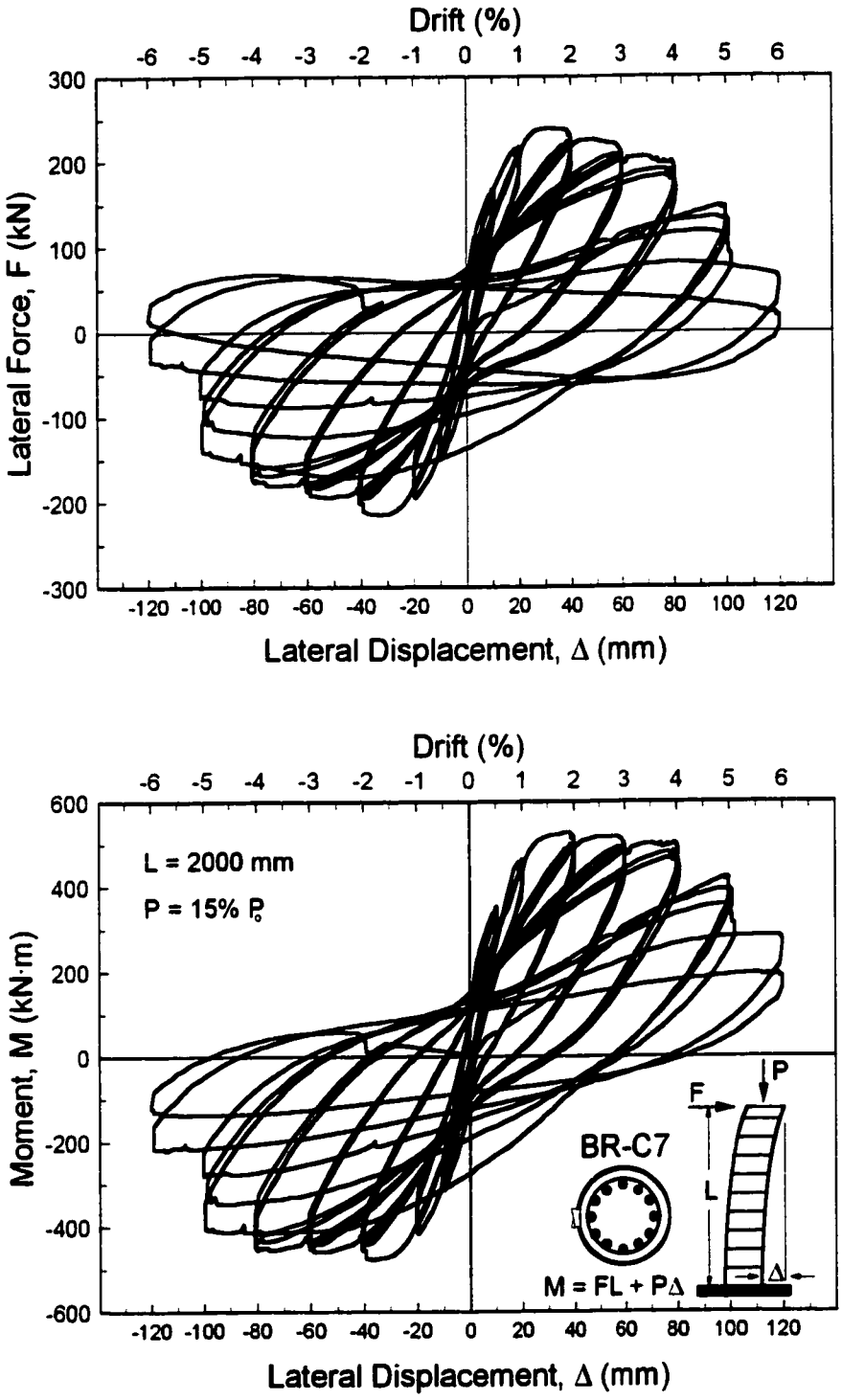

Fig. 3.7 Force and Moment-Displacement relationships for column BR-C7

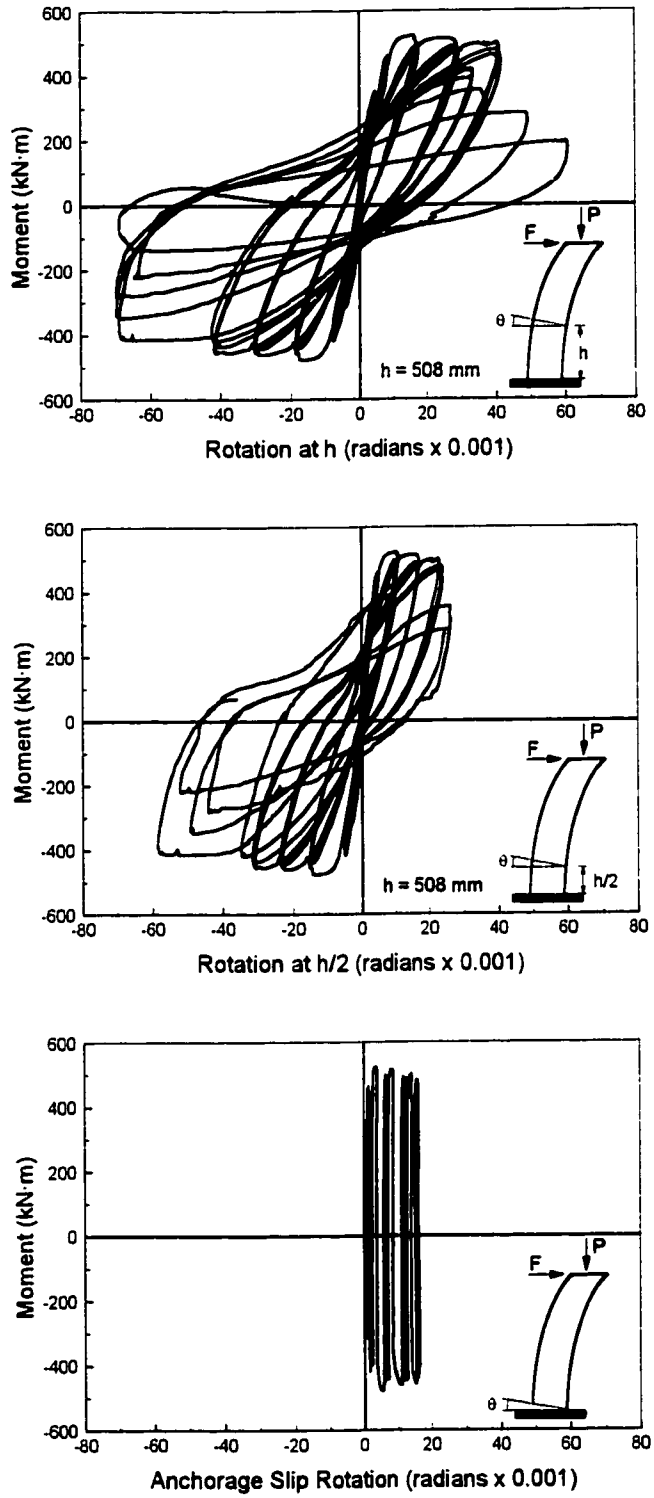

Fig. 3.8 Moment-Rotation relationships for column BR-C7

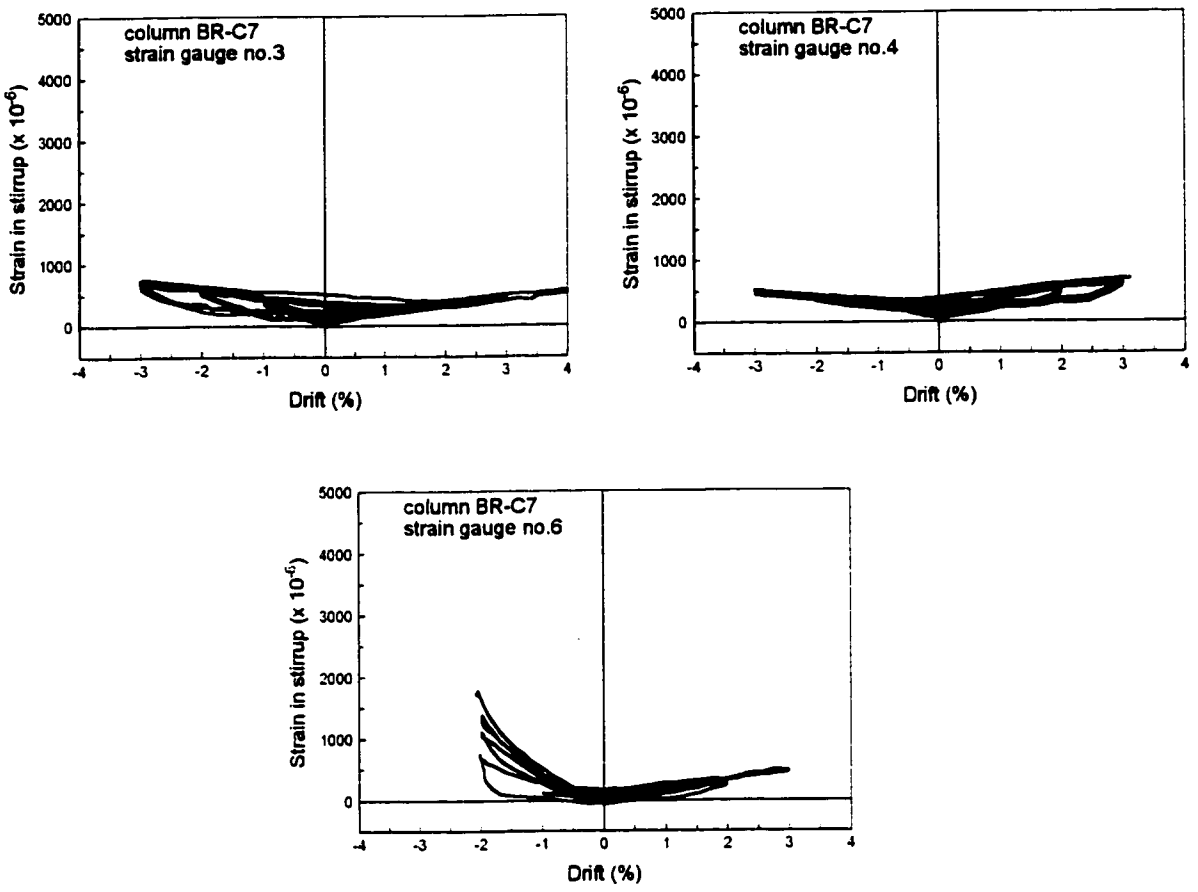

Fig. 3.9 Transverse reinforcement steel strains for column BR-C7 (for strain gauge locations refer to Fig. 2.13)

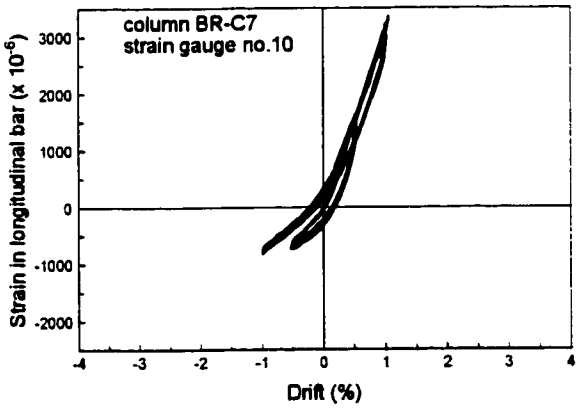

Fig. 3.10 Longitudinal reinforcement steel strains for column BR-C7 (for strain gauge locations refer to Fig. 2.13)

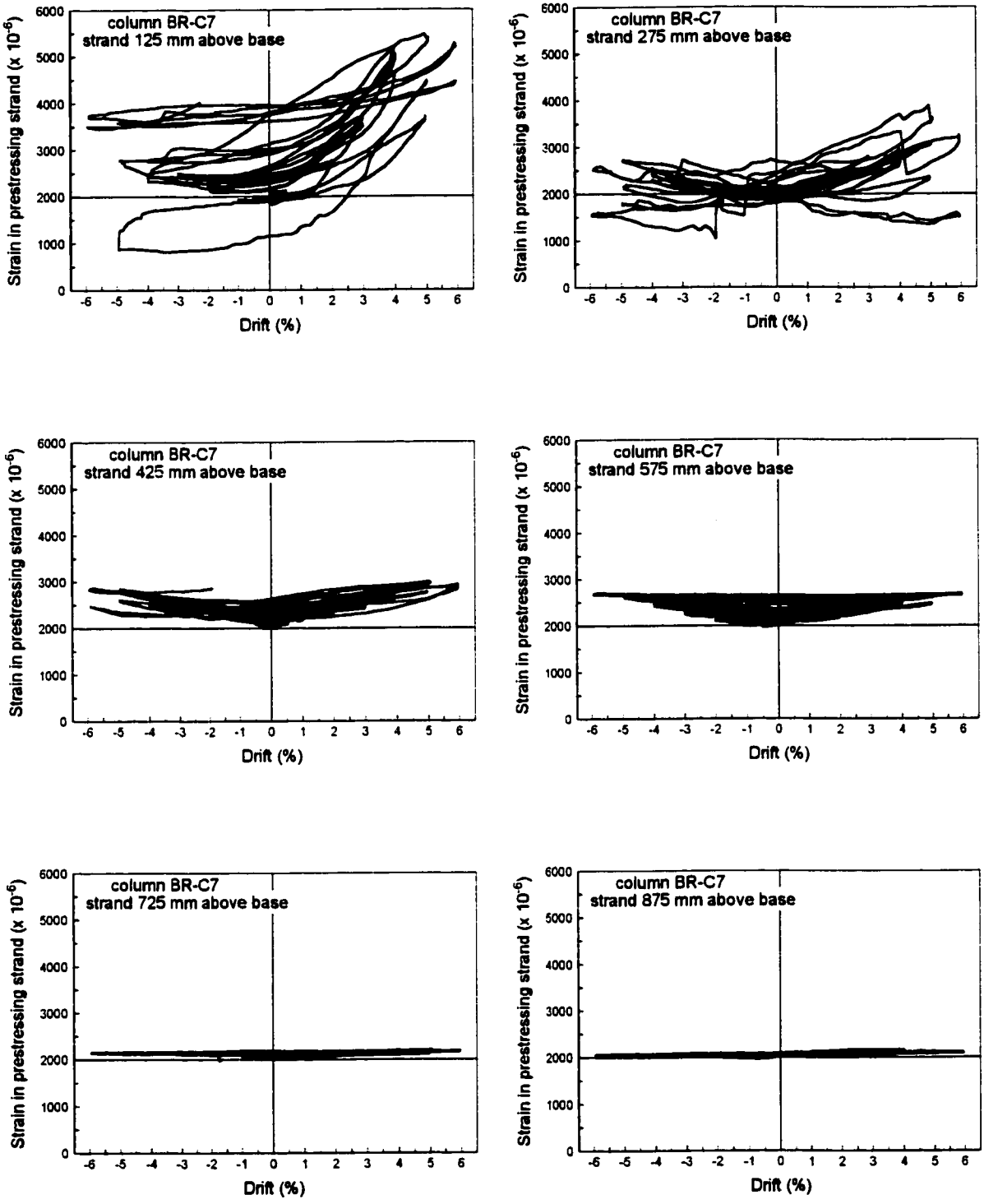

Fig. 3.11 Prestressing strand strains for column BR-C7

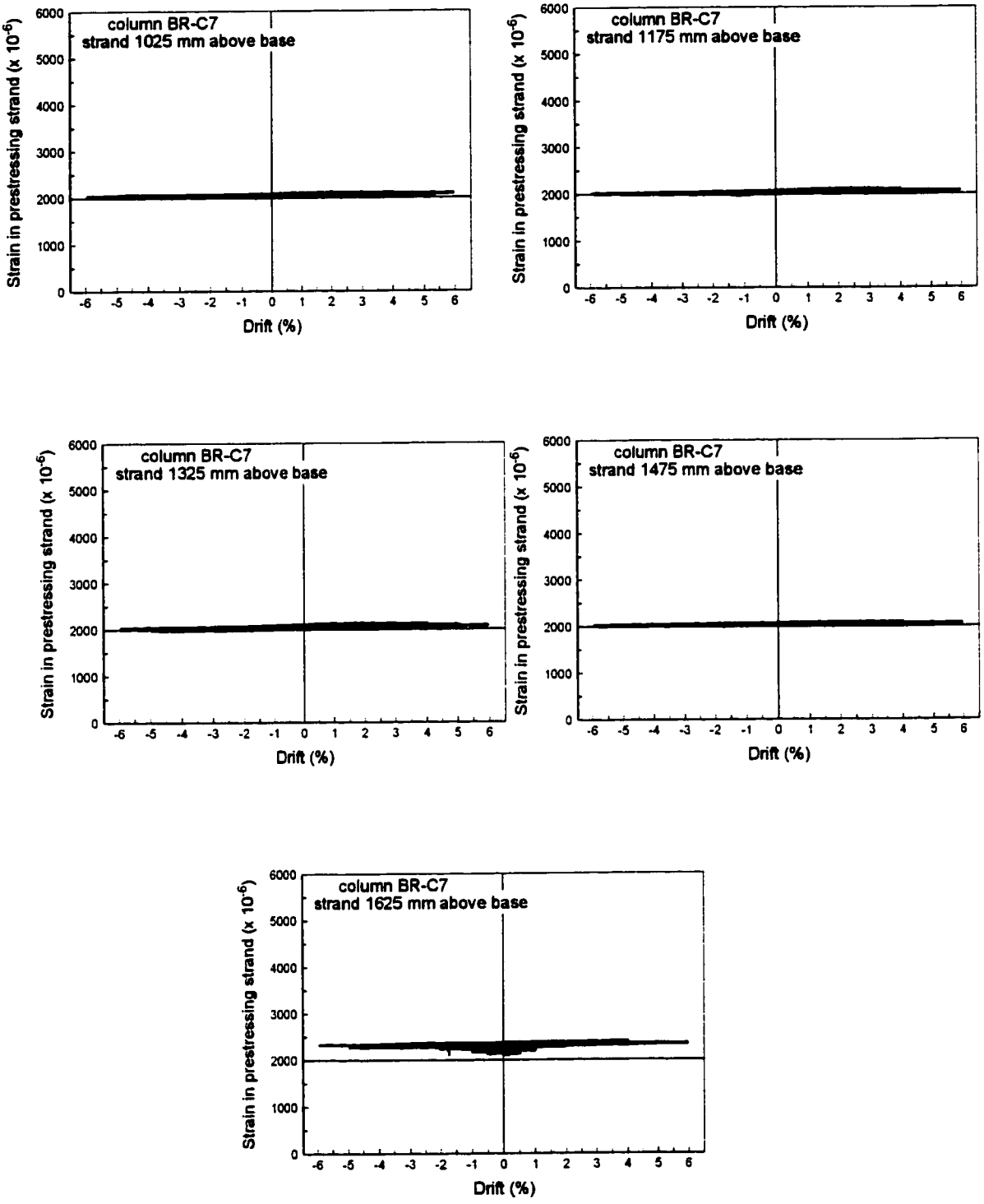

Fig. 3.11 (continued) Prestressing strand strains for column BR-C7

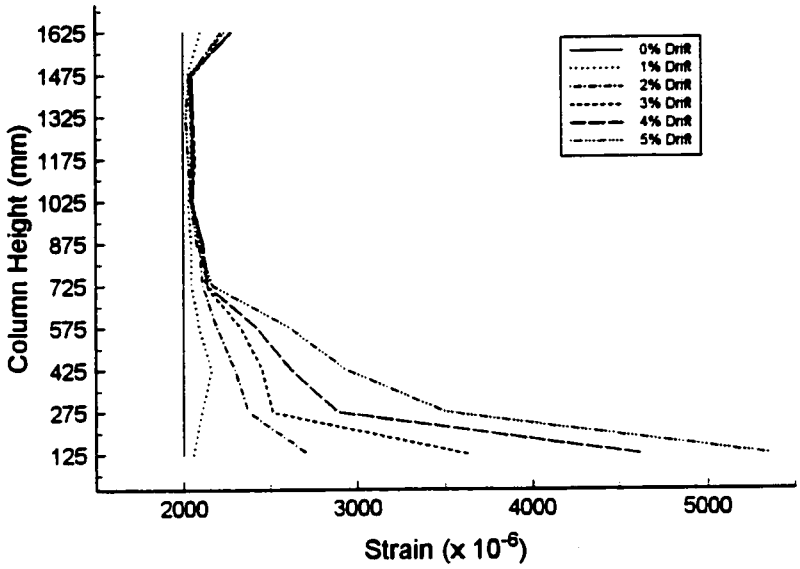

Fig. 3.12 Prestressing strand maximum strain profile for column BR-C7

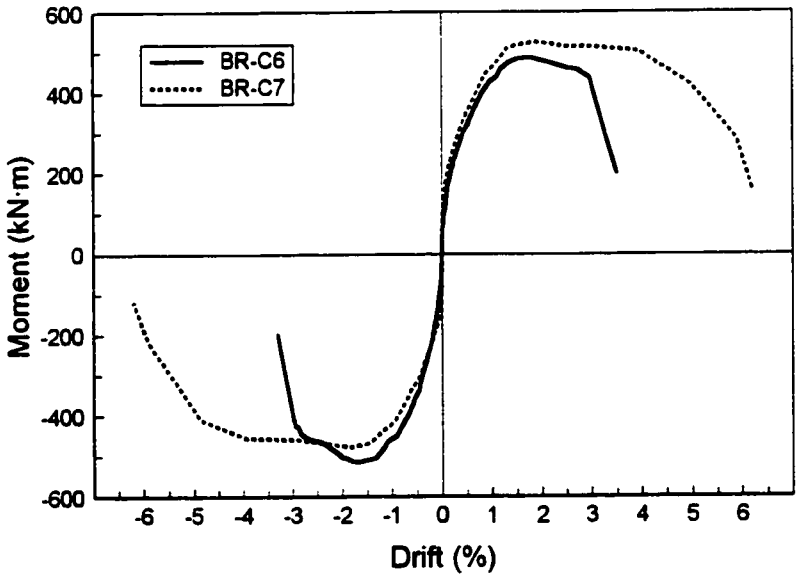

Fig. 3.13 Moment-Drift relationship envelope for columns BR-C6 and BR-C7

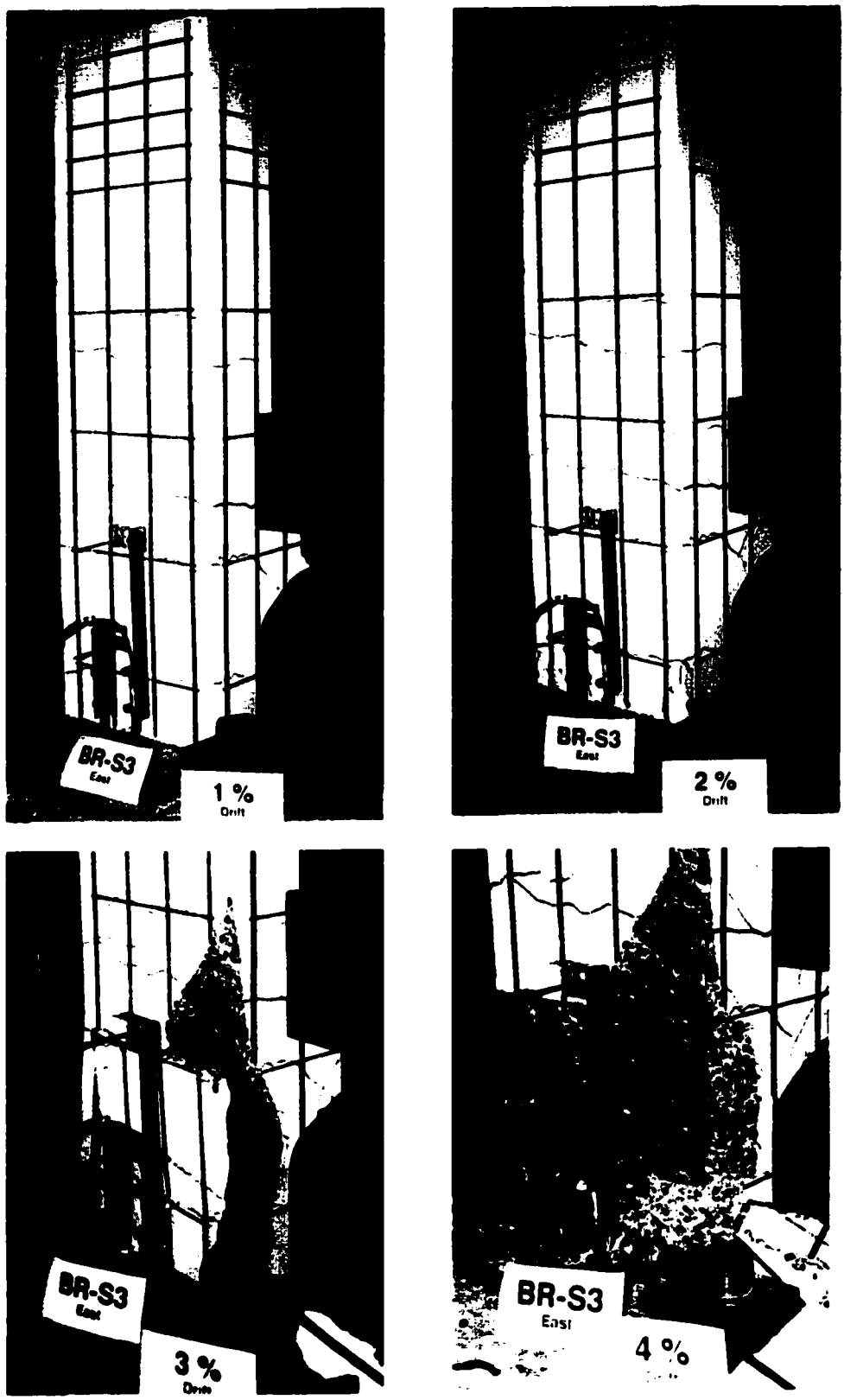

Fig. 3.14a Column BR-S3 at 1% drift (upper left), 2% drift (upper right), 3% drift (lower left) and 4% drift (lower right)

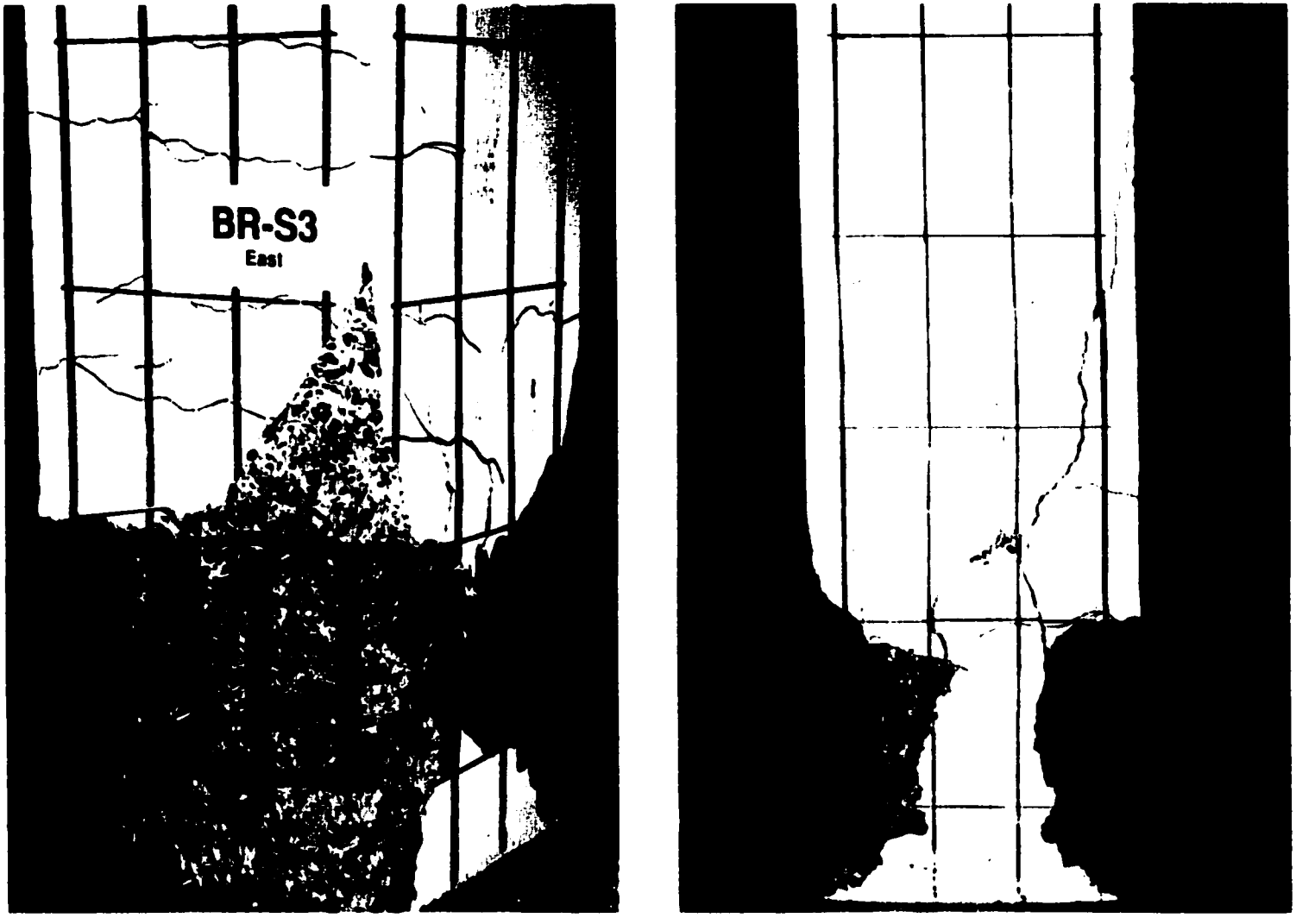

Fig. 3.14b Column BR-S3 at the end of test, east view (left) and south view (right).

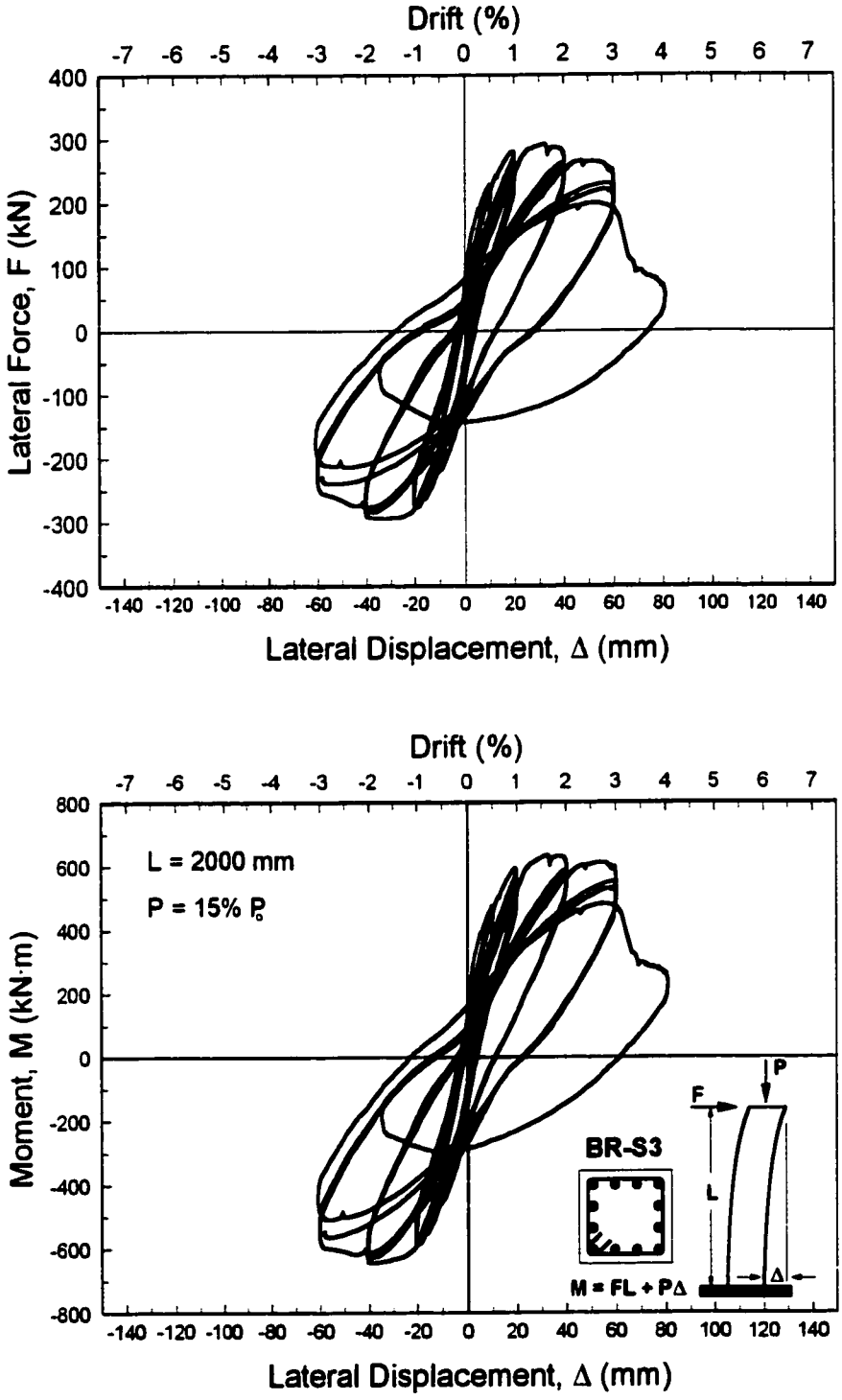

Fig. 3.15 Force and Moment-Displacement relationships for column BR-S3

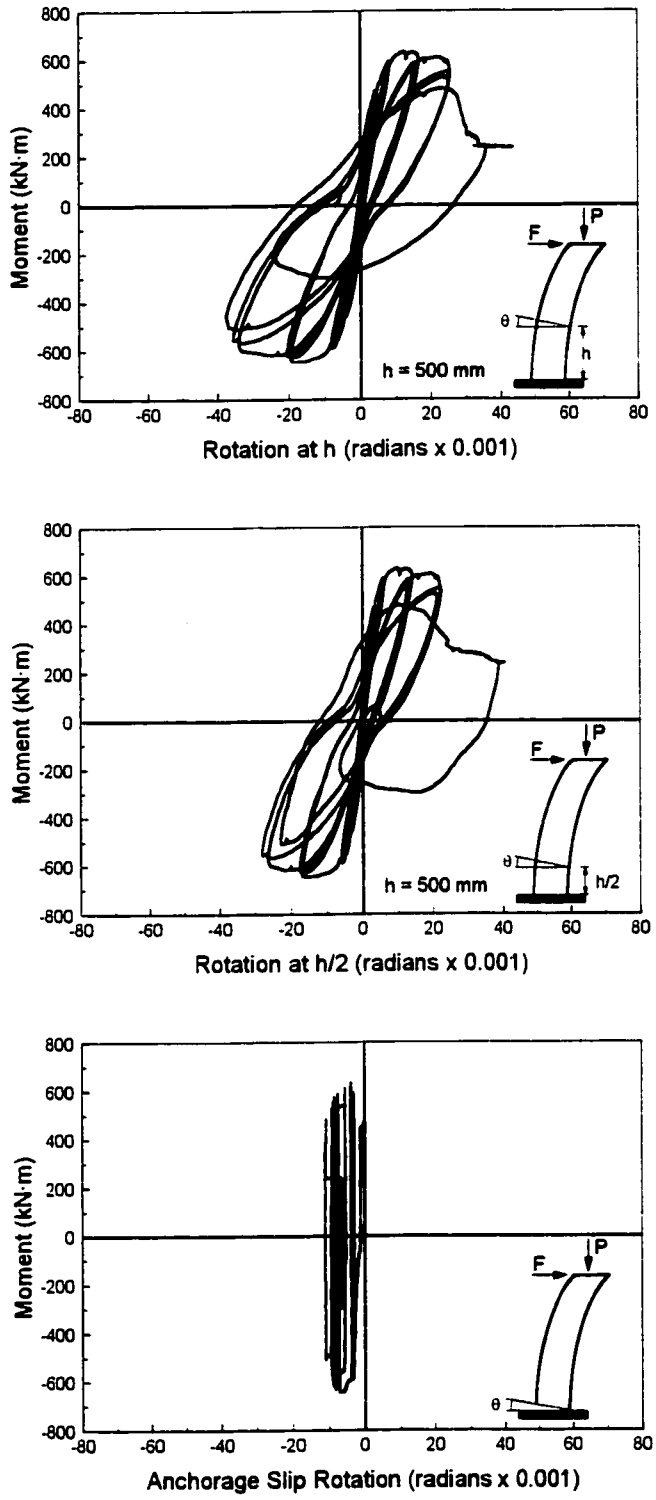

Fig. 3.16 Moment-Rotation relationships for column BR-S3

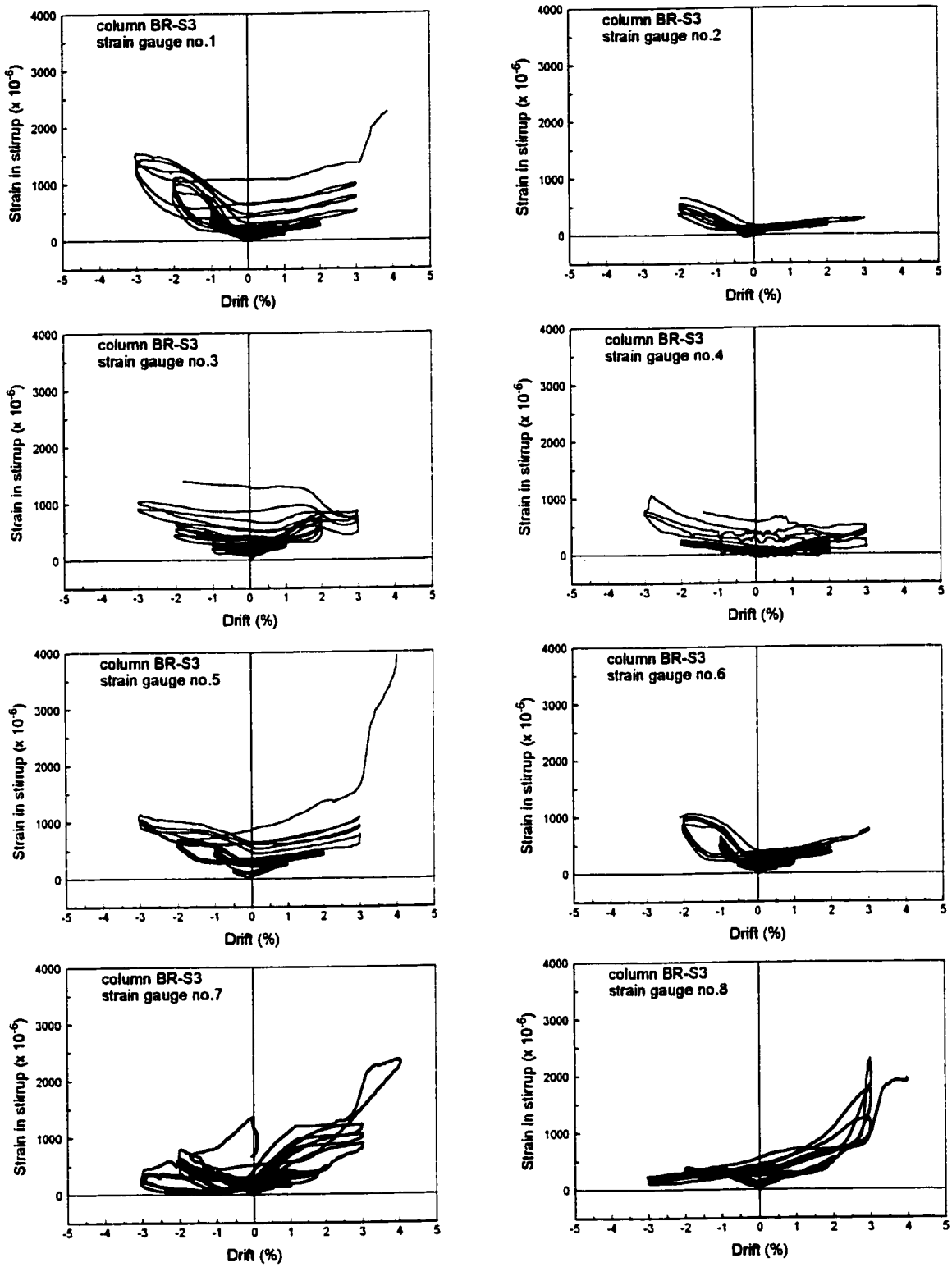

Fig. 3.17 Transverse reinforcement steel strains for column BR-S3 (for strain gauge locations refer to Fig. 2.14)

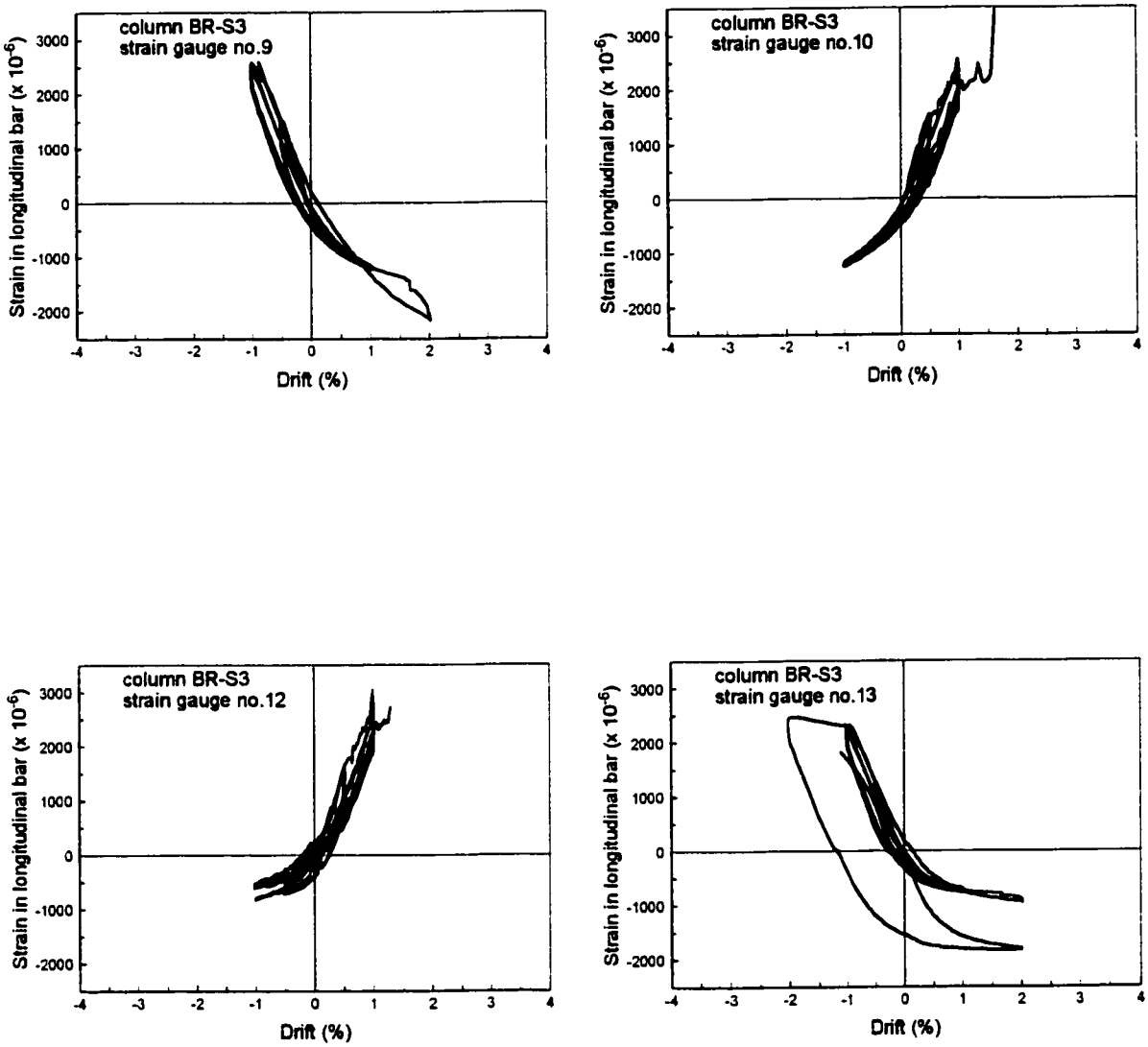

Fig. 3.18 Longitudinal reinforcement steel strains for column BR-S3 (for strain gauge locations refer to Fig. 2.14)

Fig. 3.19a Column BR-S4 at 2% drift (left) and 3% drift (right)

Fig. 3.19b Column BR-S4 at 2% drift: Crack at column/footing interface

Fig. 3.19c Column BR-S4 at 5% drift (left) and 7% drift (right)

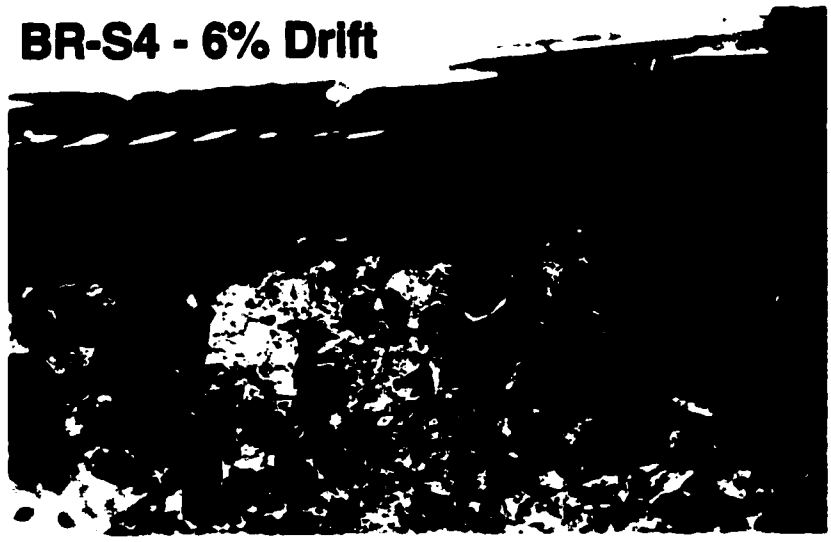

Fig. 3.19d Column BR-S4 at 6% drift: Ruptured longitudinal bars

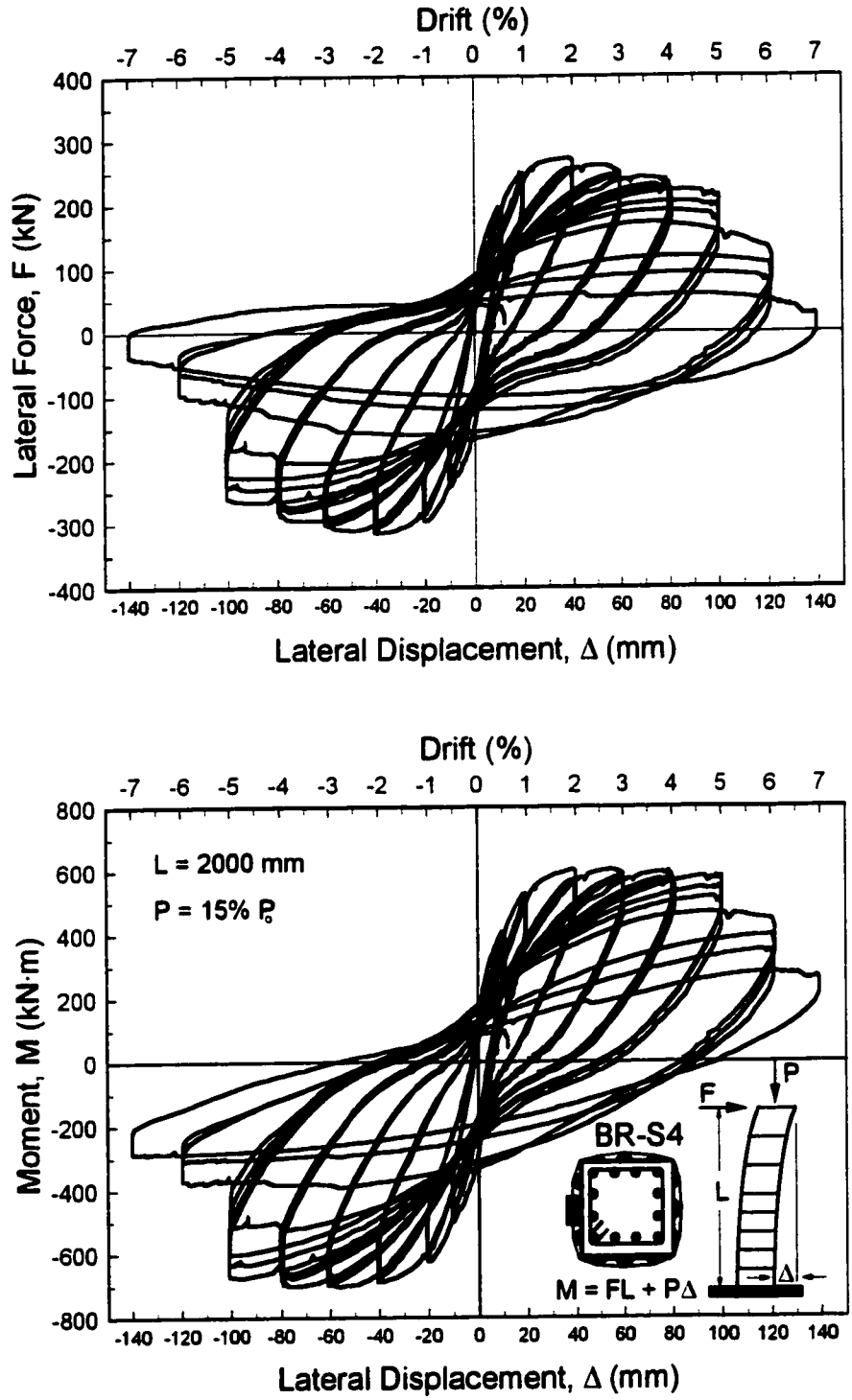

Fig. 3.20 Force and Moment-Displacement relationships for column BR-S4

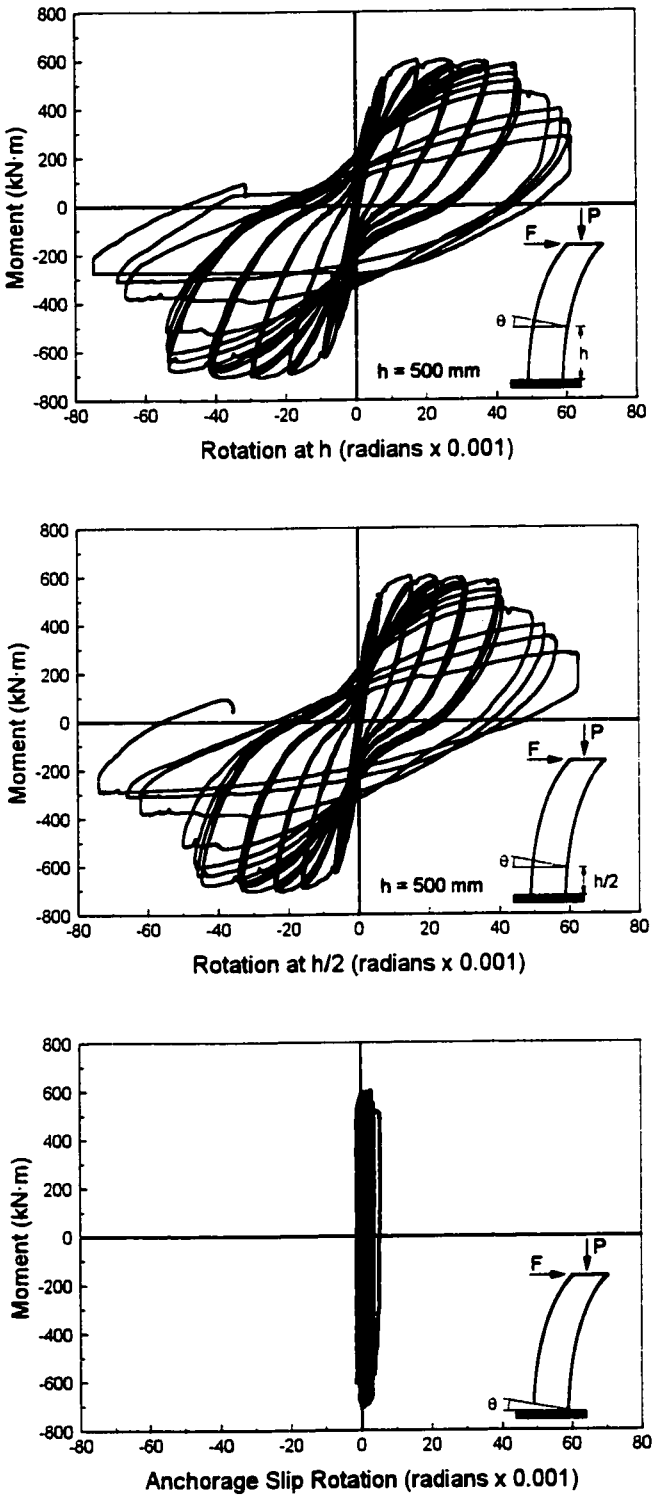

Fig. 3.21 Moment-Rotation relationship for column BR-S4

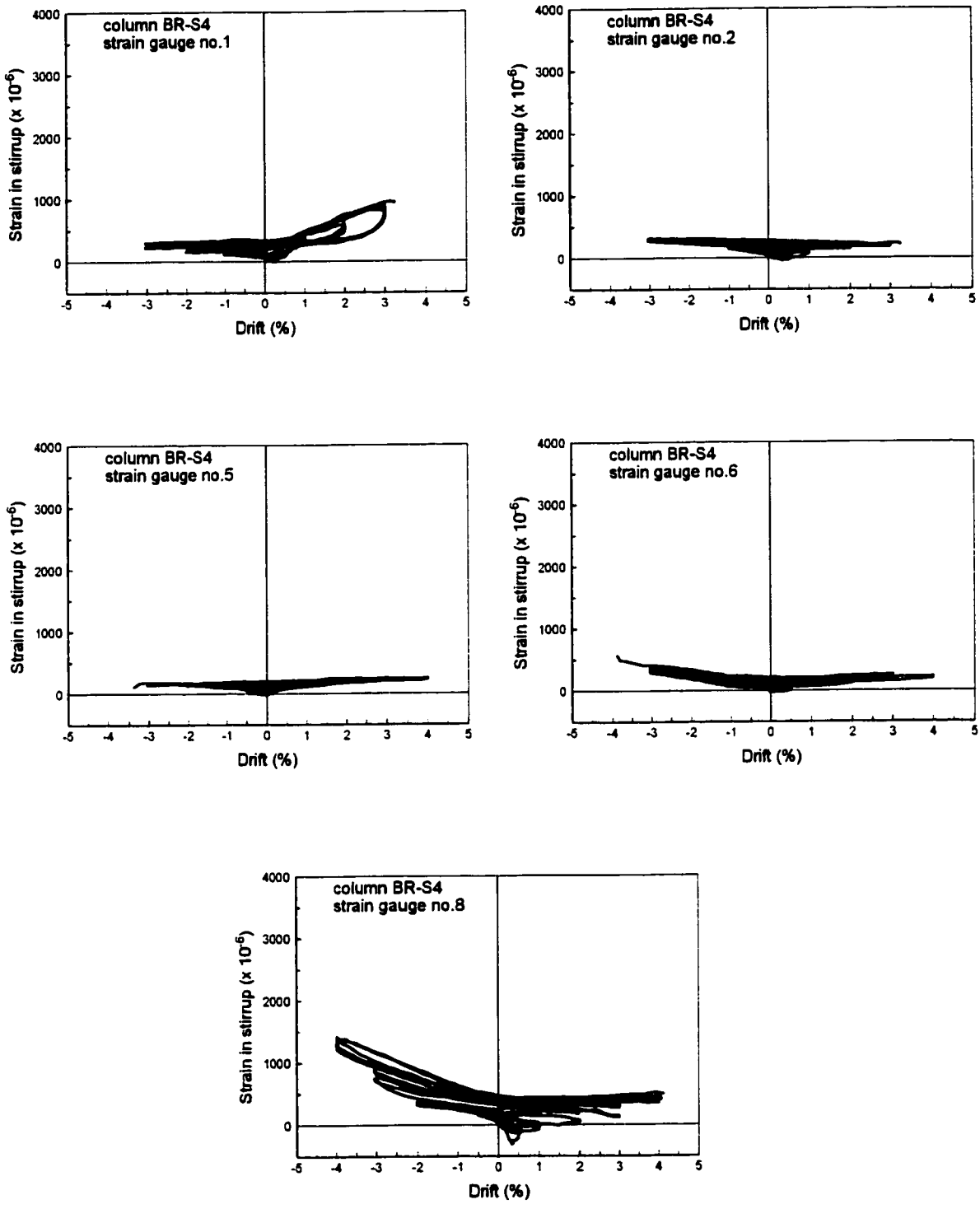

Fig. 3.22 Transverse reinforcement steel strains for column BR-S4 (for strain gauge locations refer to Fig. 2.14)

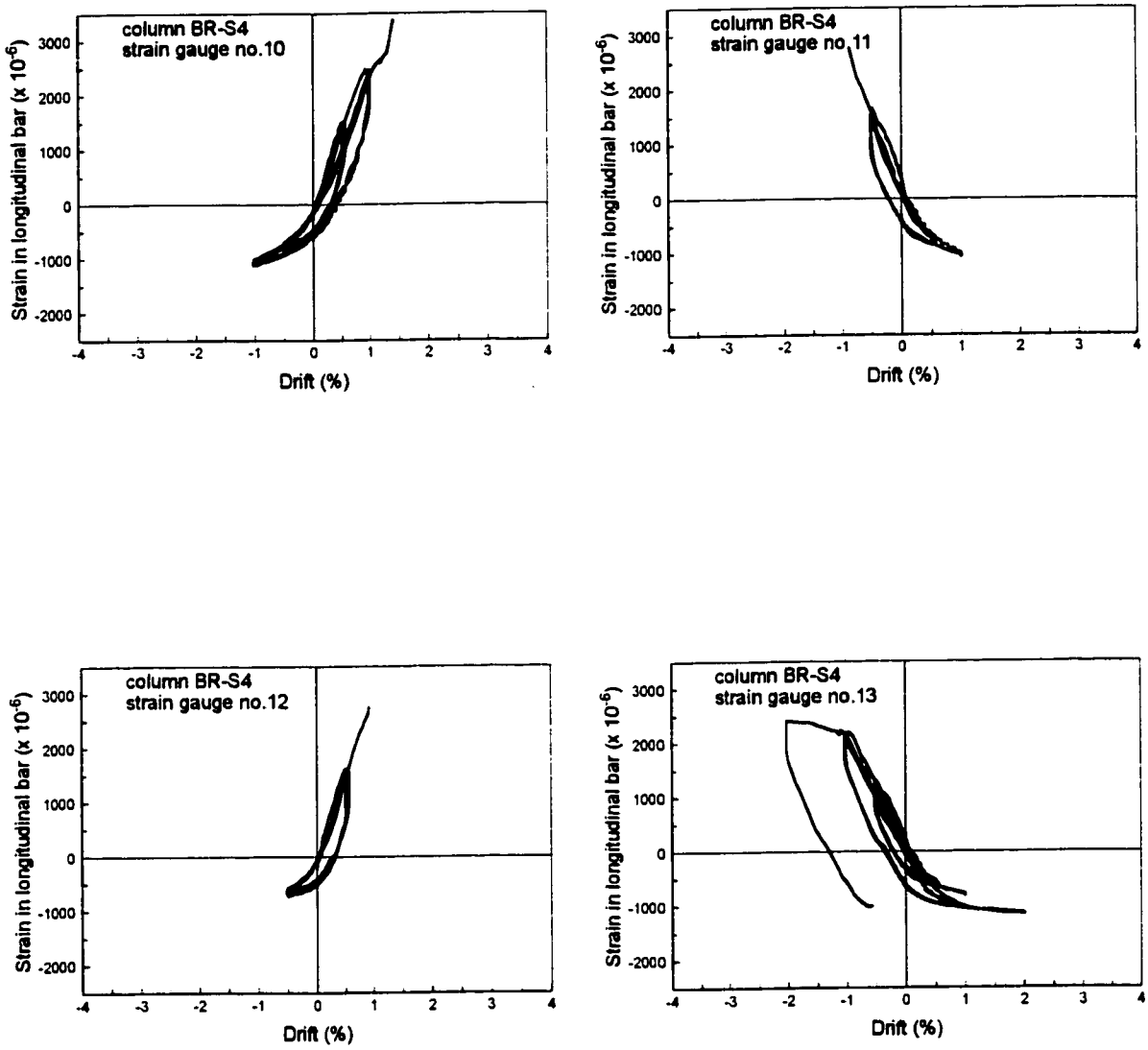

Fig. 3.23 Longitudinal reinforcement steel strains for column BR-S4 (for strain gauge locations refer to Fig. 2.14)

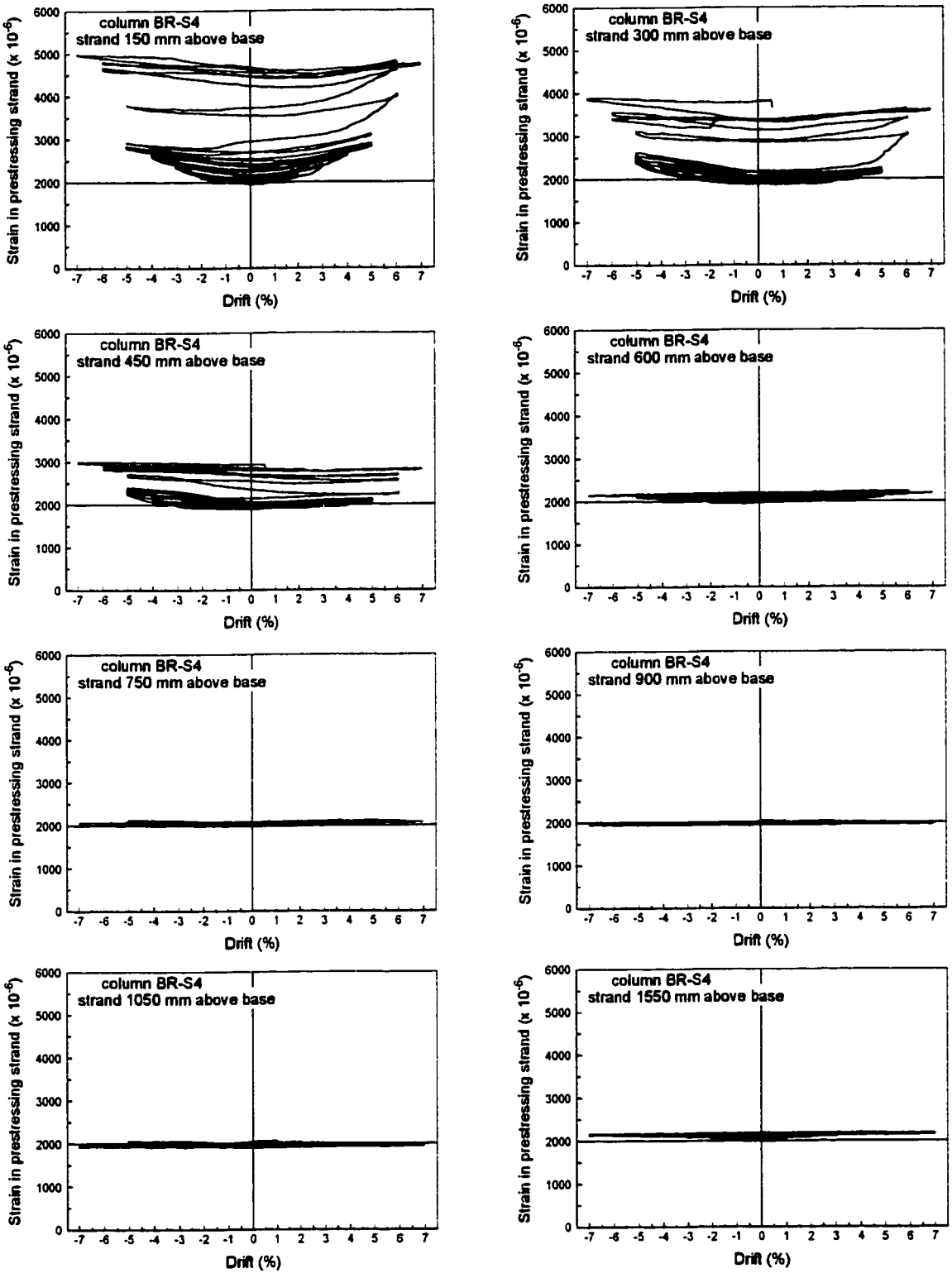

Fig. 3.24 Prestressing strand strains for column BR-S4

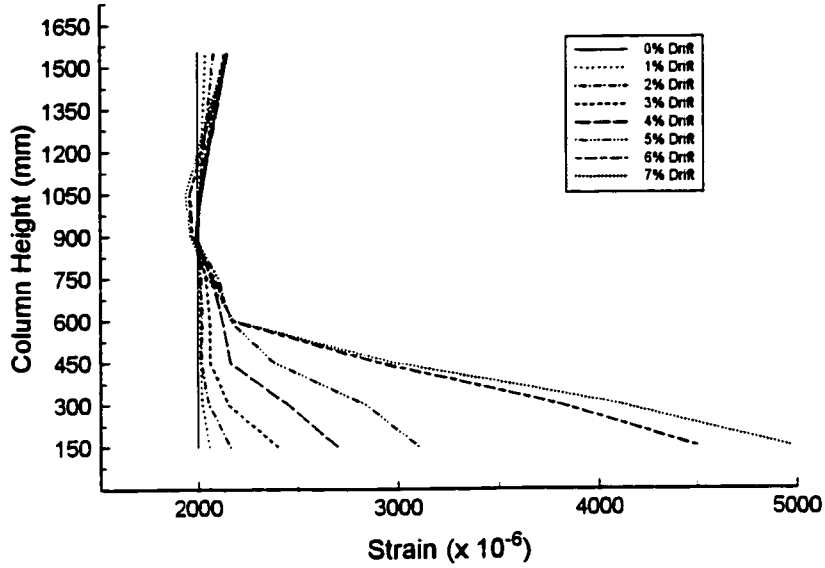

Fig. 3.25 Prestressing strand maximum strain profile for column BR-S4

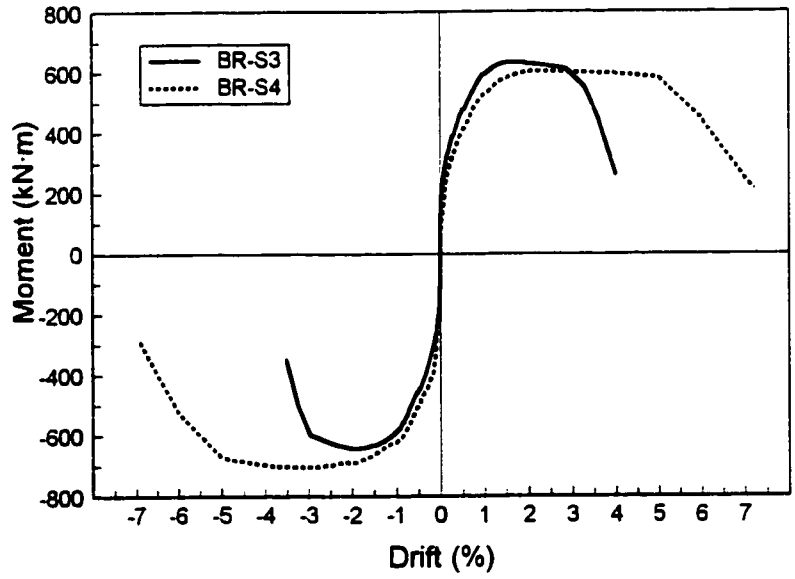

Fig. 3.26 Moment-Drift relationship envelope for columns BR-S3 and BR-S4

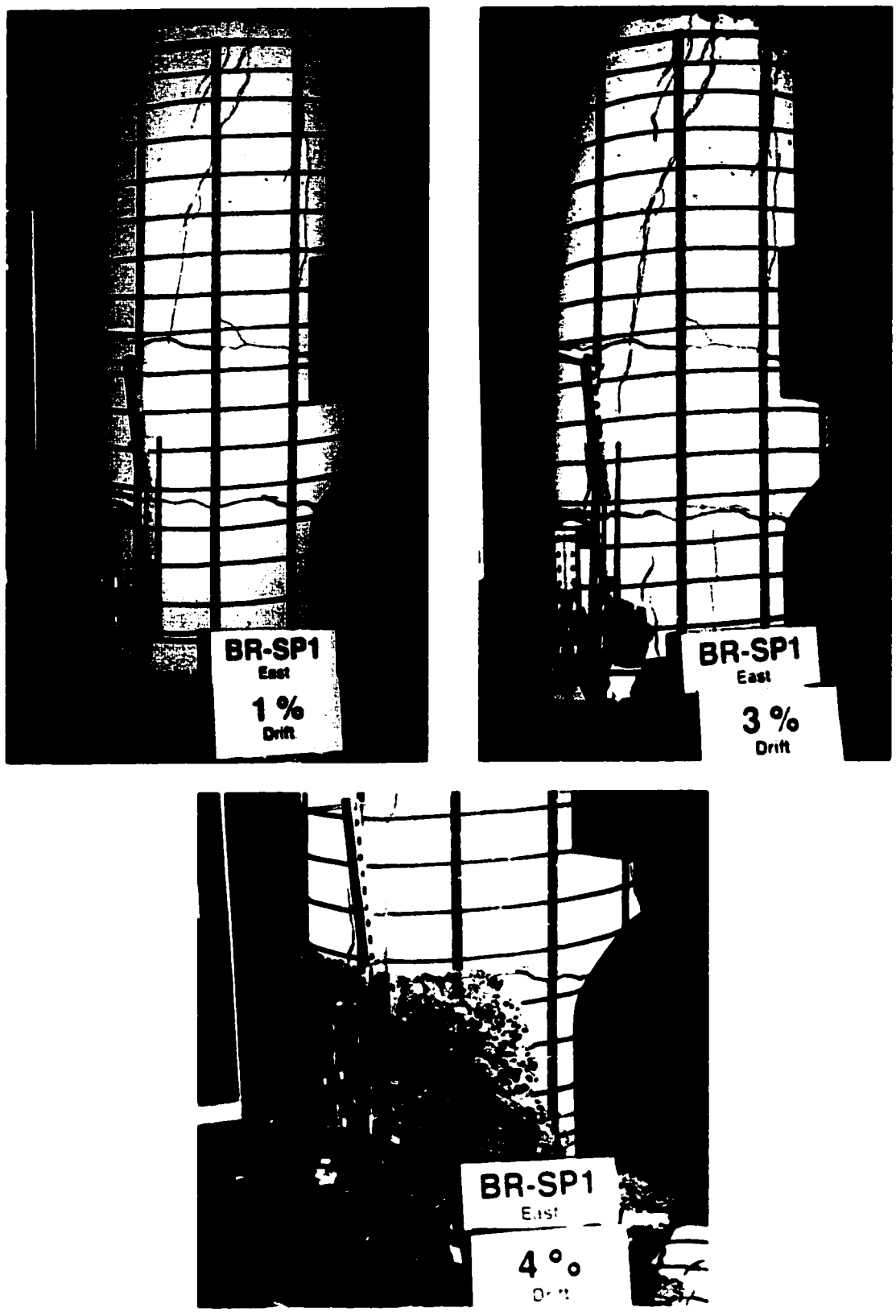

Fig. 3.27a Column BR-SP1 at 1% (upper left), 3% (upper right) and 4% (lower) drift

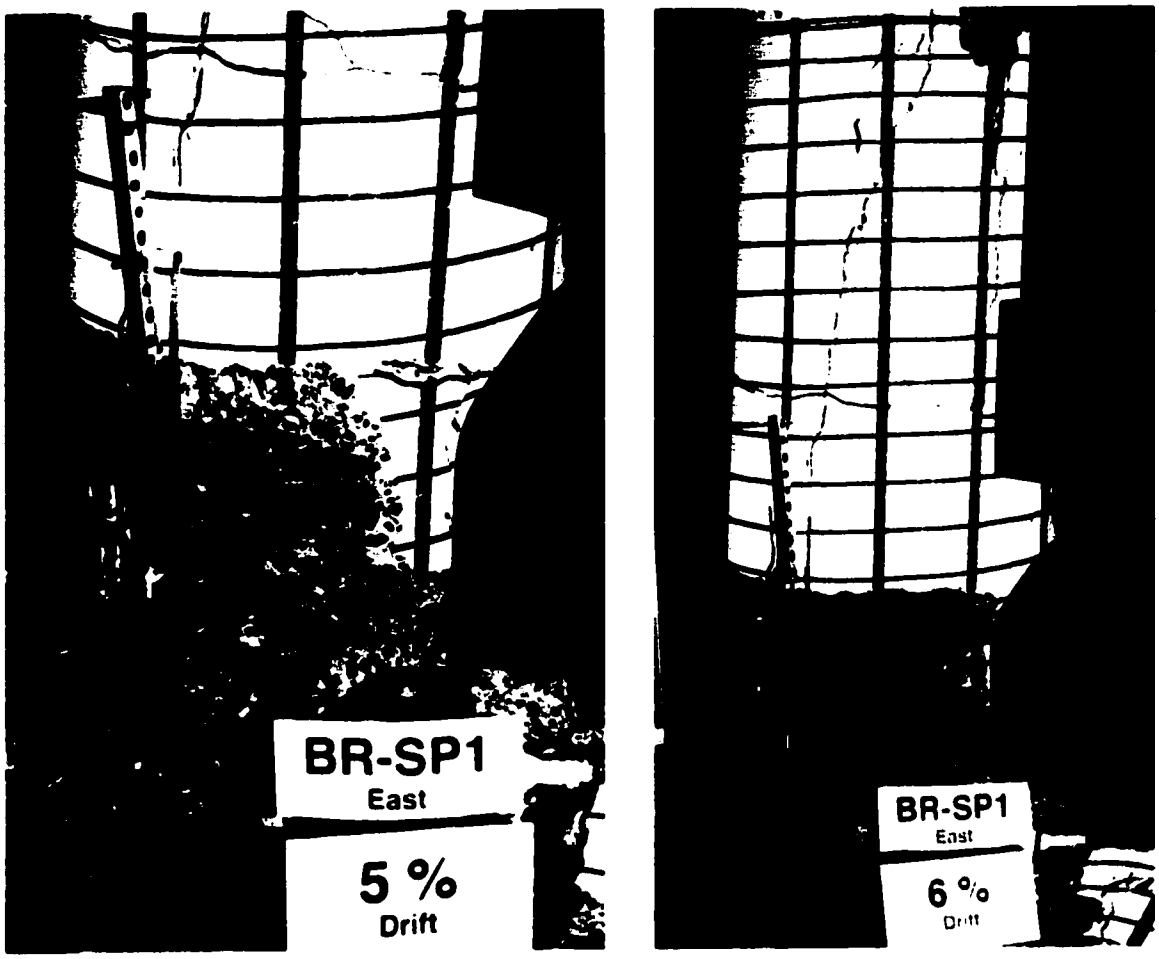

Fig. 3.27b Column BR-SP1 at 5% drift (left) and 6% drift (right)

Fig. 3.27c Column BR-SP1 at 7% drift: Ruptured longitudinal bars

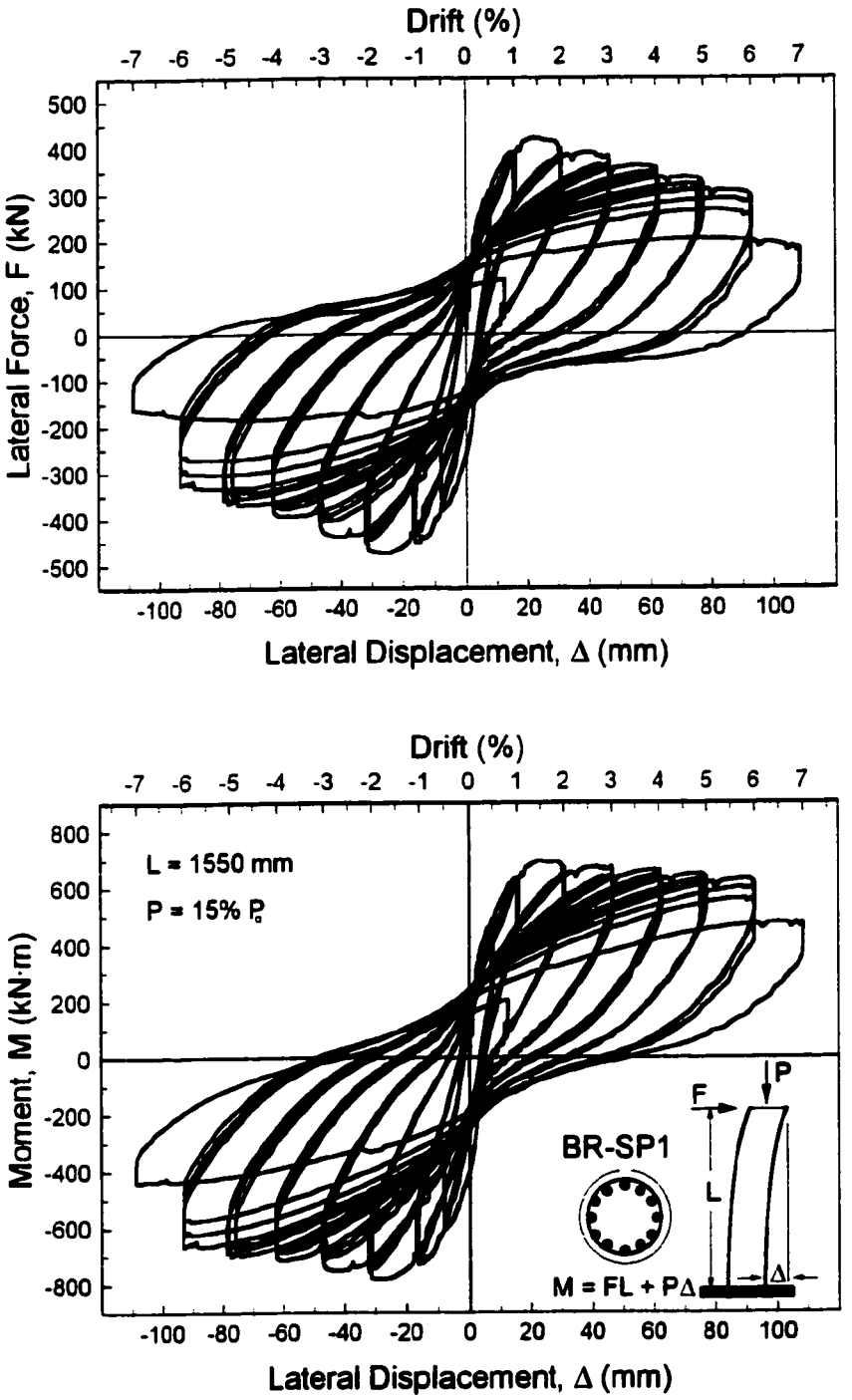

Fig. 3.28 Force and Moment-Displacement relationships for column BR-SP1

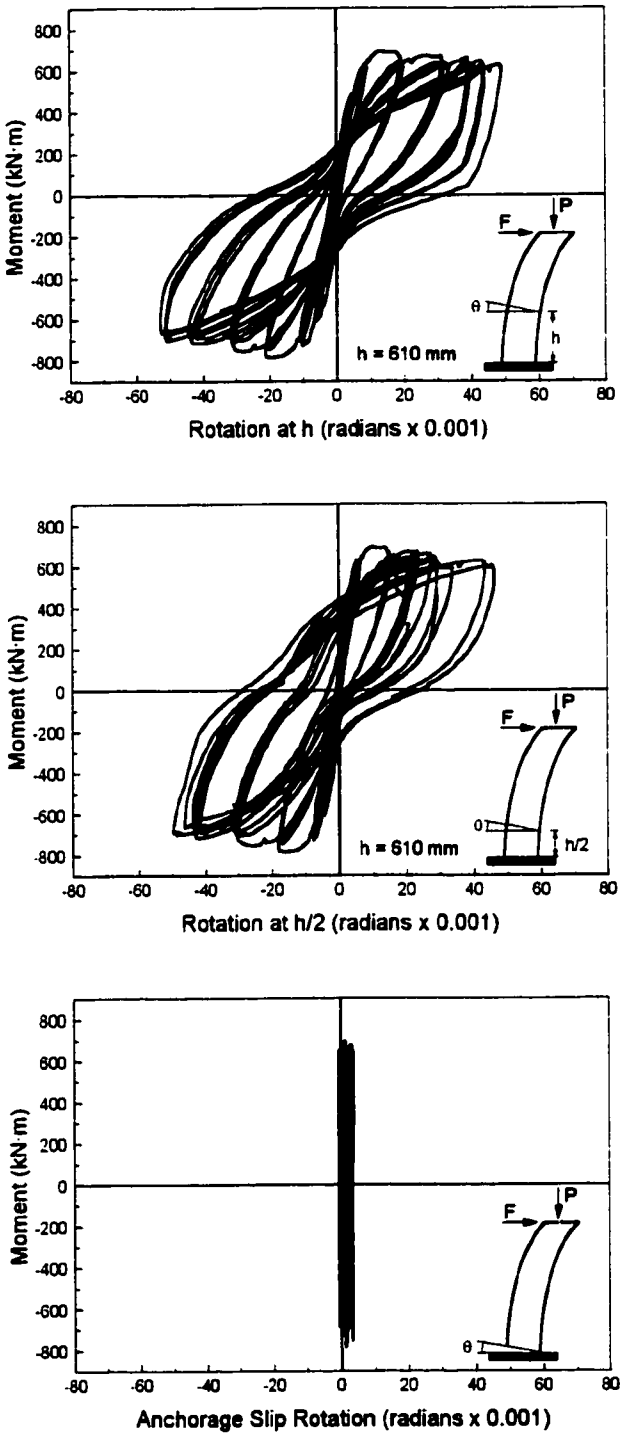

Fig. 3.29 Moment-Rotation relationships for column BR-SP1

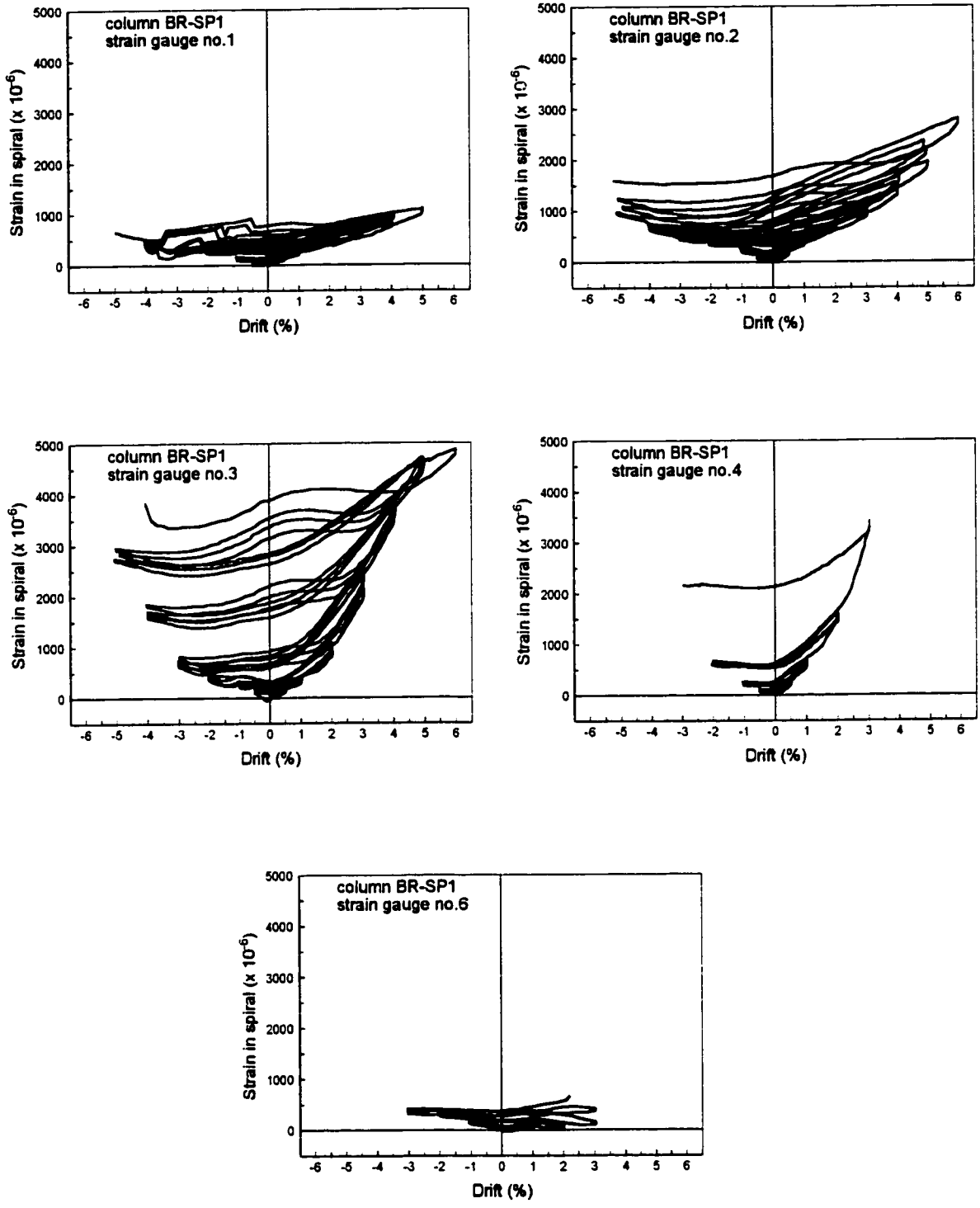

Fig. 3.30 Transverse reinforcement steel strains for column BR-SP1 (for strain gauge locations refer to Fig. 2.15)

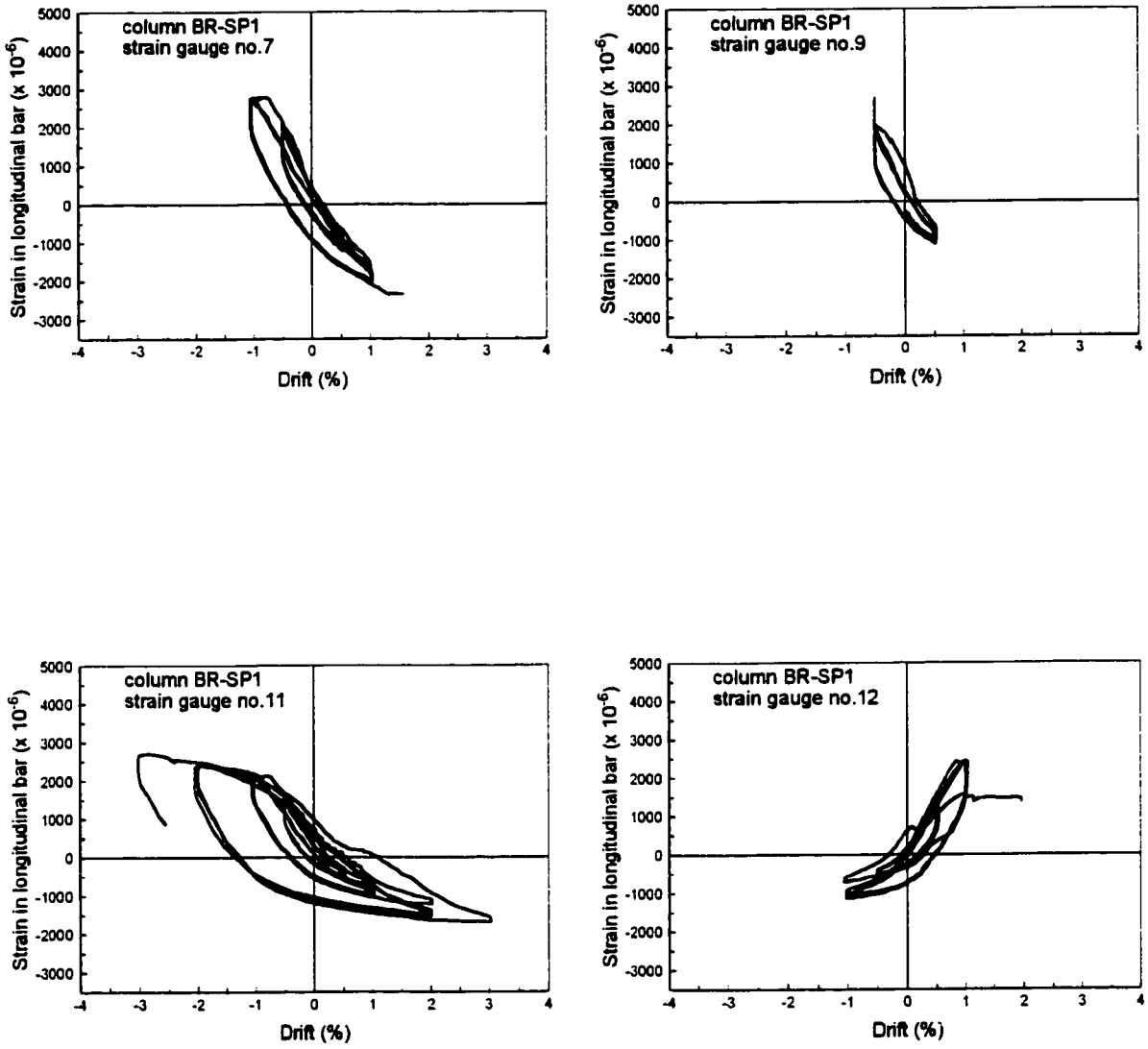

Fig. 3.31 Longitudinal reinforcement steel strains for column BR-SP1 (for strain gauge locations refer to Fig. 2.15)

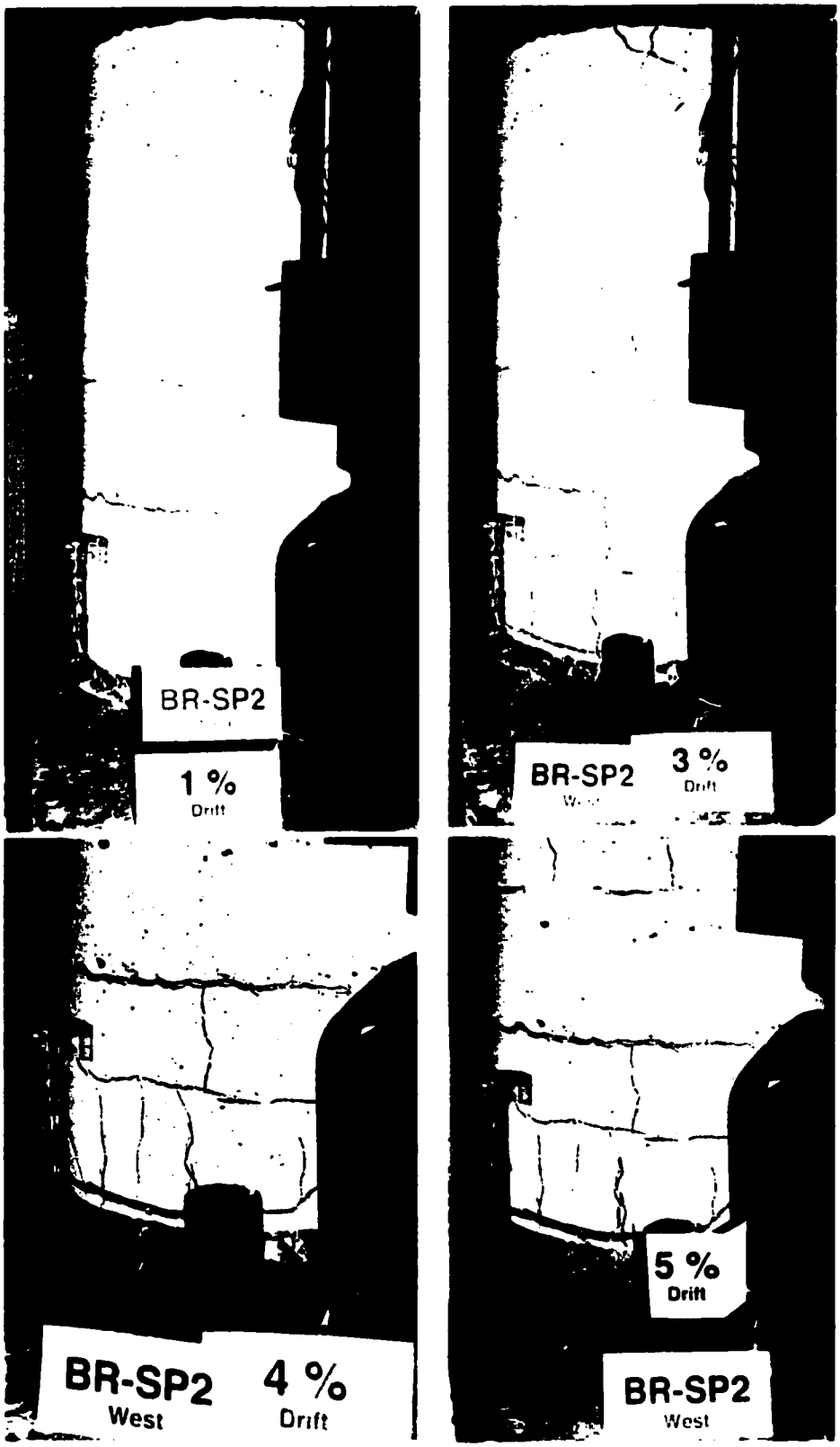

Fig. 3.32a Column BR-SP2 at 1% drift (upper left), 3% drift (upper right), 4% drift (lower left) and 5% drift (lower right)

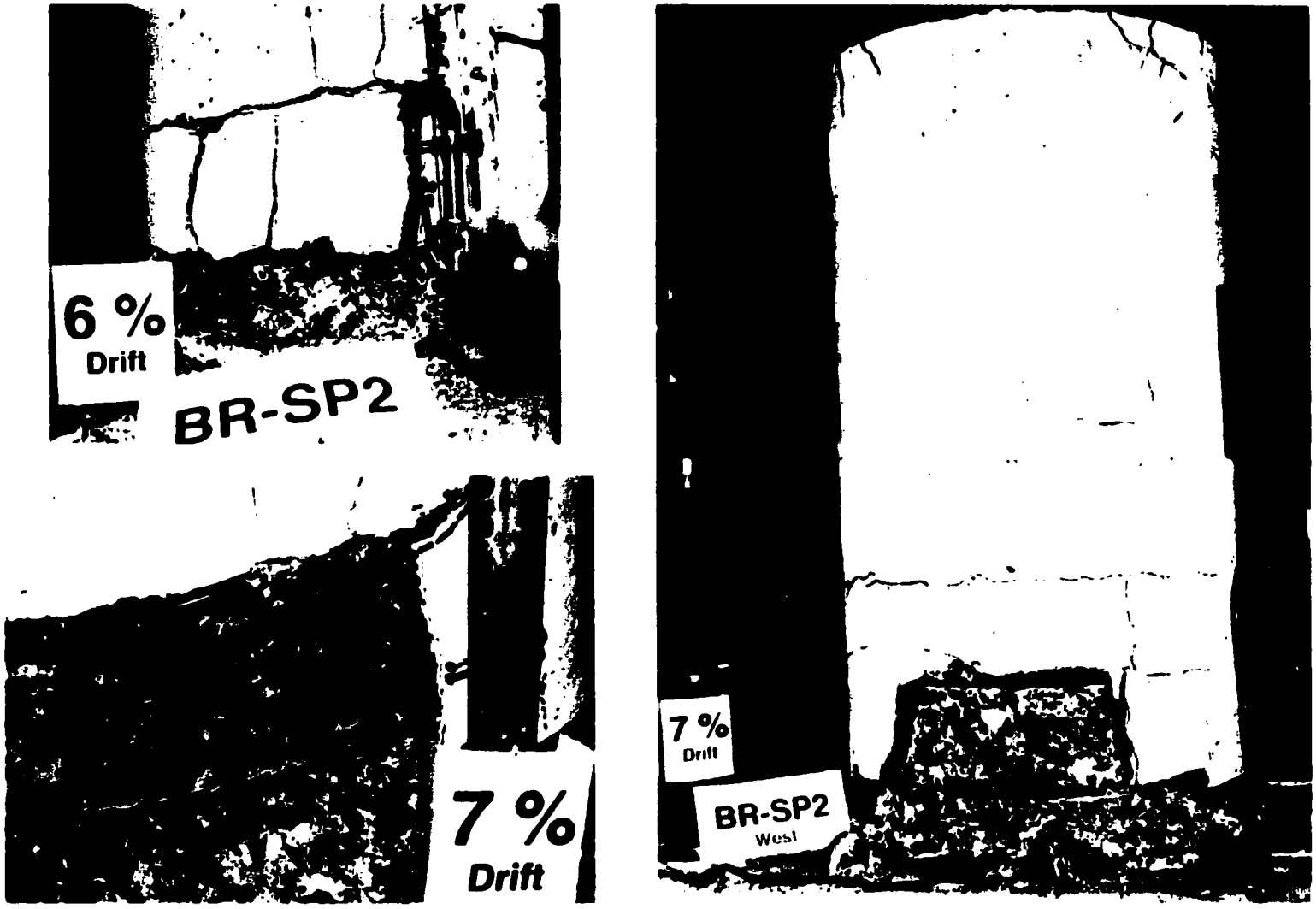

Fig. 3.32b Column BR-SP2 at 6% drift (upper left) and 7% drift (right & lower left) with ruptured longitudinal bars .

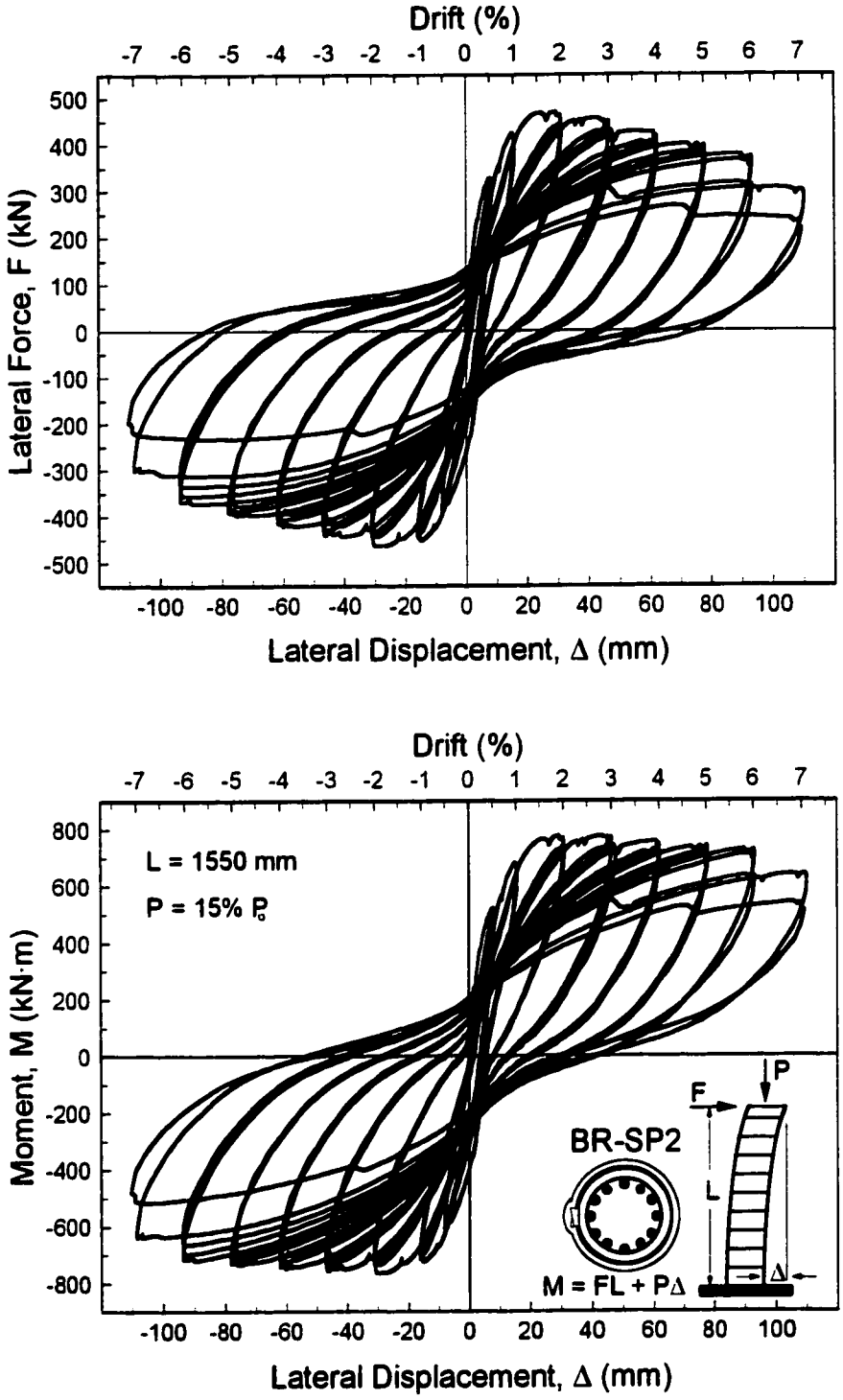

Fig. 3.33 Force and Moment-Displacement relationships for column BR-SP2

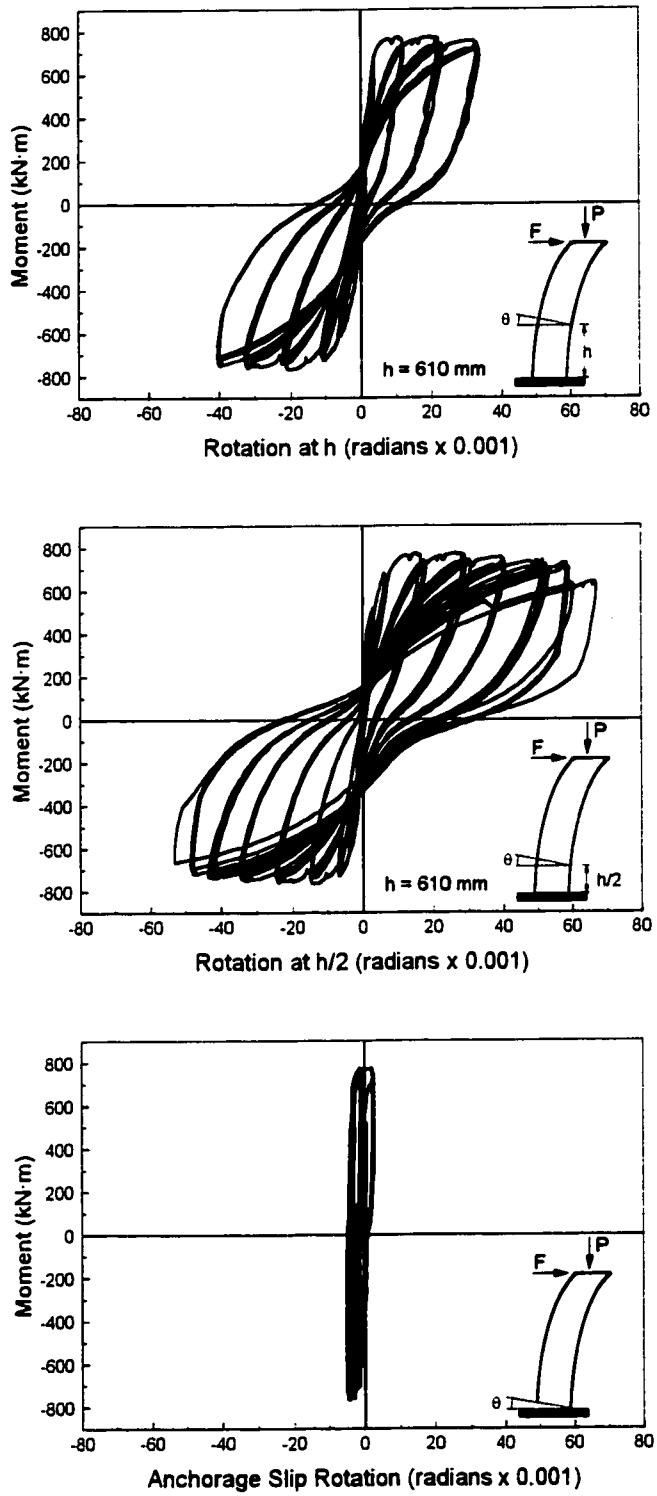

Fig. 3.34 Moment-Rotation relationships for column BR-SP2

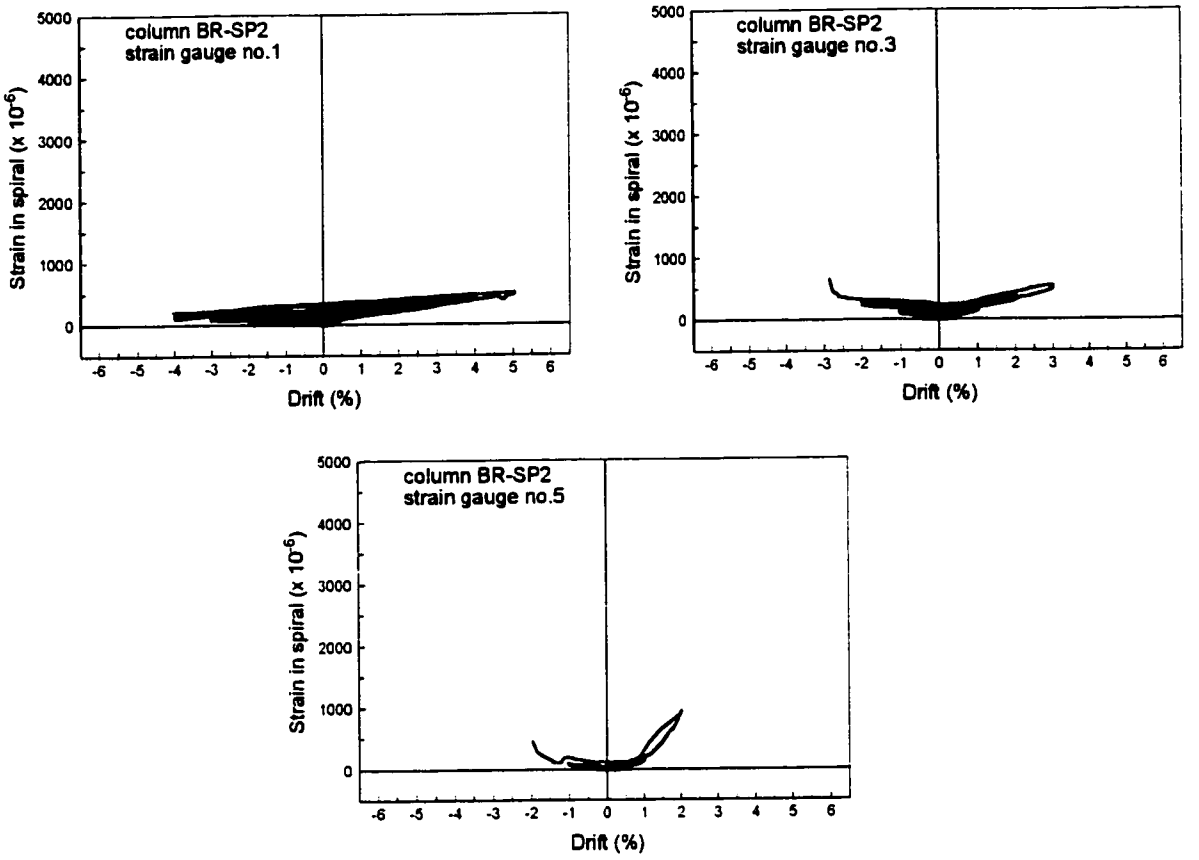

Fig. 3.35 Transverse reinforcement steel strains for column BR-SP2 (for strain gauge locations refer to Fig. 2.15)

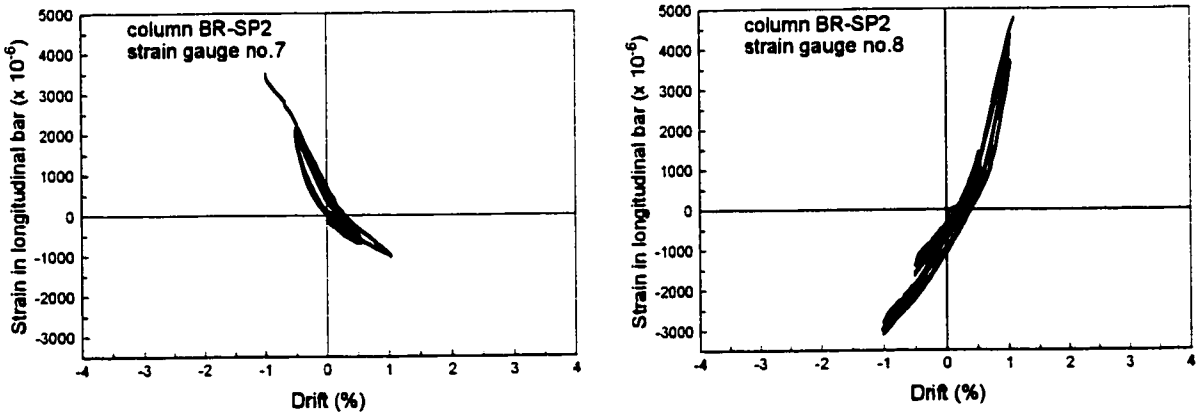

Fig. 3.36 Longitudinal reinforcement steel strains in column BR-SP2 (for strain gauge locations refer to Fig. 2.15)

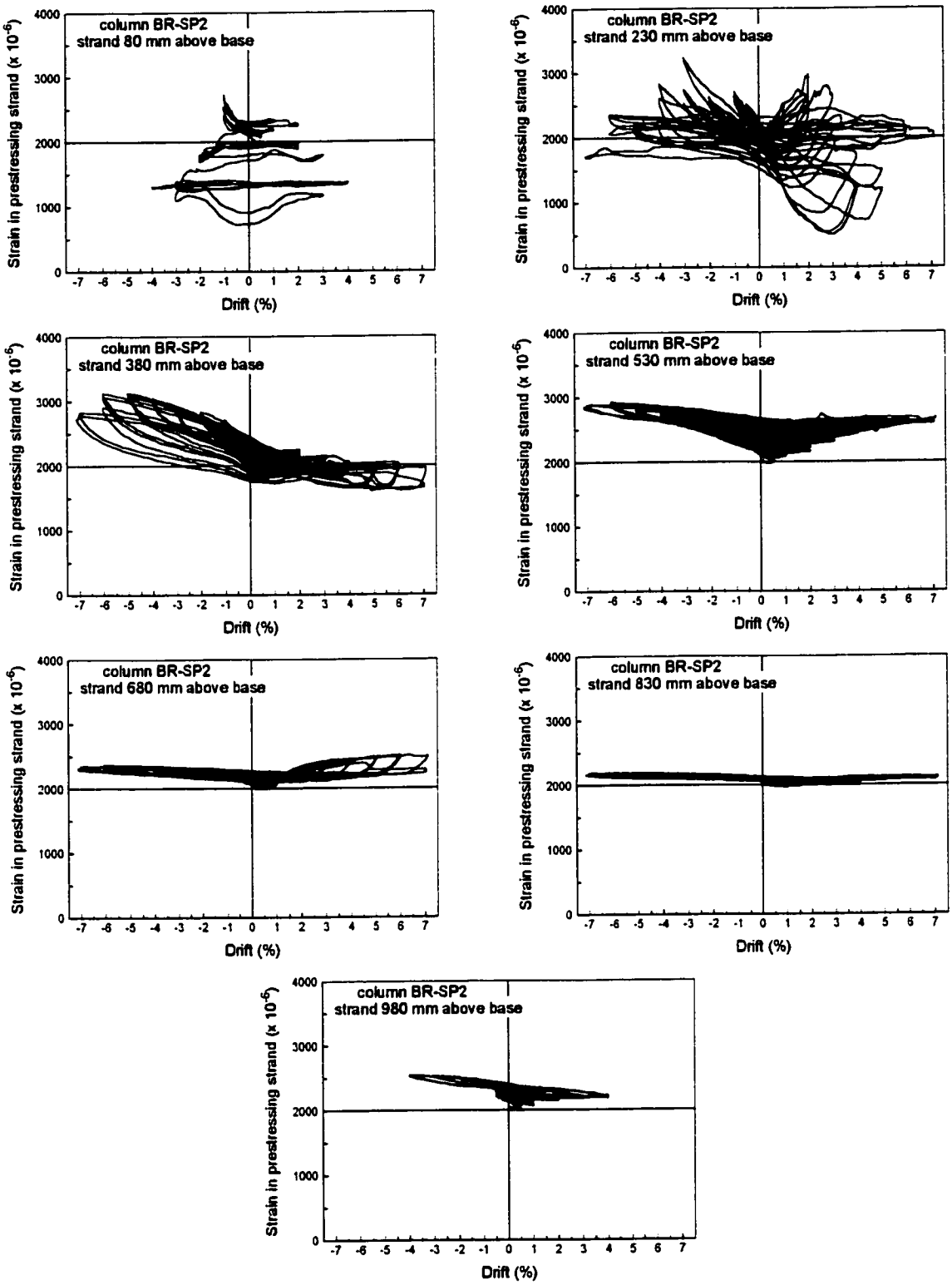

Fig. 3.37 Prestressing strand strains for column BR-SP2

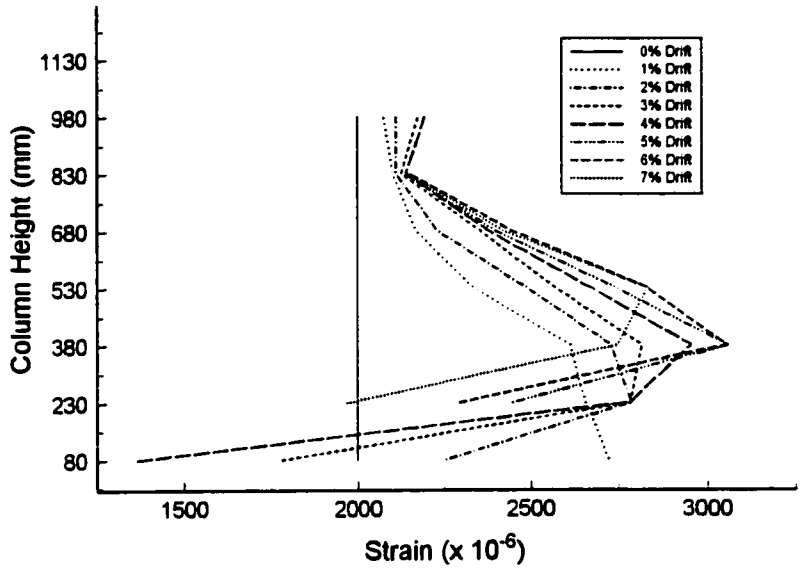

Fig. 3.38 Prestressing strand maximum strain profile for column BR-SP2

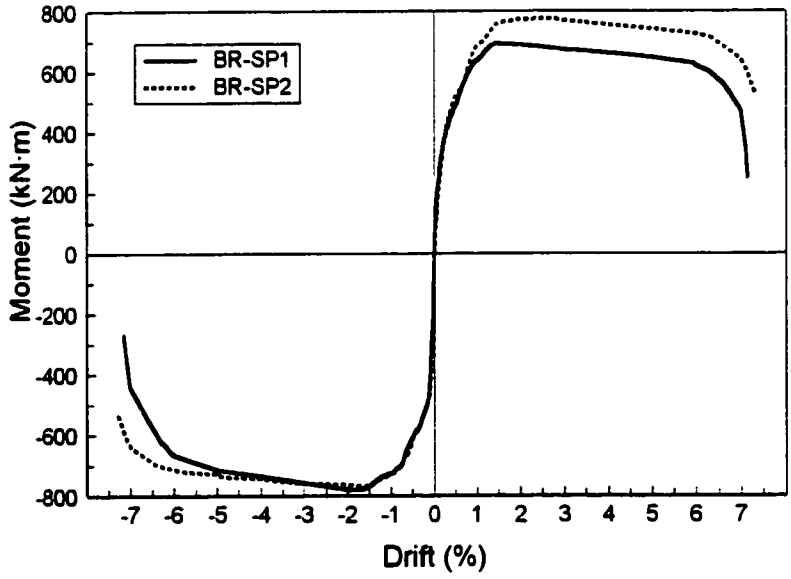

Fig. 3.39 Moment-Drift relationship envelope for columns BR-SP1 and BR-SP2

Chapter 4

Analysis and Discussion of Test Results and Retrofitting Technique

4.1 General

This chapter presents the analysis of test results obtained from both the current and previous phase of the same experimental investigation. The data obtained from the entire project constitutes a sufficiently rich data base to draw conclusions on the effectiveness of the retrofitting scheme applied to both shear-dominant and flexure-dominant columns.

4.2 Overview of Column Tests and Results

A new retrofitting technique was developed experimentally for seismic upgrading of reinforced concrete bridge columns. The new technique consisted of external prestressing, through which both active and passive lateral pressure was provided to overcome lateral expansion of concrete under compression, and to counteract diagonal tension caused by shear. The experimental program consisted of two phases. Phase 1, performed by Yalcin (1997), consisted of circular and square columns which exhibited a primarily shear dominant response. Phase 2, presented in the earlier chapters of this thesis, consisted of circular and square columns with a primarily flexure dominant response.

4.2.1 Overview of Column Tests in Phase 1

The tests performed by Yalcin (1997) consisted of 7 columns, with 1485 mm height; of which five were circular, with a cross-sectional dimension of 610 mm, and two were

square, with a cross-sectional dimension of 550 mm. The columns were designed to have reinforcement typical of those used in pre-1971 bridge columns. The reinforcement consisted of grade 400 steel, with twelve #25 longitudinal bars uniformly placed around the perimeter of the section tied with #10 perimeter ties at 300 mm spacing. The first tie was placed at 75 mm from the base. The loading regime for all columns consisted of constant axial load equal to 15% of the column concentric capacity (P_o), and incrementally increasing lateral deformation reversals, consisting of 3 cycles of lateral drift at 0.5%, 1%, 2%, 3%, etc. until failure. Drift was defined as the lateral displacement at the tip of the column divided by the total height of the column.

Among the circular columns, one was tested as the control column, another was retrofitted externally using high-strength steel straps, and the remaining three were retrofitted by external prestressing using 7-wire steel strands. The high-strength steel straps had yield strength of 910 MPa at 0.52% strain and ultimate strength of 1010 MPa at 9% strain, with strain hardening beginning at 2.1%. The straps were spaced at 150 mm. The prestressing strands were of size 9 and grade 1860 Mpa. They were wrapped and prestressed around the column as individual hoops, with the ends connected with modified versions of Dywidag twisted ring anchors. Different hoop spacing and initial prestress levels were used as test parameters.

The non-retrofitted circular column was able to sustain deformation cycles at 1% drift, and failed in shear when it was subjected to 2% drift. The column that was retrofitted with high-strength steel straps, withstood cycles at 2% drift, before it failed at the beginning of the cycles at 3% drift. The failure was initiated with rupturing of steel straps, triggering the column failure. Due to a rather premature failure of straps it was concluded that this retrofitting technique, with the strap size and strength used, was not very effective. For the columns retrofitted with prestressing strands, three different arrangements were used; strands at 300 mm prestressed to 25% f_{pu} (ultimate strand capacity); strands at 150 mm prestressed to 25% f_{pu}; and wires at 150 mm prestressed to 5% f_{pu}, essentially providing passive pressure. While all three columns showed significant improvements in column deformability, the 300 mm spacing was found to be less effective. One of the strands in this column failed

during the cycles at 3% drift. Significant strength degradation followed the strand rupture. However, 150 mm spacing with 25% f_{pu} was very effective, with no strands showing signs of failure. There was no strength degradation observed until after 5% drift. Although the columns had a short shear-span and hence were expected to show shear dominant response, the mode of failure changed from shear (observed in the control column) to flexure. The strength degradation observed during the 5% drift cycles was very slow and gradual. With 150 mm spacing and 5% f_{pu}, the behaviour was also good, but the strength degradation occurred suddenly at 5% drift. In conclusion, using prestressing strands as a method of retrofitting was effective, with best results obtained with 150 mm spacing and active pressure of 25% f_{pu}.

The non-retrofitted square column also sustained cycles at 1% drift, and failed in shear when it was forced to deform to 2% drift. A companion square column was retrofitted using external presstressing in the same manner as for circular columns, except that raiser discs were placed on column faces to raise the prestressed strand at three places on each face, so as to achieve confining force at three locations on each face, as well as on the corners. Note that the confining force at these locations became more evenly distributed over the entire face of the column because these raiser discs were attached to hollow structural steel sections that distributed the forces. The strands were placed at 150 mm spacing with an initial prestress of 25% f_{pu}. The retrofitted column demonstrated good behaviour, reaching 5% drift before any significant strength degradation occurred. At 5% drift, the strength degradation was slow, and column failure occurred at 6% drift.

Part of the results from Phase 1 are presented in this section to be compared with the columns tested in the current investigation (Phase 2). These include the two control columns and the companion columns which had retrofitting at 150 mm spacing with an initial prestress level of 25% f_{pu}. The hysteretic Moment-Drift relationship for the two circular columns, BR-C1 and BR-C2, and the two square columns, BR-S1 and BR-S2, are shown in Fig. 4.1 and Fig. 4.2, respectively.

4.2.2 Column Tests and Results - Phase 2

From the columns tested in Phase 1, the retrofitting configuration was established - 150 mm spacing and 25% f_{pu} initial prestress level. Phase 2 consisted of four columns which reflected the pre-1971 practice, as well as two spirally reinforced circular columns, representing the current practice.

The first pair of columns were circular with a diameter of 508 mm and a height of 1725 mm. These were labeled BR-C6 and BR-C7. The total effective height of the columns was 2.0 m. The reinforcing steel was of grade 400 MPa, and consisted of twelve #20 longitudinal bars and #10 circular ties with overlapping ends at 300 mm spacing. The first hoop was placed at 125 mm above the base. BR-C6 was tested as the control column and BR-C7 was retrofitted using prestressed strands at 150 mm spacing, with an initial prestress level of 25% f_{pu}. The prestressing strands used were size 9 and grade 1860 MPa 7 wire steel strands. The control column, BR-C6, sustained cycles at 2% drift, and failed in flexure during the cycles at 3% drift. The companion column with retrofitting, BR-C7, showed superior behaviour, and withstood deformation cycles up to the 5% drift level without significant strength decay. The hysteretic Moment-Drift relationship for Columns BR-C6 and BR-C7 are illustrated in Fig. 4.3.

The second pair of columns had a 500 mm square cross-section with an effective height of 2.0 m. These were labeled BR-S3 and BR-S4. The reinforcement consisted of twelve #20 longitudinal bars and #10 hoops with 135° bends at the ends at 300 mm spacing. The first hoop was placed at 150 mm from the footing. BR-S3 was tested as the control column, and BR-S4 was retrofitted with prestressing strands placed at 150 mm spacing with an initial prestress level of 25% f_{pu}. The control column, BR-S3, sustained the cycles at 2% drift, and failed in flexure during the cycles at 3% drift. The retrofitted column, BR-S4, showed improved behaviour and withstood increased deformation reversals up to the first cycle at 6% drift. The hysteretic Moment-Drift relationships are shown in Fig. 4.4.

The third pair of columns were circular with a diameter of 610 mm and a reduced effective height of 1.54 m. These were labeled BR-SP1 and BR-SP2. The reinforcement consisted of twelve #20 longitudinal bars and a #10 spiral with a 75 mm pitch. The Column

BR-SP1 was tested as the control column and BR-SP2 was retrofitted using prestressing strands placed at 150 mm spacing with an initial prestress level of 25% f_{pu}. The control column, BR-SP1, experienced strength decay at 6% drift, followed by the rupturing of longitudinal bars. This column behaved very well in flexure, even without retrofitting, because of the of spiral reinforcement. Hence the column did not need any retrofitting. The retrofitted column, BR-SP2, was prepared to investigate if any further improvement in behaviour would be obtained, while also showing the behaviour of a fiber-reinforced concrete jacket placed over the strands. It exhibited similar behaviour as the control column, in that it withstood cycles at 6% drift, followed by the rupturing of longitudinal bars. This can be seen in the hysteretic Moment-Drift relationships shown in Fig. 4.5.

4.3 Mechanism of Load Resistance and Modes of Behaviour

There are two basic modes of failure for a typical reinforced concrete column; shear and flexure. Columns are usually referred to as shear-dominant and flexure-dominant columns. Shear-dominant columns often have short shear spans, and are subjected to high levels of shear forces. Usually, these columns can not develop their full flexural capacity, showing premature failure due to diagonal tension and/or diagonal compression. Shear failure is usually regarded as a brittle form of failure, occurring with rapid strength degradation. Hence, this type of failure is prevented in design. The flexure-dominant columns often have long shear spans, and are subjected to higher flexure. These columns first develop their flexural yield point, prior to any distress in shear. Flexural yielding is associated with the yielding of longitudinal reinforcement. Therefore, these columns show ductile behaviour that results in gradual strength decay. In earthquake resistant design, where inelastic deformations are relied on for energy dissipation, it is desirable to promote this flexural mode of response. Although flexural behaviour is ductile, it may become brittle if dominated by compression concrete. Columns subjected to high compression may show brittle failure if the column capacity is attained prior to the yielding of the longitudinal reinforcement. In such cases, the behaviour of concrete, and hence the entire column can only be improved by increasing confinement.

4.3.1 Shear-Dominant Columns

Columns BR-C1 and BR-S1 had a short shear span, and developed a shear dominant mode of failure. The columns first developed flexural and shear cracks, during the early stages of testing. The shear cracks continued to widen under diagonal tension as the drift level increased. Eventually, there was a sudden failure of the column, resulting from lack of resistance to the high level of diagonal tension applied. Crossing of inclined cracks under cyclic loading also resulted in degradation of concrete.

When retrofitted, shear dominant columns improved significantly. Most importantly, the mode of failure changed from shear to flexure. The prestressed strands, spaced at 150 mm, provided excellent resistance to diagonal tension and prevented shear failure. This increased the shear capacity above the level corresponding to flexural yielding. The columns developed flexural yielding and showed a high level of deformability. As observed during testing, the drift capacity increased from 1% to approximately 5%. The shear cracks did not develop till much later, and they did not widen very much after having formed.

4.3.2 Flexure-Dominant Columns

Columns BR-C6, BR-S3 and BR-SP1 had a flexure-dominant mode of failure. The columns developed flexural cracks in early stages of testing. Some shear cracks also formed at later stages of loading, but never widened as the ones in shear-dominant columns. The flexure dominant response occurred either due to increased shear span or increased transverse reinforcement. In the former case the applied shear was low, whereas in the latter shear resistance was high. These columns showed much more ductile behaviour than columns with a shear- dominant failure mode. The non-retrofitted flexure-dominant columns withstood 2% drift before failing during or at the end of the cycles at 3% drift. Column BR-SP1 was designed to conform to current design standards and withstood 5% drift without showing any significant signs of strength degredation. The strength decay became evident during the cycles at 6% drift, occuring shortly before the longitudinal bar fracture - marking the limit of the column capacity.

4.4 Comparison of Shear-Dominant and Flexure-Dominant Columns

The columns tested in both phases of this experimental investigation had many similarities. Some had similar reinforcement details but different aspect ratios whereas others had similar aspect ratios with different reinforcement arrangements. The comparison of these columns demonstrates the effects of aspect ratio and column retrofitting. The two shear dominant columns, BR-C1 and BR-S1, are compared with flexure dominant columns, BR-C6, BR-S3 and BR-SP1, demonstrating either the effects of concrete confinement or aspect ratio. The retrofitted columns are also included in the graphs, as the retrofitting increases concrete confinement.

The comparisons are made using the envelopes of Moment-Drift relationships. It should be noted that the area under these envelopes effectively represent the amount of energy dissipated by each column. Therefore, the greater the area under the envelope is, the more ductile a column is - which improves the seismic performance. Because the tests were conducted under pseudo-static load conditions, this area does not give the actual energy dissipation. During an actual seismic event, the moment capacities of these columns would be higher (it is dependant on the rate of loading) and therefore, the area would be larger - i.e. more energy dissipation.

4.4.1 Effect of Transverse Reinforcement

Columns BR-C1 and BR-SP1 had almost the same aspect ratio, 2.4 and 2.5, respectively. They both had a circular cross-section and circular reinforcement arrangement. The only difference was in the amount of transverse reinforcement. Column BR-SP1 had four times the transverse reinforcement that Column BR-C1 had. Increased transverse reinforcement provided increased shear resistance, changing the mode of failure from that of shear to that of flexure. Furthermore, the use of higher volumetric ratio of transverse reinforcement, in the form of a spiral with a small pitch, further improved concrete confinement. The improvement in concrete confinement increased ductility of core concrete as well as the deformability of the entire column. Improved confinement often results in improved behaviour in flexural compression and shear induced diagonal compression.

Figure 4.6 shows the comparison of these two columns with different amounts of transverse reinforcement. The difference in moment resistance can be explained by the larger size of longitudinal reinforcement used, as well as the higher strength of concrete in Column BR-C1.

The difference in transverse reinforcement resulted in a brittle shear failure in the Column BR-C1, whereas Column BR-SP1, with increased volumetric ratio of transverse reinforcement, developed ductile response in flexure. The flexural response resulted in a higher drift capacity. In this case, Column BR-SP1 was adequately confined and no retrofitting was necessary. However, Column BR-C1 with a shear-dominant failure mode, did require retrofitting for improved deformability. The companion column, BR-C2, was retrofitted by means of external prestressing. As indicated earlier, retrofitting increased both the shear capacity, as well as concrete confinement. The result, was improved column deformability.

4.4.2 Aspect Ratio

Two distinctly different levels of column aspect ratio (shear-span-to-depth ratio) were used in the test program. The circular columns, BR-C1 and BR-C6, generally had the same reinforcement configuration. Similarly, the square columns, BR-S1 and BR-S3, had the same reinforcement arrangement, but distinctly different aspect ratio. Because of the differences in column height and cross-sectional dimension, the aspect ratios were quite different. For Columns BR-C1 and BR-C6, the aspect ratios were 2.4 and 3.9, respectively. For Columns BR-S1 and BR-S3, the aspect ratios were 2.7 and 4.0, respectively. The comparison of columns with different aspect ratios are presented for circular and square columns in Fig. 4.7 and Fig. 4.8, respectively.

The results reveal that differences in aspect ratio resulted in different modes of behaviour. Columns BR-C1 and BR-S1, with a lower aspect ratio failed in shear, whereas Columns BR-C6 and BR-S3, with a high aspect ratio failed in flexure. The columns that behaved in flexure showed increased ductility, with higher drift capacity. In all cases, retrofitting improved column performance. The effect of retrofitting on columns with low aspect ratio was to improve diagonal tension resistance, increasing column shear capacity.

Retrofitting also changed the mode of behaviour to flexure. It improved confinement of column concrete, resulting in increased deformability of columns in flexure. The confinement provided by external prestressing was highly effective, not only because the prestressing hoops provided active and passive confinement pressures, but also because of the increased area of confined concrete, as the external hoops confined both the cover and core concrete.

4.4.3 Retrofitting of Shear-Dominant and Flexure-Dominant Columns

The control columns consistently suffered from brittle behaviour associated with lack of transverse reinforcement, with the exception of the spirally reinforced column, which had a sufficient volumetric ratio of transverse steel. Hence, the basic rationale behind providing external prestressing as column retrofitting was to make up for this deficiency in transverse reinforcement. External prestressing of shear-dominant columns provided extra diagonal tension resistance, while also controlling diagonal cracks in concrete. The initial prestress in strands reduced crack widths and improved the mechanism of aggregate interlock, thereby increasing shear resistance of cracked concrete. Once the active lateral pressure has been overcome by increased shear, the strands then behaved as shear reinforcement, adding to the diagonal tension resistance. Once the diagonal tension failure was eliminated, the strands also helped improve ductility of compression concrete through confinement. Closely spaced transverse prestressing hoops confined both the cover and core concrete, and increased column deformability.

Although flexure dominant members generaly exhibit improved deformability, columns under combined axial compression and flexure may show limited ductility, especially under cyclic loading. Retrofitting flexure-dominant columns that have high aspect ratios, with external prestressing, improves concrete confinement. It was shown experimentally that a maximum hoop spacing of approximately one quarter of column cross-sectional dimension was adequate to provide the required confinement.

The spacing of prestressing strands was examined in Phase I of the current investigation. It was concluded that a spacing of 300 mm, which was approximately equal to one half the cross-sectional dimension, was too large for shear dominant columns, and that

a spacing of 150 mm was more appropriate. Columns BR-C2 and BR-S2, had a large drift capacity. These columns developed in excess of 5% lateral drift, which is certainly higher than the level expected in a strong seismic activity.

For the flexure-dominant columns the 150 mm spacing worked very well but is not necessarily needed throughout the whole height of the column. In the plastic hinging zone, this small spacing may be required, but elsewhere the spacing can be increased. Caution should be exercised not to allow shear failure in these parts of the column or other failure due to redistribution of stresses. For the retrofitted square column, BR-S4, the prestressing strand spacing in the top half of the column was increased to 250 mm without any ill effects to the column behaviour. Care should be taken if the spacing is to be increased. However, based on limited data available, it is difficulty to recommend more accurate requirements for hoop spacing.

4.5 Retrofit Needs - Column Analysis

The first step in determining whether or not a column needs retrofitting is to analyse the column to find out the failure mode and drift capacity. This can be accomplished by using a computer program. A COLumn Analysis program (COLA) was developed by Yalcin (1997) to establish the flexural capacity of columns, as well as their deformations. This analysis program is based on models which predict deformations due to flexure as well as anchorage slip. Confined and unconfined concrete behaviour have been modelled and introduced in the form of material models. The formation and progression of plastic hinging was considered through the algorithm developed by Razvi and Saatcioglu (1996).

The computer program was used to generate extensive data by Yalcin (1997) to establish force and deformation capacities of existing bridge columns. Some typical tables and charts were prepared, expressing column drift capacity as a function of different parameters. The parameters considered were: column aspect ratio, transverse and longitudinal reinforcement ratio, gross-to-core-concrete area ratio, and concrete and steel strength. These tables and charts can be utilized to predict column shear and flexural capacities, as well as drift capacity.

4.5.1 Column Evaluation Based on Charts

The Tables and Charts developed by Yalcin (1997), as part of the first phase of current research program, were used to establish strength and deformability of the control columns. Three control columns from the current phase, and two control columns from the earlier phase were used for this purpose. Unfortunately, these tables and charts were prepared as sample charts, and were not general in scope. Therefore, only a limited use of them could be made. Figures 4.9 and 4.10 illustrate the charts adopted from Yalcin (1997). To use these charts, the information shown below had to be prepared first.

	BR-C1	BR-C6	BR-SP1	BR-S1	BR-S3
r	0.054	0.076	0.275	0.059	0.084
Aspect Ratio	2.43	3.94	2.54	2.7	4.0
P/Po	15%	15%	15%	15%	15%
ρ_l	2.1%	1.8%	1.23%	1.98%	1.44%

The r value is a function of the volumetric ratio of transverse steel (ρ_v), the yield strength of transverse steel (f_{yh}), the concrete strength (f'_c), and the gross and core concrete area of the column (A_g and A_c). It is expressed as indicated below:

$$r=\rho_v \frac{f_{yh}}{f'_c} \frac{1}{(A_g/A_c-1)}$$

The column strength was determined from Fig. 4.9, and gave analytical predictions that matched the experimental values. These charts help predict whether the column fails in shear or flexure. For the five columns listed above, the charts indicate that Columns BR-C1 and BR-S1 should experience shear failure, whereas the other three columns should experience flexural failure. These results are in agreement with experimental observations.

The drift capacity for each circular columns was estimated using the charts in Fig. 4.10. These charts specify circular columns, therefore the square columns were not

evaluated using these charts. The axial load level for all columns was P/P_o = 15%. Hence the values in the charts, given for P/P_o = 10% and 20%, had to be interpolated. Using Chart C for Column BR-C1, the drift capacity was estimated to be 1.8%. The aspect ratio of 2.43 and ρ_l of 2.1 were close to the chart values (ρ_l is the volumetric longitudinal reinforcement ratio). The experimental results suggested a drift capacity of approximately 1.4%. The agreement between the value obtained from the chart and experimentally recorded value appear to be good.

The estimated drift capacity for Column BR-C6, using Charts C and D, was about 2.5%. The aspect ratio of 3.94 was interpolated between the two charts, and ρ_l of 1.8% was taken as 2% to simplify the interpolation. The experimental results suggest a drift capacity of about 3%. Therefore, the estimation was not too far off.

The drift capacity for Column BR-SP1, using Charts A and C, was estimated to be 3.5% or above. In this case, the Chart A shows a plateau for P/P_o = 10%. Having P/P_o = 15% was difficult to interpolate. The aspect ratio of 2.54 was very close to the chart value, and for ρ_l of 1.23% the value was interpolated between the two charts putting more emphasis on Chart A (ρ_l = 1%). The 3.5% drift estimation was a poor estimation when compared with the experimental results which suggested 6% drift capacity.

In conclusion, these charts may be a good starting point, and may be applicable if the purpose is to prioritize columns within a retrofitting program. However, the results obtained for the five columns do not show these charts to be very accurate. This inaccuracy may be due, in large part, to the limited number of charts that were available, and their generalized format. The chart which seemed to work the best was the one which determined the column's failure mode (fig. 4.9), but this is based on limited trials. It should be noted that a more detailed analysis, using COLA for example, should be done before discounting any columns from a retrofitting program and deeming them safe with no need of retrofitting. The results of a more detailed analysis using COLA will be displayed in this next section. The results from COLA can be compared to the results obtained from the column evaluation using the charts, as these results will also be included in the tables.

4.5.2 Column Analysis Using COLA

The three control columns from this experimental program as well as the two control columns from Yalcin (1997) were analysed using COLA. The results are displayed in the table below and compared with the chart evaluation and experimental results. The shear capacity could not be calculated by COLA. However, the computed shear capacities based on CSA A23.3 (1994) were included in the same tables. Also, the drift capacity was computed at 80% of its ultimate capacity. Note that the material strengths used in the analysis were taken as determined by coupon tests to get as close to experimental results as possible.

Column BR-SP1	COLA-analysis	Chart-analysis	Experimental
Shear Capacity	850 kN	N/A	N/A
Shear Capacity x Span	1310 kNm	N/A	N/A
Flexural Moment Capacity	650 kNm	N/A	775 kNm
Failure Mode	flexural	flexural	flexural
Drift Capacity [1]	6.5% [1]	> 3.5%	6.0% [1]
1) Drift capacity was governed by the failure of the longitudinal bars, not 80% of column capacity.			

Column BR-C1	COLA-analysis	Chart-analysis	Experimental
Shear Capacity	480 kN	N/A	N/A
Shear Capacity x Span	715 kNm	N/A	850 kNm
Flexural Moment Capacity	850 kNm	N/A	N/A
Failure Mode	shear	shear	shear
Drift (80% Capacity)	2%	1.8%	1.6%

Column BR-C6	COLA-analysis	Chart-analysis	Experimental
Shear Capacity	320 kN	N/A	N/A
Shear Capacity x Span	640 kNm	N/A	N/A
Flexural Moment Capacity	435 kNm	N/A	480 kNm
Failure Mode	flexural	flexural	flexural
Drift (80% Capacity)	3.5%	2.5%	3.0%

Column BR-S1	COLA-analysis	Chart-analysis	Experimental
Shear Capacity	495 kN	N/A	N/A
Shear Capacity x Span	735 kNm	N/A	800 kNm
Flexural Moment Capacity	920 kNm	N/A	N/A
Failure Mode	shear	shear	shear
Drift (80% Capacity)	2.2%	N/A	1.8%

Column BR-S3	COLA-analysis	Chart-analysis	Experimental
Shear Capacity	390 kN	N/A	N/A
Shear Capacity x Span	780 kNm	N/A	N/A
Flexural Moment Capacity	565 kNm	N/A	600 kNm
Failure Mode	flexural	flexural	flexural
Drift (80% Capacity)	3.2%	N/A	3.0%

From these tables it is apparent that COLA slightly underestimates the column moment capacity. As for drift capacity, COLA overestimates lateral drift capacity slightly. However, in view of the types of experimental test conducted, this slight overestimation may be insignificant and expected. In order to match how COLA calculates the drift capacity, the experimental drift capacity results presented are taken at the point when the capacity dropped below 80% of peak. Based on these predictions, this program would appear to be an excellent way of determining the seismic adequacy of existing columns.

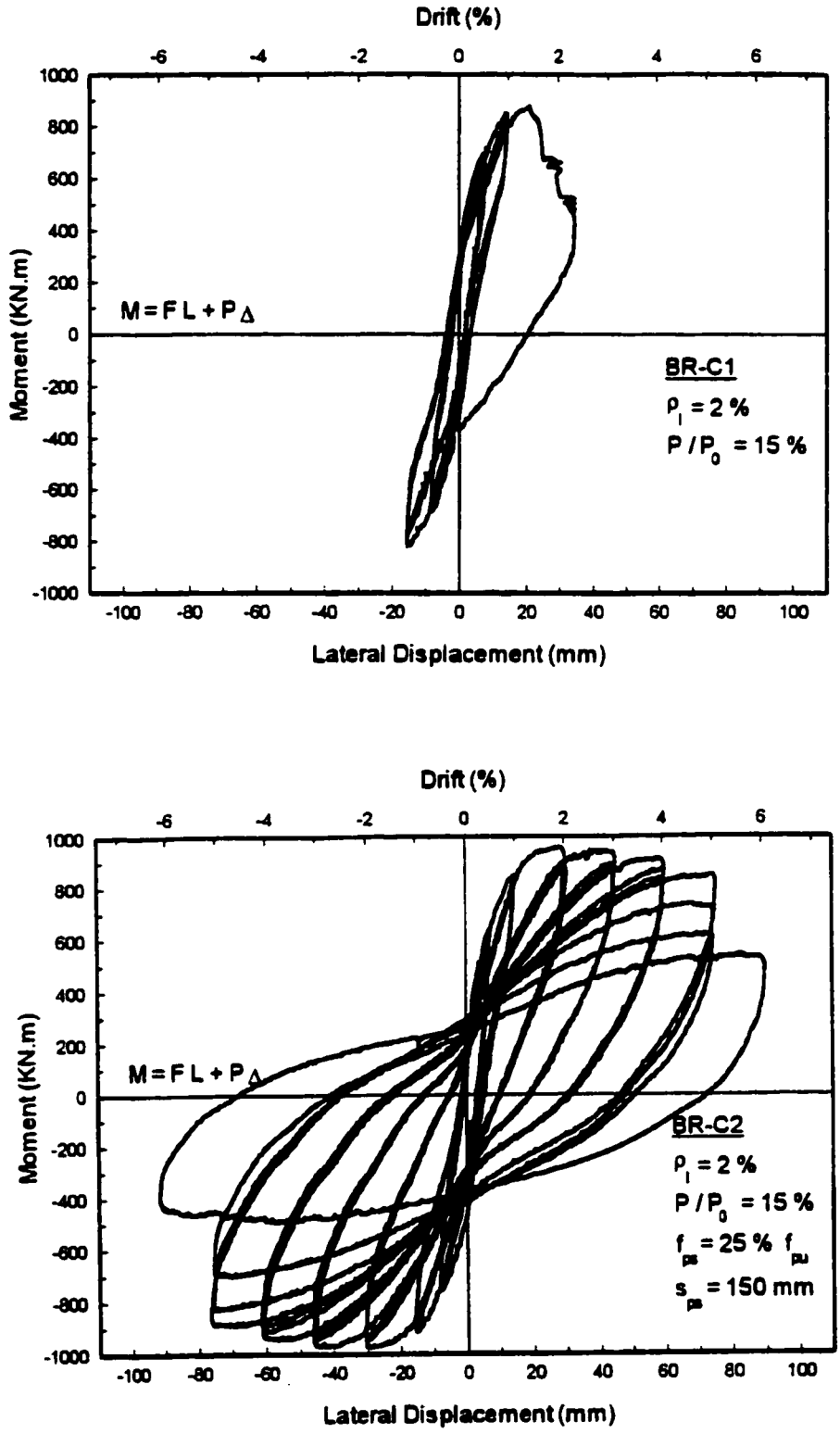

Fig. 4.1 Moment-Drift relationship for columns BR-C1 and BR-C2 (Yalcin 1997)

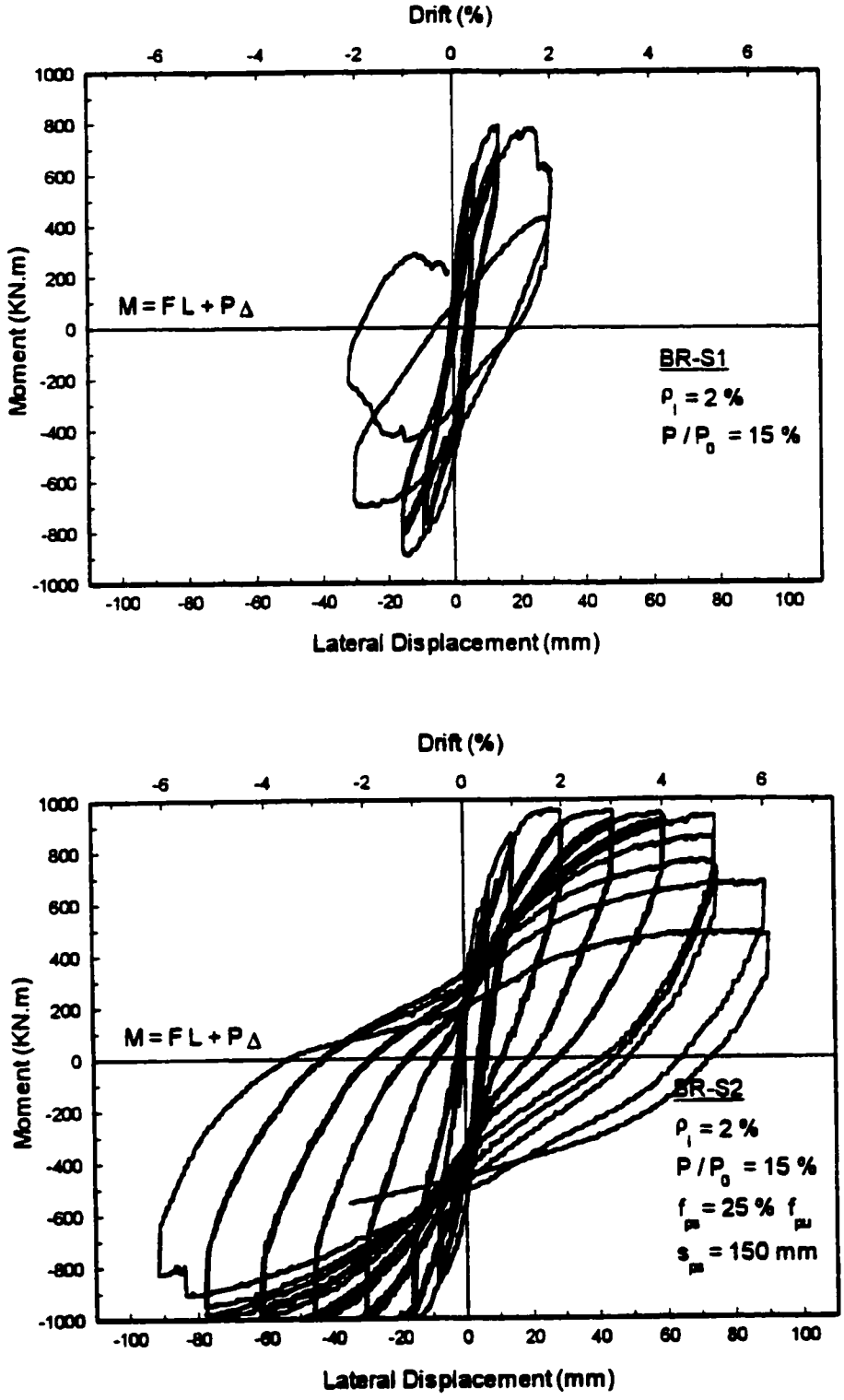

Fig. 4.2 Moment-Drift relationship for columns BR-S1 and BR-S2 (Yalcin 1997)

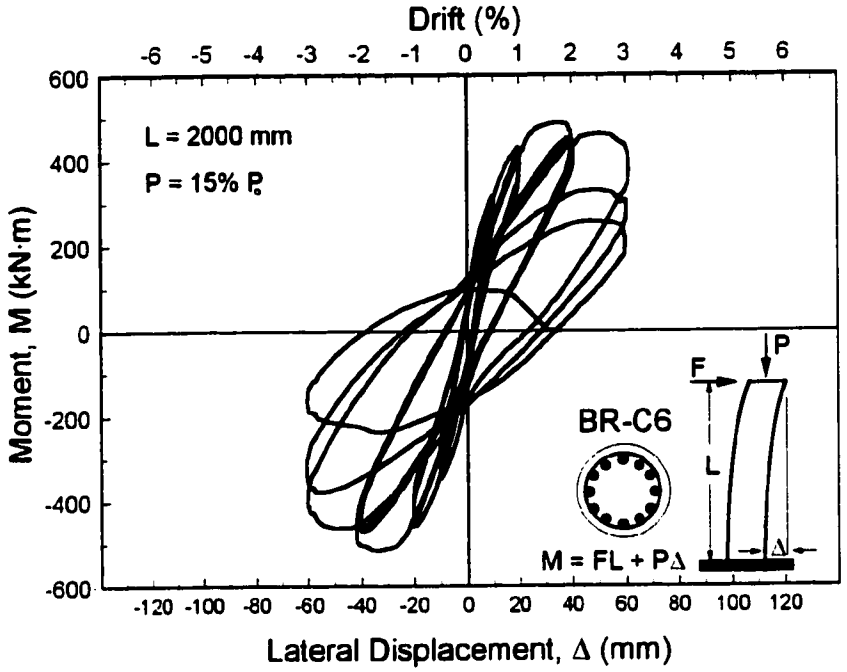

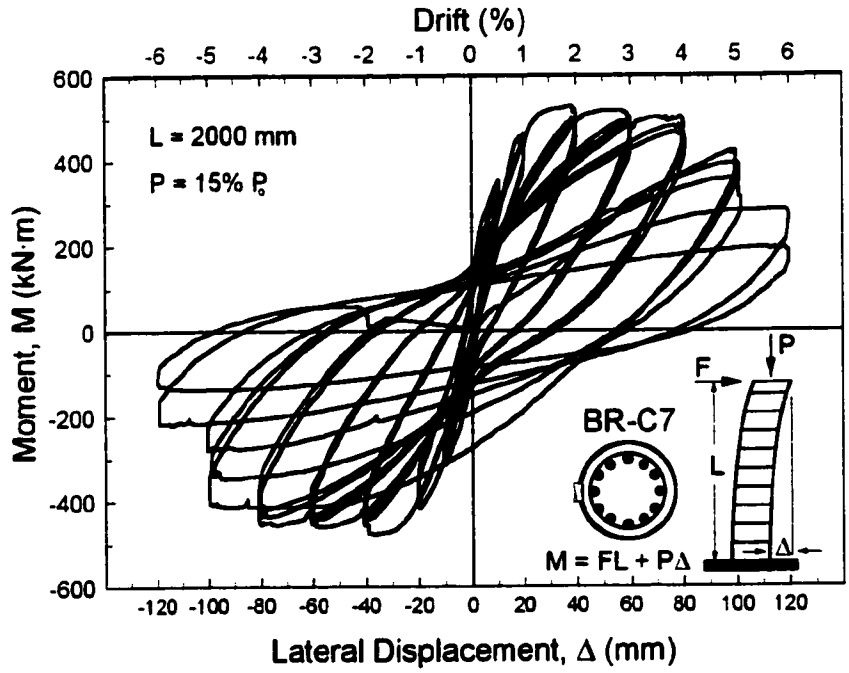

Figure 4.3 Moment-Drift relationship for columns BR-C6 and BR-C7

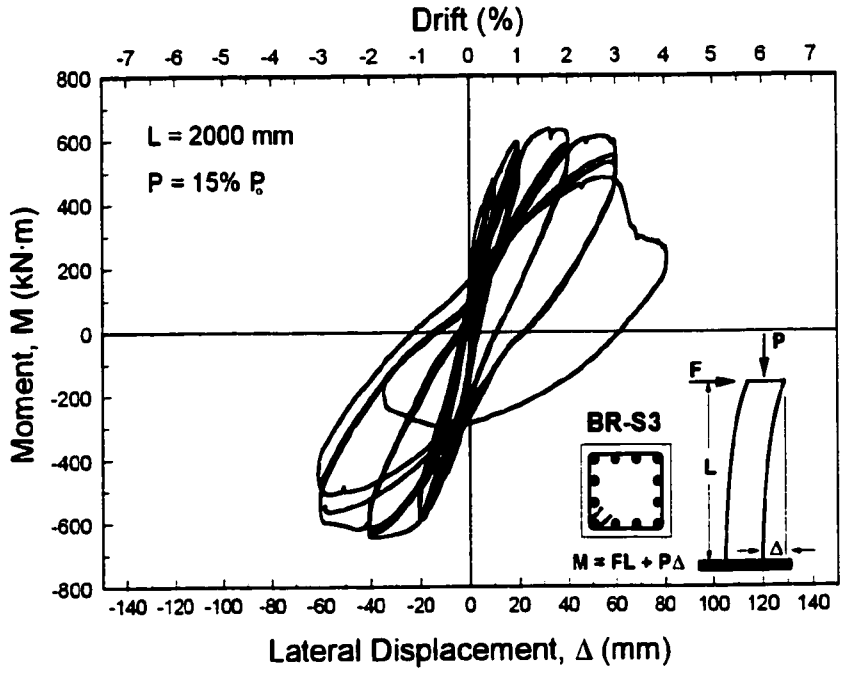

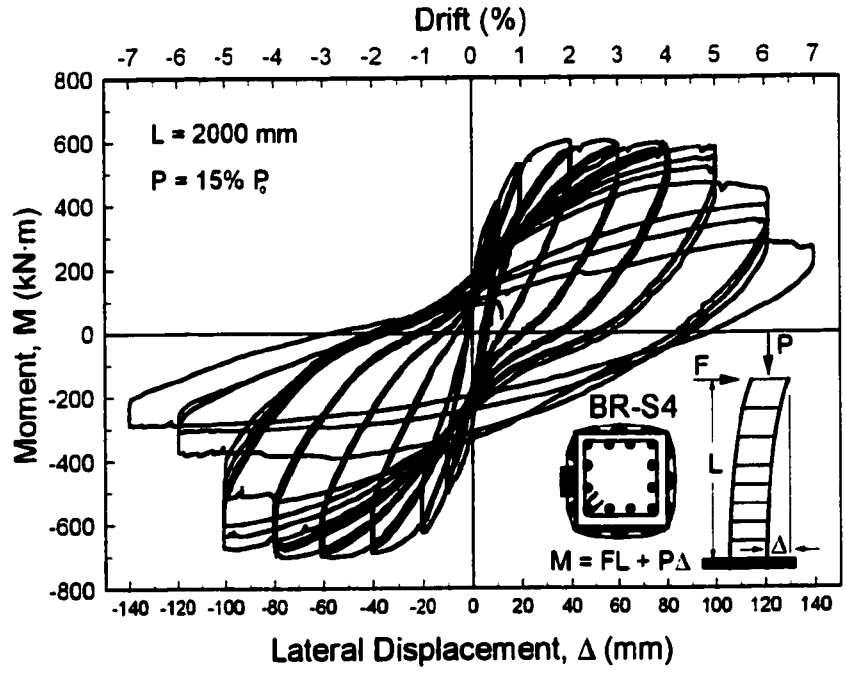

Figure 4.4 Moment-Drift relationship for columns BR-S3 and BR-S4

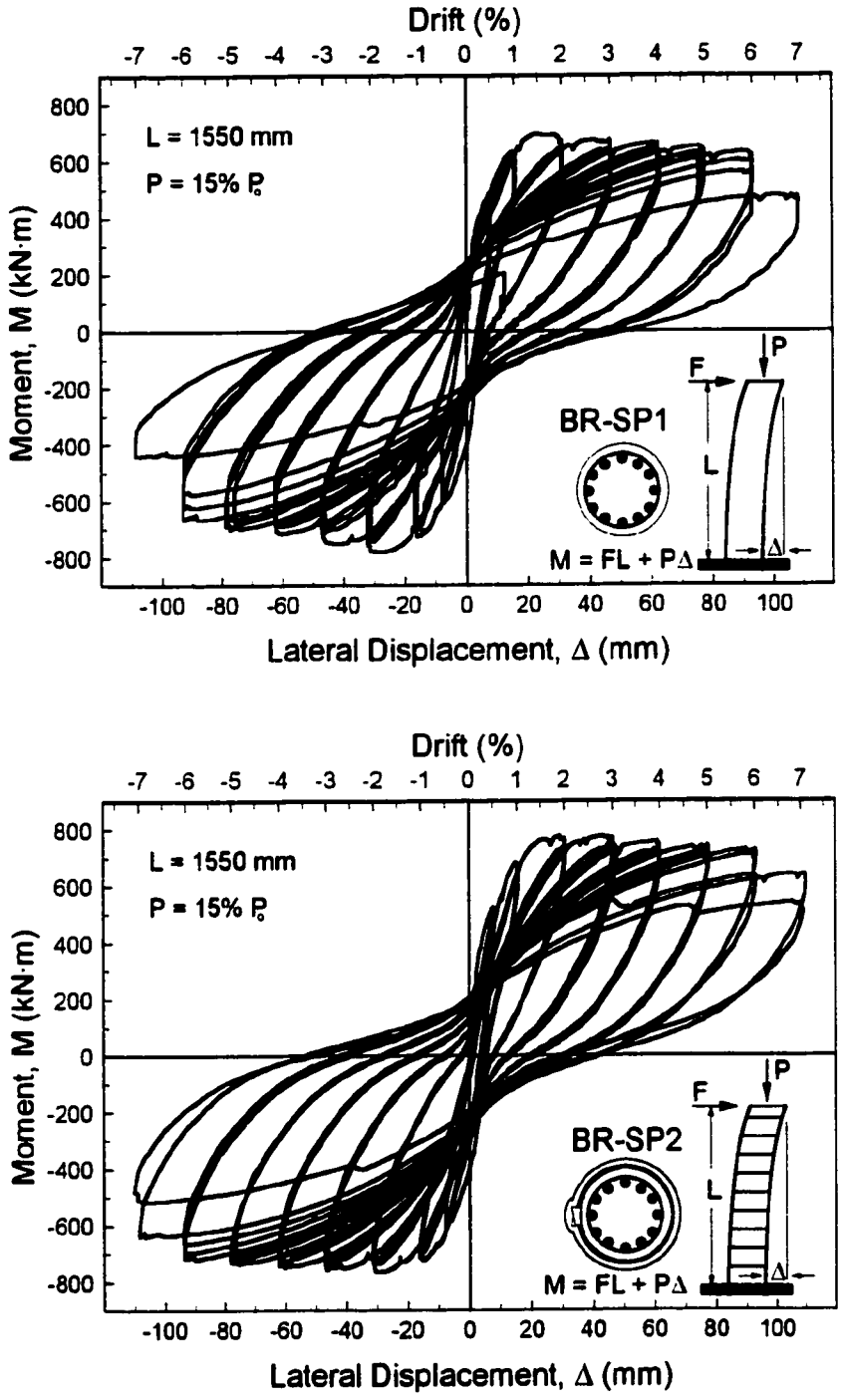

Figure 4.5 Moment-Drift relationship for columns BR-SP1 and BR-SP2

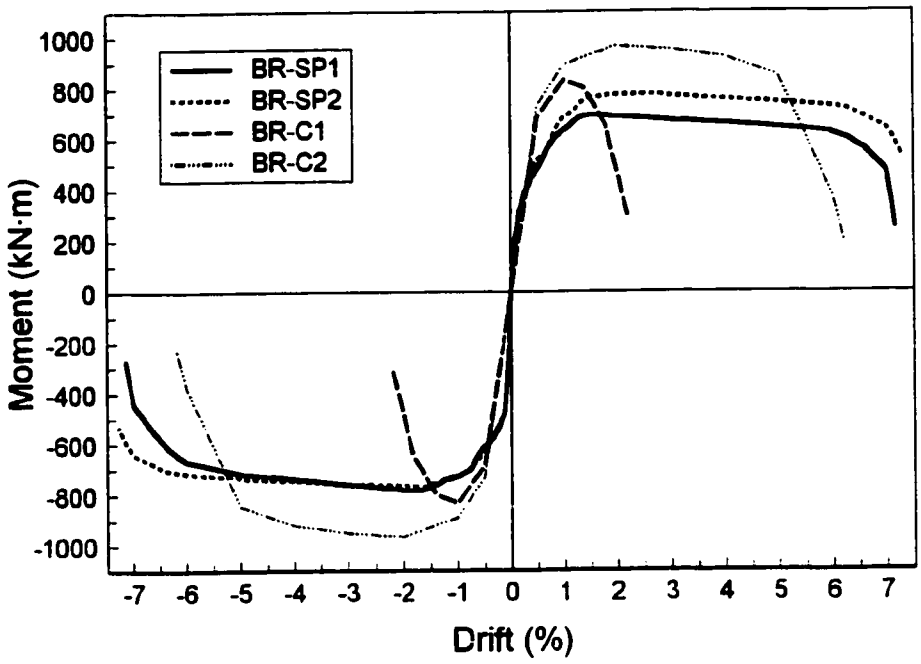

	BR-C1	BR-C2	BR-SP1	BR-SP2
shear span, L (mm)	1485	1485	1550	1550
outside diameter of column, D (mm)	610	610	610	610
spacing of #10 tied hoops, in mm	300	300	N/A	N/A
pitch of #10 spiral reinforcement (mm)	N/A	N/A	75	75
volumetric ratio of transverse reinforcement	0.267%	0.267%	1.067%	1.067%
spacing of prestressing strands (mm)	N/A	150	N/A	150
number and size of longitudinal bars	12 #25	12 #25	12 #20	12 #20
reinforcement ratio of longitudinal bars	2.1%	2.1%	1.23%	1.23%
concrete strength (MPa)	45	45	35	35
axial load (in % of P_o)	15%	15%	15%	15%

Fig. 4.6 Comparison of circular columns with an aspect ratio of approximately 2.5

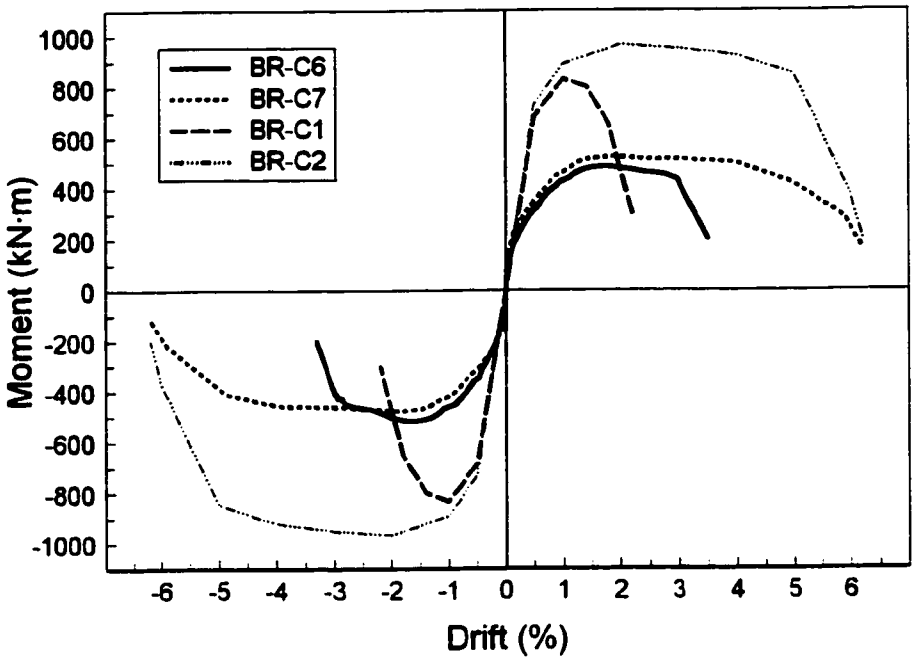

	BR-C1	BR-C2	BR-C6	BR-C7
shear span, L (mm)	1485	1485	2000	2000
outside diameter of column, D (mm)	610	610	508	508
column aspect ratio (L/D)	2.43	2.43	3.94	3.94
spacing of #10 tied hoops (mm)	300	300	300	300
volumetric ratio of transverse reinforcement	0.267%	0.267%	0.325%	0.325%
spacing of prestressing strands (mm)	N/A	150	N/A	150
number and size of longitudinal bars	12 #25	12 #25	12 #20	12 #20
reinforcement ratio for longitudinal bars	2.1%	2.1%	1.8%	1.8%
concrete strength (MPa)	45	45	35	35
axial load (in % of P_o)	15%	15%	15%	15%

Fig. 4.7 Comparison of circular columns with different aspect ratios

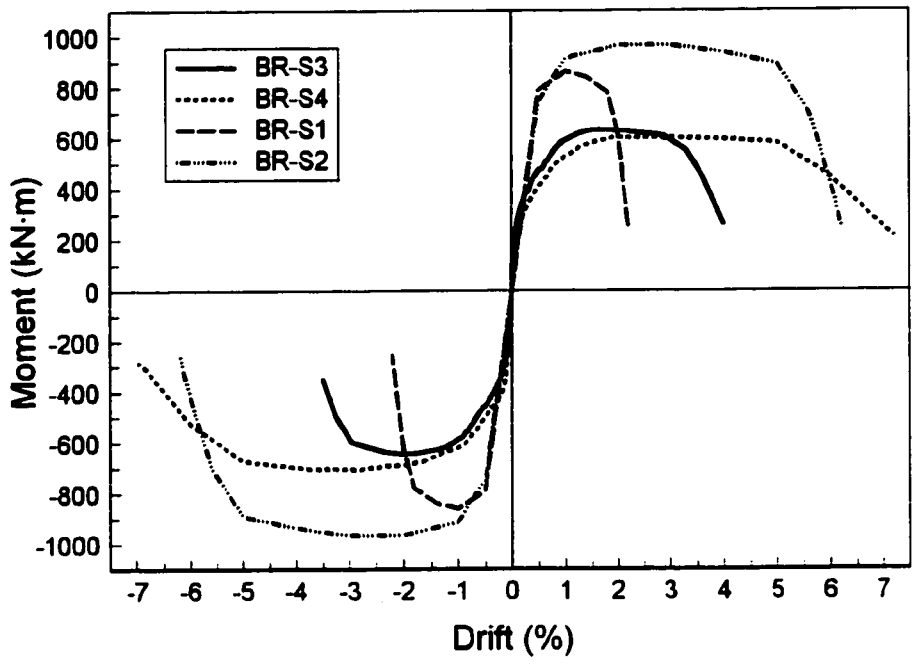

	BR-S1	BR-S2	BR-S3	BR-S4
shear span, L (mm)	1485	1485	2000	2000
outside dimension of column, D (mm)	550	550	500	500
column aspect ratio (L/D)	2.7	2.7	4.0	4.0
spacing of #10 tied hoops (mm)	300	300	300	300
volumetric ratio of transverse reinforcement	0.296%	0.296%	0.325%	0.325%
spacing of prestressing strands (mm)	N/A	150	N/A	150
number and size of longitudinal bars	12 #25	12 #25	12 #20	12 #20
reinforcement ratio for longitudinal bars	1.98%	1.98%	1.44%	1.44%
concrete strength (MPa)	45	45	35	35
axial load (in % of P_o)	15%	15%	15%	15%

Fig. 4.8 Comparisson of square columns with different aspect ratios

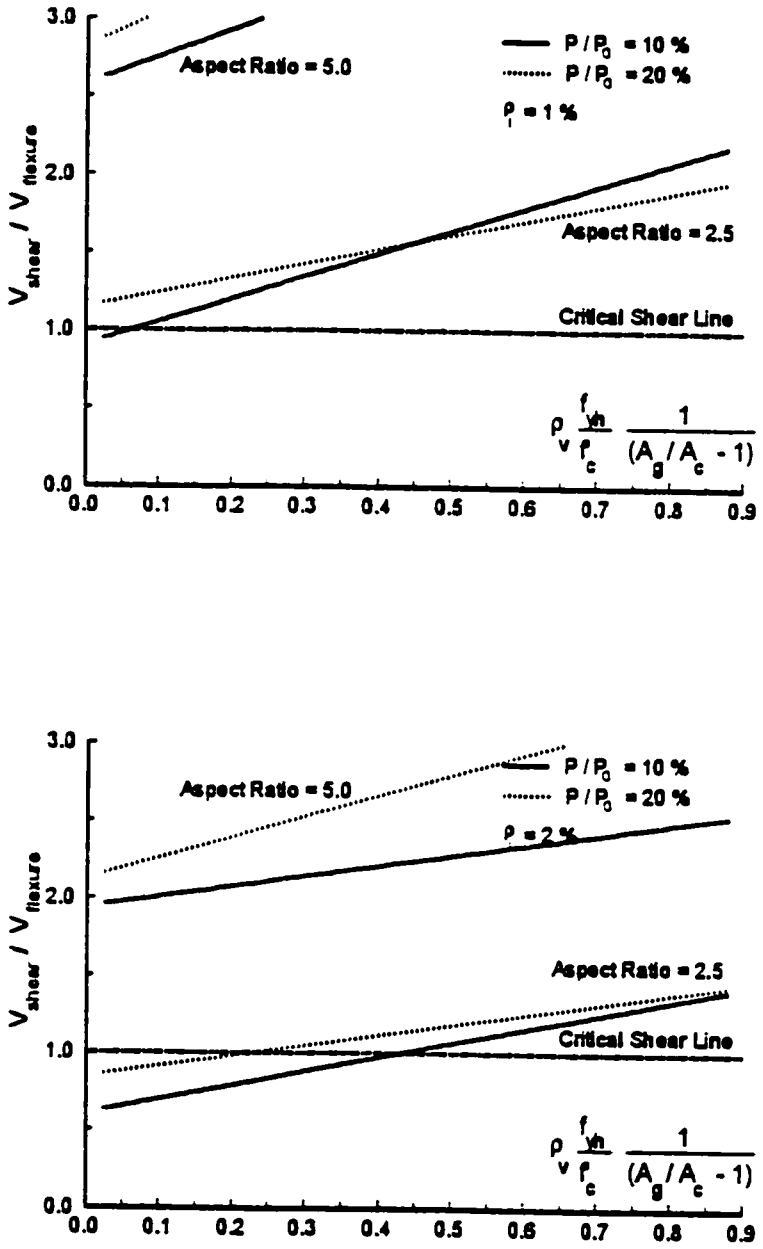

Fig. 4.9 Charts for prediction of shear and flexural behaviour of columns for various longitudinal reinforcement (Yalcin 1997)

Chart A

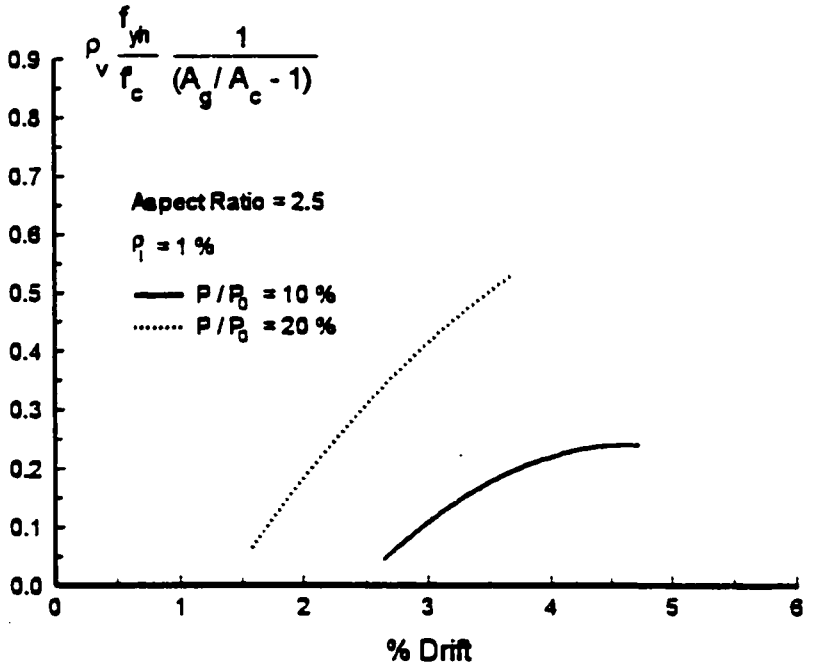

Chart B

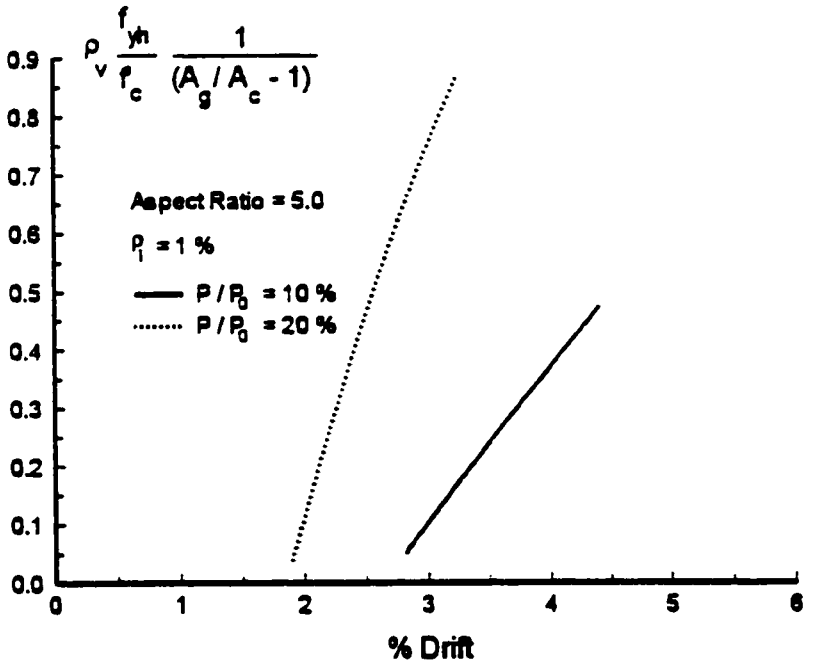

Fig. 4.10 Design charts for circular columns (Yalcin 1997)

Chart C

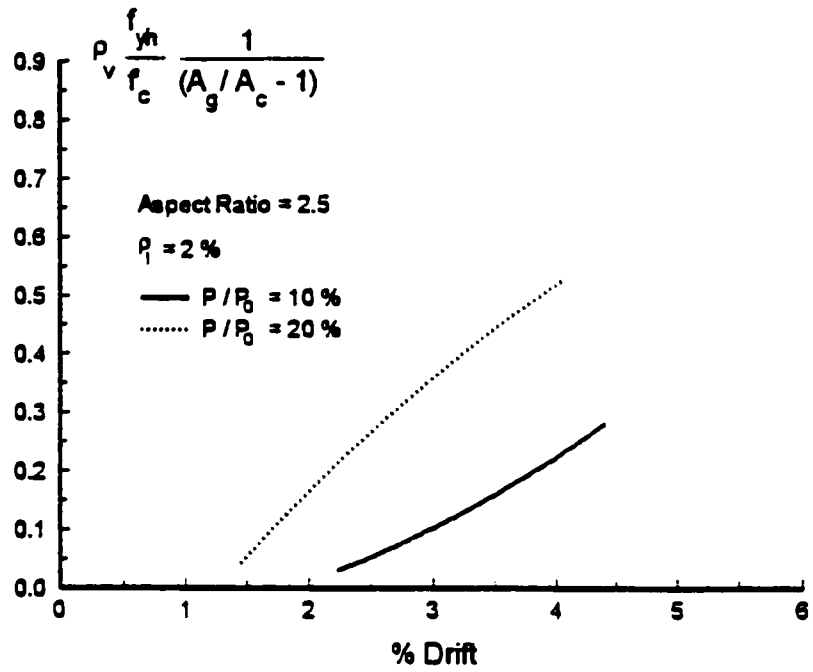

Chart D

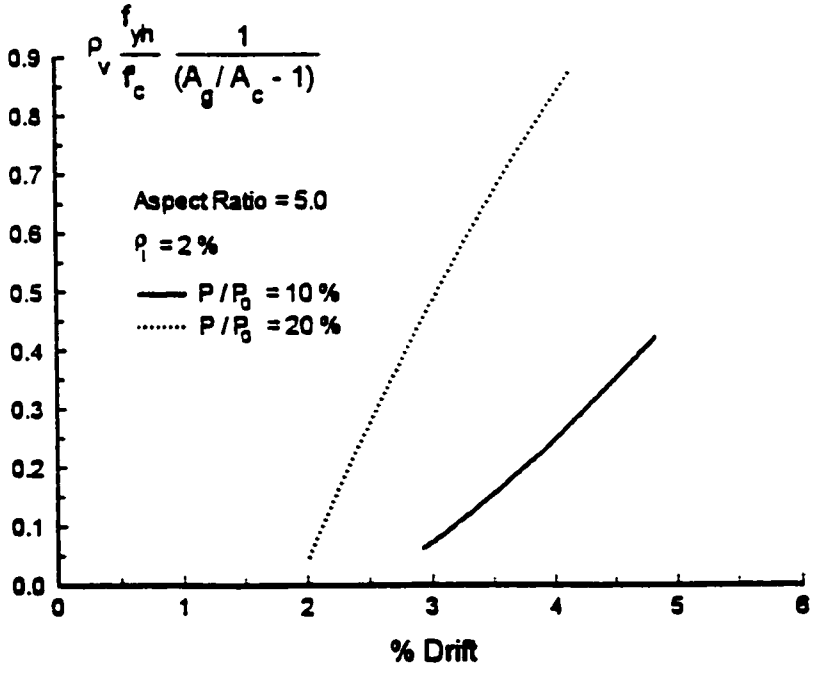

Fig. 4.10 Design charts for circular columns (Yalcin 1997)

Chapter 5

Summary and Conclusions

5.1 Summary

An experimental investigation was carried out to test a new retrofitting technique for circular and square bridge piers, which consisted of external prestressing by means of high-strength steel strands. The first phase of the experimental program (Yalcin, 1997) included shear-dominant columns and different retrofitting schemes. The second phase was based on the results of the previous phase, and included columns with different aspects ratios, covering a range of shear-dominant and flexure-dominant columns. In all, 13 near full size columns were tested, which consisted of square and circular columns with tied reinforcement, based on pre-1971 design practice, as well as circular columns with spiral reinforcement, reflecting the current practice. Of the 13 columns tested, 6 were tested in the current phase. The test program, experimental findings, as well as analytical predictions for these columns are presented in detail in the thesis. A literature review was also conducted on research involving other retrofitting strategies.

5.2 Conclusions

From the literature review, it can be concluded that bridge columns built on the basis of pre-1971 codes have inadequate seismic resistance when located in zones of high seismicity. For reinforced concrete bridge columns, the problems are due, in large part, to inadequate concrete confinement, lack of shear resistance, and poor reinforcement overlap details. To overcome these inadequacies, research has been done to develop retrofitting techniques to properly confine the existing columns. All the techniques researched have successfully improved the columns. However, some were more noteworthy and proved to have wider applications. Different techniques also had

different economic implications. By far the most commonly used technique in practice is steel jacketing. However, this technique is expensive and labour and material intensive. Therefore, other techniques, such as carbon fibre wrap and external prestressing, may be viable alternatives.

The following conclusions may be drawn from the experimental investigation reported in this thesis.

- The majority of existing concrete bridge columns, designed prior to 1971, are seismically deficient. Columns with low aspect ratio, behaving predominantly in the shear mode, develop brittle failure. Columns with approximately 2.4 aspect ratio showed a lateral drift capacity of approximately 1% prior to a significant strength decay. Those with increased shear span of approximately 4.0 showed somewhat higher lateral drift capacity of about 2%, prior to strength decay. Present day American and Canadian codes suggest that columns in regions of high seismicity should be able to resist deformations of 2% to 3% drift without significant strength degredation.
- A spirally reinforced column, conforming to the current code requirements (with 75 mm spiral pitch), showed a ductile response, in spite of the relatively low aspect ratio of 2.5. This column was able to sustain incrementally increasing deformation reversals of up to 6% lateral drift. This indicates that, for the given volumetric ratio of transverse reinforcement tested, spirally reinforced concrete columns are well designed for regions of high seismicity.
- The new retrofitting technique, developed at the University of Ottawa, consisting of external prestressing by high-strength steel strands, was very effective in improving strength and deformability of test columns. The technique was effective in both shear-dominant and flexure-dominant columns.
- The retrofitting technique worked best when the external prestressing strands had a spacing of 150 mm with an initial prestress of 25% f_{pu}. This spacing was found to control shear cracking, while enhancing diagonal tension resistance in shear-dominant columns. The same spacing was sufficiently small to provide effective confinement to compression concrete in flexure-dominant columns. However, it is conceivable that a larger spacing may be adequate for less critical portions of columns.

- The retrofitting scheme was equally effective for circular and square columns. The raiser discs and the related attachments used to distribute external prestressing over faces of square columns, proved to be very effective in achieving near-uniform lateral pressure.
- Retrofitting flexure-dominant columns resulted in improvements of drift capacity from 2% to 4%. Furthermore, the failure observed was more gradual than that of non-retrofitted columns.
- Retrofitting a properly designed spirally reinforced column did not result in any appreciable improvement in column deformability. The fibre-reinforced concrete jacket implemented on this column, providing corrosion protection, performed very well. There was little damage to the jacket during many cycles of lateral load. The jacket maintained its integrity until after 5% drift.
- The analytical approach used to establish inelastic force-displacement relationships of columns was able to provide good predictions of inelastic drift. The computer program, incorporating the approach, produced fairly accurate estimates of lateral drift and flexural strength for non-retrofitted columns.
- Laboratory experiments with the new retrofitting technique revealed that the technique could be implemented in practice with little difficulty. Both the labour and material costs are likely to be reduced, as compared to steel jacketing, while attaining similar improvements in column behaviour.

References

Aboutaha, R.S.; Engelhardt, M.D.; Jirsa, J.O.; and Kreger, M.E. (1996), "Retrofit of Concrete Columns with Inadequate Lap Splices by the Use of Rectangular Steel Jackets", Earthquake Spectra, Vol.12, No.4, Nov. 1996, pp. 693-714.

Chai, Y.H. (1996), "An Analysis of the Seismic Characteristics of Steel-Jacketed Circular Bridge Columns", Earthquake Engineering and Structural Dynamics, Vol.25, No.2, Feb. 1996, pp. 149-161

Chai, Y.H.; Priestly, N.;and Seible, F. (1991), "Seismic Retrofit of Circular Bridge Columns for Enhanced Flexural Performance",ACI Structural Journal, Vol.88, No.5, Sept.-Oct. 1991, pp. 572-584

Coffman, H.L.; Marsh, M.L.; and Brown, C.B. (1993), "Seismic Durability of Retrofitted Reinforced-Concrete Columns", Journal of Structural Engineering, Vol.119, No.5, May 1993, pp. 1643-1661

Jaradat, O.A.; McLean, D.I.; and Marsh, L. (1996), "Strength Degradation of Existing Bridge Columns Under Seismic Loading", Transportation Research Record, No. 1541, 1996, pp. 29-42.

Mitchell, D.; Bruneau, M.; Williams, M.; Anderson, D.; Saatcioglu, M.; and Sexsmith, R. (1994), "Performance of bridges in the 1994 Northridge earthquake", Canadian Journal of Civil Engineering, Vol. 22, 1995, pp. 415-427

Mitchell, D.; Sexsmith, R.; and Tinawi, R. (1994), "Seismic Retrofitting Techniques for Bridges - a state-of-the-art report", Canadian Journal of Civil Engineering, Vol.21, 1994, pp. 823-835.

Razvi, S.R. and Saatcioglu, M. (1996), "Design of R/C Columns for Confinement Based on Lateral Drift", Report to OCEERC (Ottawa Carleton Earthquake Engineering Research Centre), January 1996.

Rodriguez, M.; and Park, R. (1994), "Seismic Load Tests on Reinforced Jacketed Columns", ACI Structural Journal, Vol.91, No.2, March-April 1994, pp. 150-159.

Saadatmanesh, H.; Ehsani, M.R.; and Jin, L. (1996), "Seismic Strengthening of Circular Bridge Columns with Composite Straps", ACI Structural Journal, Vol.93, No.6, Nov.-Dec. 1996, pp. 639-647.

Saadatmanesh, H.; Ehsani, M.R.; and Jin, L. (1997), "Seismic Retrofitting of Rectangular Bridge Pier Models with Fiber Composites", Earthquake Spectra, Vol.13, No.2, May 1997, pp. 281-304.

Saatcioglu, M. and Yalcin, C. (1998), "Seismic Retrofitting Concrete Bridge Columns", Proceedings of the 5th International Conference on Short and Medium Span Bridges, CSCE, 1998.

Seible, F.; Priestly, N.; Hegemier, G.A.; and Innamorato, D. (1997), "Seismic Retrofit of RC Columns with Continuous Carbon Fiber Jackets", Journal of Composites for Construction, Vol.1, No.2, May 1997, pp. 52-62.

Xiao, Y. and Ma, R. (1997), "Seismic Retrofit of RC Circular Columns Using Prefabricated Composite Jacketing", Journal of Structural Engineering, Vol.123, No.10, Oct. 1997, pp. 1357-1364.

Yalcin, C. (1997), "Seismic Evaluation and Retrofitting of Existing Reinforced Concrete Bridge Columns", PhD Thesis, University of Ottawa, Ottawa, Ontario, Canada.